

THE EFFECT OF CHROMIUM ON THE ACTIVITY COEFFICIENT
OF SULPHUR IN LIQUID Fe-S-Cr ALLOYS

THE EFFECT OF CHROMIUM ON THE ACTIVITY COEFFICIENT
OF SULPHUR IN LIQUID Fe-S-Cr ALLOYS

By

JACQUES GUSTAVE DONDELINGER
Ingénieur des Arts et Manufactures

A Thesis

Submitted to the Faculty of Graduate Studies
in Partial Fulfilment of the Requirements
for the Degree
Master of Science

McMaster University

September 1969

MASTER OF SCIENCE (1969)
(Metallurgy)

McMASTER UNIVERSITY
Hamilton, Ontario.

TITLE: The Effect of Chromium on the Activity
Coefficient of Sulphur in Liquid Fe-S-Cr Alloys

AUTHOR: Jacques Gustave Dondelinger, Ingénieur des Arts
et Manufactures

SUPERVISOR: Professor D. A. R. Kay

NUMBER OF PAGES: (xv), 58

SCOPE AND CONTENTS:

The effect of chromium on the activity coefficient of sulphur in the ternary system Fe-S-Cr has been investigated over an extended range of temperature and chromium concentrations. A levitation-melting technique was used and H_2 - H_2S gas mixtures were passed over levitated droplets of iron and iron-chromium alloys. By comparing the experimental results obtained for both binary and ternary systems the effect of chromium on the activity coefficient of sulphur was derived in terms of first order free energy, enthalpy and entropy coefficients. Thermal diffusion effects were cancelled out by carrying out binary and ternary runs under the same experimental conditions.

ACKNOWLEDGMENTS

The author wishes to thank Dr. A. McLean for proposing the present study and for assisting in the early stages of the project, and Dr. D. A. R. Kay, whose guidance and encouragement led to a successful completion of this work.

Thanks are due to the members of the Iron and Steelmaking group of the McMaster Metallurgy Department, especially to Dr. C. K. Cooper and Dr. R. J. Pomfret for their helpful discussion and assistance during the preparation of this thesis.

The author would like to thank Mr. H. Neumayer for his technical advice in gas and chromium analyses. Thanks are also due to Mrs. A. Miltimore and Miss I. Sinanan for their skilful and accurate typing.

The author is indebted to McMaster University for the award of a graduate fellowship.

The financial support provided by Dominion Foundries and Steel Limited is gratefully acknowledged.

TABLE OF CONTENTS

	<u>Page</u>
Introduction	1
CHAPTER I	
SOLUTION THERMODYNAMICS AND LITERATURE REVIEW	3
1.1 Thermodynamics of Liquid Metallic Solutions	3
1.1.1 Mole Fraction and Weight Percent as Concentration Variables Wagner's Formalism and Lupis' Extension	3
1.1.2 Lattice Ratio as a Concentration Variable	
1.2 Literature Review	6
1.2.1 Binary System Fe-S	6
1.2.2 Ternary System Fe-S-Cr	7
CHAPTER II	
EXPERIMENTAL TECHNIQUES	10
2.1 Introduction	10
2.2 Apparatus	10
2.2.1 Reaction Chamber	11
2.2.2 Levitation Coil	11
2.2.3 Power Generator	12
2.2.4. Gas System	12
2.2.5 Temperature Measurement	12
2.3 Materials Used	13
2.3.1 Iron	13
2.3.2 Iron-Chromium Alloys	13
2.3.3 Gas Supply	13

	<u>Page</u>
2.4 Experimental Procedure	14
2.4.1 Description of an Experimental Run	14
2.4.2 Temperature Control	15
2.4.3 Method of Temperature Reading	15
2.4.4 Use of Prepared Gas Mixtures	16
2.5 Analysis	16
2.5.1 Droplet Sulphur Analysis	16
2.5.2 Chromium Analysis	17
2.5.3 Gas Analysis	17
2.6 Pyrometer Calibration	17
 CHAPTER III	
EXPERIMENTAL RESULTS	19
3.1 Binary System Fe-S	19
3.1.1 Gas Analysis Results	19
3.1.2 Kinetic Runs	20
3.1.3 <Equilibrium>Results	22
3.2 Ternary System Fe-S-Cr	23
3.2.1 Gas Analysis	23
3.2.2 Chromium Analyses	24
3.2.3 Kinetic Results	24
3.2.4 <Equilibrium>Results	25
 CHAPTER IV	
METHODS OF CALCULATION	27
4.1 Hydrogen Sulphide Dissociation	27
4.2 Chromium Loss	28
4.3 Thermodynamic Derivations	29

	<u>Page</u>
4.3.1 Binary System	29
4.3.2 Ternary System Fe-S-Cr	32
CHAPTER V DISCUSSION	34
5.1 Thermal Diffusion	34
5.1.1 Effect of Thermal Diffusion	34
5.1.2 Control of Thermal Diffusion	35
5.2 Binary System Fe-S	37
5.2.1 < Apparent Equilibrium Constant > and < Self Interaction Parameter >	37
5.2.2 Discussion	40
5.3 Ternary System Fe-S-Cr	41
5.3.1 Temperature Dependence of e_{S}^{Cr}	41
5.3.2 Discussion	43
Summary	46
Appendix I	48
Appendix 2	52
References	56

LIST OF FIGURES

Figure

- 1 Schematic diagram of the levitation apparatus
- 2 Reaction chamber
- 3 Former and levitation coil
- 4 Gas sampling device
- 5 Pyrometer calibration apparatus
- 6 Pyrometer calibration curve
- 7 Attainment of < equilibrium > at 1600°C, effect of flow rate
- 8 Attainment of < equilibrium > at 1755°C, effect of flow rate
- 9 Attainment of < equilibrium > at 1755°C, effect of flow rate
- 10 Attainment of < equilibrium > for a very low value of P_{H_2S}/P_{H_2} , effect of temperature
- 11 Attainment of < equilibrium > for a low value of P_{H_2S}/P_{H_2} , effect of temperature
- 12 Attainment of < equilibrium > for a medium value of P_{H_2S}/P_{H_2} , effect of temperature
- 13 Attainment of < equilibrium > for a high value of P_{H_2S}/P_{H_2} , effect of temperature

Figure

- 14 Attainment of $\langle \text{equilibrium} \rangle$ for a very high value of $P_{\text{H}_2\text{S}}/P_{\text{H}_2}$ effect of temperature
- 15 Effect of levitation time on Cr loss at 1590^o and 1755^o C
- 16 Chromium loss during levitation, effect of temperature
- 17 Effect of thermal diffusion
- 18 $\langle \log K'(\%) \rangle$ versus wt. % S at 1525^o C
- 19 $\langle \log K'(\%) \rangle$ versus wt. % S at 1600^o C
- 20 $\langle \log K'(\%) \rangle$ versus wt. % S at 1755^o C
- 21 Effect of temperature upon $\log K'(\%)$ and $\langle \log K'(\%) \rangle$
- 22 Comparative diagram: Temperature dependence of $\log K(\%)$ and $\langle \log K(\%) \rangle$
- 23 Comparative diagram: Temperature dependence of e_{S} and $\langle e_{\text{S}} \rangle$
- 24 Effect of Cr on the activity coefficient of S at 1525^o C
- 25 Effect of Cr on the activity coefficient of S at 1600^o C
- 26 Effect of Cr on the activity coefficient of S at 1690^o C
- 27 Effect of Cr on the activity coefficient of S at 1755^o C
- 28 Effect of Cr and temperature on the activity coefficient of S.

Figure

- 29 Comparative study of the effect of Cr on the activity coefficient of S on a lattice ratio basis, $v_{Cr} = +1$
- 30 Effect of Cr and temperature on the activity coefficient of S on a lattice ratio basis, $v_{Cr} = +1$
- 31 Temperature dependence of e_S^{Cr} , comparative study
- 32 Effect of gas composition upon the thermal diffusion effect, schematic diagram
- 33 Effect of gas composition upon the thermal diffusion effect, experimental estimation

LIST OF TABLES

Table

- 1 Comparison of Systems Used for Expressing Concentrations, Activities and Interaction Coefficients
- 2 Attainment of <equilibrium> at 1600° with low P_{H_2S}/P_{H_2} ratio, effect of flow rate
- 3 Attainment of <equilibrium> at 1755° with low P_{H_2S}/P_{H_2} ratio, effect of flow rate
- 4 Attainment of <equilibrium> at 1755° with high P_{H_2S}/P_{H_2} ratio effect of flow rate
- 5 Attainment of <equilibrium> for very low and low values of P_{H_2S}/P_{H_2} , effect of temperature
- 6 Attainment of <equilibrium> for medium, high and very high values of P_{H_2S}/P_{H_2} , effect of temperature
- 7 <Equilibrium> results at 1525°C
- 8 <Equilibrium> results at 1600°C
- 9 <Equilibrium> results at 1755°C
- 10 Chromium content of the prepared iron-chromium alloys
- 11 Chromium loss during levitation, effect of temperature and levitation time

Table

12	Attainment of <equilibrium> in iron-chromium alloys
13	System Fe-S-Cr, <equilibrium> results at 1525°C
14	System Fe-S-Cr, <equilibrium> results at 1600°C
15	System Fe-S-Cr, <equilibrium> results at 1690°C
16	System Fe-S-Cr, <equilibrium> results at 1755°C
17	System Fe-S, temperature dependence of log K'(%)
18	System Fe-S, temperature dependence of log K'(X) and log K'(Z)
19	System Fe-S-Cr, effect of Cr on the activity coefficient of S at 1525°C, weight percent scale
20	System Fe-S-Cr, effect of Cr on the activity coefficient of S at 1600°C, weight percent scale
21	System Fe-S-Cr, effect of Cr on the activity coefficient of S at 1690°C, weight percent scale
22	System Fe-S-Cr, effect of Cr on the activity coefficient of S at 1755°C, weight percent scale
23	System Fe-S-Cr, effect of Cr on the activity coefficient of S at 1525°C, lattice ratio scale
24	System Fe-S-Cr, effect of Cr on the activity coefficient of S at 1600°C, lattice ratio scale
25	System Fe-S-Cr, effect of Cr on the activity coefficient of S at 1690°C, lattice ratio scale
26	System Fe-S-Cr, effect of Cr on the activity coefficient of S at 1755°C, lattice ratio scale

LIST OF SYMBOLS

log	logarithm to the base 10
ln	natural logarithm
P	pressure
V	volume
R	gas constant
t	temperature in degree centigrade
T	temperature in degree Kelvin
M	molecular weight
m	square root of molecular weight
n	number of moles
a	activity
2, i, j, k, m	solutes in solvent l
X_i	mole fraction of component i
γ_i	activity coefficient of i, mole fraction scale
%i	weight percent of component i
f_i	activity coefficient of i, weight percent scale
z_i	concentration variable of component i, lattice ratio scale
b	number of interstitial sites per lattice atom in a solid solution

v_i	$v_i = 1$ for substitutional solute $v_i = -1/b$ for interstitial solute
ψ_i	activity coefficient of i , lattice ratio scale
ϵ_i^j	first order free energy interaction coefficient, mole fraction scale
ϵ_i^i	first order self interaction parameter, mole fraction scale
η_i^j	first order enthalpy interaction coefficient, mole fraction scale
σ_i^j	first order entropy interaction coefficient, mole fraction scale,
ρ_i^j	second order free energy interaction coefficient, mole fraction scale
F_i^E	excess partial molar free energy of mixing, mole fraction scale
H_i^E	partial molar enthalpy of mixing mole fraction scale
S_i^E	excess partial molar entropy of mixing, mole fraction scale
e_i^j	first order free energy interaction coefficient, weight percent scale

e_i^i	first order self interaction parameter, weight percent scale
h_i^j	first order enthalpy interaction coefficient, weight percent scale
s_i^j	first order entropy interaction coefficient weight percent scale
\mathcal{F}_i^E	excess partial molar free energy of mixing weight percent scale
\mathcal{H}_i^M	partial molar enthalpy of mixing weight percent scale
\mathcal{S}_i^M	excess partial molar entropy of mixing, weight percent scale
$r_i^{j,k}$	second order free energy interaction coefficient
Ψ_i^j	free energy interaction coefficient, lattice ratio scale
E_i^j	free energy interaction coefficient using lattice ratio variable and logarithm to the base 10
K	equilibrium constant in system Fe-S
< K >	equilibrium constant in system Fe-S with thermal diffusion error
K'	apparent equilibrium constant in binary system Fe-S

K''	apparent equilibrium constant in ternary system Fe-S-Cr
$K(\%)$	equilibrium constant in system Fe-S, weight percent scale
$K(x)$	equilibrium constant in system Fe-S, mole fraction scale
$K(z)$	equilibrium constant in system Fe-S lattice ratio scale
$S(g)$	gaseous sulphur
\underline{S}	dissolved sulphur
ΔG	free energy change in chemical reaction
ΔG°	standard free energy change of reaction

INTRODUCTION

Levitation-melting techniques have been used several times in the past for the study of gas-metal reaction kinetics and metallic solution thermodynamics.

However, the use of a levitation melting technique has not yet been reported in studies of the Fe-S system. It is thought that this lack of data is due to the difficulties which are likely to arise with such a technique, namely:

- 1) the strong decrease in surface tension with increasing sulphur content;
- 2) the large thermal diffusion effect when using H_2-H_2S mixtures.

Thermal diffusion leads to uncertainties in the gas composition at the gas-metal interface. Hence no accurate thermodynamic data for the equilibrium between a gaseous and liquid phase can be expected from a levitation technique. It follows that self interaction parameters cannot be derived accurately, for their determination is based on a knowledge of the gas composition at the gas-metal interface.

However, the effect of a second solute can be derived by comparison of binary and ternary results and uncertainties in the gas composition can be cancelled out, provided the degree of thermal diffusion is kept constant.

In the present work a levitation-melting technique is used to study the effect of chromium on the activity of sulphur in the ternary system Fe-S-Cr by comparing binary and ternary results obtained under conditions of constant thermal diffusion. Interaction coefficients of chromium on the activity of sulphur are obtained for four temperatures,

1525, 1600, 1690 and 1755^oC, and for chromium concentrations up to 40 weight percent.

CHAPTER I

SOLUTION THERMODYNAMICS and LITERATURE REVIEW

1.1 Thermodynamics of Liquid Metallic Solutions

The thermodynamic description of liquid metallic solutions aims to give an analytical representation of the activities of the various elements in a liquid multi-component solution. However, no representation is satisfactory over an extended range of concentration. Thus, different ways of expressing concentration variables, (Table 1), such as weight percent⁽¹⁾, atom fraction⁽²⁾, atom ratio^(3,4), lattice ratio⁽⁵⁾ have been used. Quadratic representation⁽⁶⁾ on an atom fraction basis has also been attempted. In the following, we shall briefly review the formalisms used in this work.

1.1.1. Mole Fraction and Weight Percent as Concentration Variables

Wagner's Formalism and Lupis' Extension

Wagner⁽²⁾ has described the thermodynamic behaviour of a liquid metallic solution consisting of solutes $i, j \dots$ in solvent 1, in terms of the excess partial molar free energy, of say solute i , ($RT \ln \gamma_i$), or the logarithm of the activity coefficient, ($\ln \gamma_i$). He expanded $\ln \gamma_i$ by a Taylor series in terms of the mole fractions of the infinitely diluted solutes (see Appendix 1). Limiting the expansion to the first order terms, Wagner and Chipman⁽⁷⁾ defined the first order free energy interaction coefficient:

$$\epsilon_i^j = \left(\frac{\partial \ln \gamma_i}{\partial x_j} \right)_{x_1 \rightarrow 1} \quad 1.1$$

Lupis and Elliott^(8, 9) expanded this formalism to include higher order interaction coefficients (see Appendix 1). They also proposed that Wagner's treatment of excess partial molar free energy be extended to excess partial molar enthalpy and excess partial molar entropy.

$$F_i^E = H_i^E - T.S_i^E \quad 1.2$$

Expressed in terms of the free energy, enthalpy and entropy interaction coefficients, ϵ_i^j , η_i^j and σ_i^j respectively, equation 1.2 becomes:

$$\epsilon_i^j = \frac{\eta_i^j}{RT} - \frac{\sigma_i^j}{R} \quad 1.3$$

Although expressing concentrations as mole fractions is more fundamental, weight percentages are often used for their practical convenience. On the latter scale, the free-energy interaction coefficient, e_i^j , becomes:

$$e_i^j = \left(\frac{\partial \log f_i}{\partial (\%j)} \right)_{\text{wt. \%}1 \rightarrow 100} \quad 1.4$$

and is related to the enthalpy and entropy interaction coefficients by:

$$e_i^j = \frac{h_i^j}{2.3 RT} - \frac{s_i^j}{2.3R} \quad 1.5$$

A brief derivation of these interaction coefficients together with conversions from mole fraction scale to weight percent scale will be found in Appendix 1.

1.1.2 Lattice Ratio as a Concentration Variable

For the description of a solid metallic solution containing interstitial solutes, the thermodynamic behaviour can be expressed in

terms of the lattice ratio, which is the ratio of filled to unfilled interstitial sites. Thus, for a binary solution of the interstitial solute i in solvent 1, Chipman⁽⁵⁾ suggested the use of a concentration variable z_i , proportional to this ratio:

$$z_i = k \frac{n_i}{bn_1 - n_i} \quad 1.6$$

where b is the number of interstitial sites per lattice atom. The proportionality factor k is taken equal to b . Hence

$$z_i = b \frac{n_i}{bn_1 - n_i} = \frac{n_i}{n_1 - n_i/b} \quad 1.7$$

Extending this definition to a multi-component solid solution of both interstitial and substitutional solutes, $i, j \dots$, z_i becomes:

$$z_i = \frac{n_i}{n_1 + \sum v_j n_j} \quad 1.8$$

where $v_j = +1$ for a substitutional solute and $v_j = -1/b$ for an interstitial solute. Note that z_i equals x_i , the mole fraction, in a solution containing only substitutional solutes. In infinitely dilute solution the activity of a solute is taken to be equal to the variable z . The departure from this direct relationship occurring in solutions of finite solute concentrations is expressed in terms of activity coefficients, Ψ_i^j , and interaction coefficients, θ_i^j , as for other representations. This formalism was successfully applied to the description of iron solid solutions⁽⁵⁾. Chipman checked its adequacy for liquid solutions of non-metallic solutes, such as carbon, sulphur, nitrogen, silicon in iron. Although the interstitial nature of these components in the liquid state may have lost its significance, Chipman found that using z as a concentration variable and taking $v_S = -1$ and $v_C = -1$, $v_{Al} = -1$, $v_{Si} = -1$, $v_P = -1$,

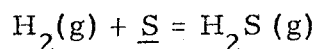
$v_{\text{Mn}} = +1$, the effects of the latter components on the activity coefficient of sulphur in iron solutions could be expressed by a linear relationship between $\log \Psi_{\text{S}}^i$ and z_i , valid up to high concentrations.

In the present work mole fraction, weight percent and lattice ratio formalisms will be used.

1.2 Literature Review

1.2.1. Binary System Fe-S

For the last thirty years the binary system Fe-S has been repeatedly investigated by numerous workers⁽¹⁰⁻²⁰⁾ who, in general, studied the reaction



$$K = \frac{P_{\text{H}_2\text{S}}}{P_{\text{H}_2} \cdot a_{\text{S}}} \quad 1.9$$

where the activity of sulphur was expressed either on a mole fraction scale or on a weight percent scale for the reference state of infinitely dilute solution. All studies were carried out using crucible melting techniques in either resistance^(12-14, 17, 20) or induction furnaces^(10, 15, 16). The temperature was generally measured by sighting a disappearing-filament type optical pyrometer^(10, 14-17) on to the melt and more rarely by using thermocouples⁽²⁰⁾. All these investigations have been critically reviewed by Sherman, Elvander and Chipman⁽¹⁵⁾, and more recently by Ban-Ya and Chipman⁽²⁰⁾. All investigations but one⁽¹⁹⁾, prior to 1967, reported a most uncommon behaviour for the activity coefficient of sulphur in the binary system in that the deviation from Henry's law increased with increasing temperature. Ban-ya and Chipman

thought that errors in data due to thermal diffusion and temperature measurement with optical pyrometers were responsible for this unusual behaviour. Thermal diffusion, often present in induction furnaces is due to insufficient radiation shielding. The emissivity of a melt varies with solute concentration and thus temperatures measured with disappearing-filament type optical pyrometers are liable to error. Because of the reported anomalous behaviour of S in Fe-S melts, Ban-ya and Chipman⁽²⁰⁾ decided to reinvestigate this binary system. In order to eliminate inaccuracies, due to thermal diffusion and erroneous temperature measurement, they used a wire-wound resistance furnace and measured the temperature by means of calibrated thermocouples. Their work was carried out over the range 1500°C to 1600°C and showed that the deviation from Henry's law decreased with increasing temperature (see Fig. 23). Moreover, they recalculated other authors⁽¹⁴⁻¹⁹⁾ results using the latest thermodynamic data⁽²¹⁻²²⁾ for H₂S dissociation at high temperatures. All these data are compiled in Fig. 22 and 23.

1.2.2. Ternary System Fe-S-Cr

At the present time, only three studies report the effect of chromium on the activity coefficient of sulphur in Fe-S-Cr melts.

Griffing and Healy⁽²³⁾ investigated the effect of Cr on the activity coefficient of S for Cr contents ranging from 0 to 100 weight percent. At 1600°C and for chromium concentrations up to 20 weight percent, their results are given by the equation

$$\log f_S^{\text{Cr}} = -0.019 (\% \text{ Cr}) \quad 1.10$$

This relationship is to be considered with some reserve since it is

derived from a set of only three points, showing a noticeable scattering. Their results obtained with higher chromium contents do not follow this linear relationship. Furthermore, those runs had to be carried out at higher temperatures because of the limiting liquidus surface in the Fe-S-Cr system^(24, 25). The effect of Cr in the ternary system was obtained by comparing ternary and binary results. However, Griffing and Healy did not re-establish the binary system Fe-S themselves but used instead the data given by Chipman et al⁽¹⁵⁾. This treatment would be adequate if all operating conditions were identical in both works. This, however, is not the case. Griffing and Healy used an induction - heated carbon-tube furnace, measured the temperature with a standardized thermocouple immersed in the melt, and bubbled H₂-H₂S gas mixtures into the melt. Because of these experimental precautions, thermal diffusion effects were probably eliminated and the temperature measurement accurate. However, in the work reported by Chipman et al⁽¹⁵⁾ an induction furnace was used. Although radiation shields and "vigorous" gas preheating were used to eliminate thermal diffusion, the temperature was measured by a disappearing-filament type optical pyrometer. These considerations leave some doubts whether or not the operating conditions were identical in both works. If any discrepancy in the effect of Cr on the sulphur activity coefficient arose from these differences, it would be most evident at low Cr concentrations and would be progressively attenuated with increasing Cr concentrations. In this respect, it should be noticed that Griffing's plot (Fig. 29) of $\log \psi_S^{Cr}$ versus z_{Cr} shows a systematic error at zero Cr concentration.

Adachi and Morita⁽²⁶⁾ reported a value of the interaction coefficient $e_S^{Cr} = -0.020$, valid at 1650°C for concentrations up to 20% Cr, which is in good agreement with the value of -0.019 reported by Griffing.

Although this result was derived from a set of twenty-five data points, it should be noticed that the data were largely scattered. Adachi and Morita used a carbon tube resistance furnace with a gas bubbling technique and measured the temperature with a disappearing-filament type optical pyrometer. As a binary system reference, they used their own results previously obtained by the same experimental procedure⁽¹⁷⁾.

A recent study by Ban-ya and Chipman⁽²⁷⁾ gave a value of $e_S^{Cr} = -0.0107$, valid at 1550° for chromium concentrations up to 18 wt.%. This value was obtained from a set of four points that showed very little scattering. Their data disagreed with both Griffing's and Adachi's results, although Ban-ya and Chipman claimed that they agreed with Griffing's. The reason is that Ban-ya and Chipman reported only one data point from Griffing's work that happened to fall in the range of concentrations they investigated, in (Fig. 29).

It can be seen from the above review that the effect of Cr on the activity of sulphur has not been studied by many workers, and that agreement amongst these workers is incomplete. Furthermore, there has been no investigation of the temperature dependence of the interaction coefficient e_S^{Cr} . These facts, together with a recent trend in industry to produce steels of chromium content higher than twenty weight percent have motivated a more extensive study of the combined effect of chromium and temperature on the activity coefficient of sulphur in the ternary system Fe-S-Cr.

CHAPTER II

EXPERIMENTAL TECHNIQUES

2.1 Introduction

In the present work a levitation-melting technique was used because of the following advantages:

- 1) Approach to equilibrium is accelerated by the strong stirring produced by the high-frequency current in the levitated droplet.
- 2) The surface to volume ratio is greater than in conventional crucible techniques and favours high mass transfer rates.
- 3) Segregation problems on freezing are avoided because the whole sample is analysed for sulphur.
- 4) Operations at high temperatures are possible without crucible contamination or failure.

However, thermal diffusion was inevitably present and its effect and control are discussed in 5.1. The experimental method consisted in passing H_2-H_2S mixtures of known composition for the required length of time past a levitated liquid Fe or Fe-Cr droplet and subsequently analysing the quenched droplets for sulphur.

2.2 Apparatus

In Fig. 1 is shown a schematic diagram of the levitation apparatus,

the main components of which are:

- 1) Reaction chamber
- 2) Levitation coil
- 3) High-frequency generator
- 4) Gas system
- 5) Temperature measurement device.

2.2.1. Reaction Chamber

The reaction chamber, shown in Fig. 2, consisted of a vertical 15 mm O. D. Vycor tube, surrounded by the levitation coil. The upper end of the tube was connected by a ground glass union to a 15 mm O. D. three-branched tube. The different branches were used for a gas outlet, a temperature reading port and a sample inlet. The lower end of the reaction tube was connected by a ground glass union to a 50 mm O. D. pyrex chamber, furnished with a gas inlet and sealed at the bottom by a rotatable aluminium disc, supporting a quartz charging rod, a 45° prism and a copper mould. This latter device had been used in a previous study⁽²⁸⁾.

2.2.2. Levitation Coil

The coils used in this work were similar in design to those used in previous studies⁽²⁸⁻³¹⁾. They were constructed from 1/8" O. D. copper tubing and wound helically in a conical former in two parts, one for levitation and the other for stabilization (Fig. 3). For temperatures of 1525°C and 1600°C, the lower part consisted of four turns. For temperatures of 1690°C and 1755°C, it consisted of five turns, thus increasing the induction field and consequently, the heat generated in the sample. In both cases the stabilizing part consisted of two reverse turns.

2.2.3. Power Generator

The high frequency power for levitation was supplied by a Tocotron high frequency generator, rated as 10 kW at 200A and 450 kHz. The current was conveyed to the water-cooled levitation coil via a 7.5:1 step-down transformer.

2.2.4. Gas System

The different gases and gas mixtures were supplied from gas cylinders and passed over different purifying materials, (Fig. 1). Commercial grade hydrogen was deoxidized by a platinum catalyst, A, which converted oxygen into water vapour, and was subsequently dried by magnesium perchlorate, B. The H_2 - H_2S mixtures were also dried by magnesium perchlorate, B. Commercial grade helium was used without purification. The H_2 - H_2S gas mixtures were led through a gas sampling device, C which was designed in such a way, Fig. 4, that gas analysis could be carried out during levitation runs. The flow of the H_2 - H_2S mixture was controlled by a rotameter-type flowmeter, D. Needle valves, E, regulated the flow of all gases which were conveyed to the reaction chamber via glass tubing. Leaving the reaction tube the gases were bubbled in dibutyl phthalate, F, and then passed to waste.

2.2.5. Temperature Measurement

The temperature was measured using a Millitron two-colour radiation pyrometer. Temperature measurements with this pyrometer depend upon the ratio of the intensities at two particular wave lengths. The measurement is thus independent of any variations in emissivity of the surface due to the solute, and of any absorption effects, provided that both wave lengths are equally attenuated. Nevertheless, a

reliable use of this pyrometer required a calibration of this instrument carried out over the range of operating temperatures, (see 2.6.).

2.3 Materials Used

2.3.1. Iron

The iron used was Armco Magnetic Ingot Iron, supplied by Corey Steel in 1/4" cold drawn rods of the following analysis:

C	Mn	P	S	Cu	Si
.024	.033	.005	.015	.018	.001

Samples weighing about one gram were cut from these rods, ground with emery paper and washed in acetone.

2.3.2. Iron-Chromium Alloys

The Fe-Cr alloys were made from Armco Iron, (as above), and 99.95 weight percent electrolytic chromium supplied by McKay Inc. A total iron and chromium weight of about 40 g was melted in an argon-arc furnace and cast into an ingot about 2 1/2" long. The cast ingot was then swaged down to a rod of 1/4" diameter. This rod was checked for homogeneity of chromium content (Table 10) and subsequent sample preparation was identical to the one described for iron.

2.3.3. Gas Supply

Commercial grade helium and hydrogen were supplied by Liquid Air. The H₂-H₂S gas mixtures were supplied by the Matheson Company of Canada, who used prepurified grade hydrogen and commercial grade hydrogen sulphide to make up gas mixtures. Specific hydrogen sulphide concentrations were ordered in the range 0.1 to 1.5 volume percent.

2.4 Experimental Procedure

2.4.1. Description of an Experimental Run

The clean sample was introduced into the reaction chamber through the sample inlet and held on top of a quartz rod above the levitation coil. The reaction chamber was flushed with helium for one to two minutes. After this time, the power was switched on and raised to its maximum value. The sample was lowered into the coil where it levitated immediately. The power input was then decreased, allowing the sample to approach the lower regions of the coil where the induction flux was highest. At the same time, the helium flow rate was reduced and under these conditions, the sample melted rapidly. The aluminum disc was rotated to permit sighting of the pyrometer at the bottom of the levitated droplet. Helium, which was used during melting for its relatively low thermal conductivity, was then replaced by hydrogen for its efficient deoxidizing ability. The sample was deoxidized at about 1550°C for four to five minutes, after which time the oxygen level in the quenched droplet was generally found to be less than $10\text{ ppm}^{(30)}$. After this deoxidation the hydrogen atmosphere was replaced by a stream of $\text{H}_2\text{-H}_2\text{S}$ mixture, the flow of which was kept at the constant level of 2.6 l/min . With increasing sulphur content, the surface tension of the levitated droplet decreased markedly⁽³²⁾ and led to problems of both mechanical and thermal instabilities. The form of the levitation coil was then repeatedly adjusted until a stable and trouble free operation was achieved. In normal operating conditions, the temperature reading could be kept within $\pm 10^{\circ}\text{C}$.

After the sample had levitated at the desired temperature for the required length of time, the aluminium disc was rotated to bring the copper mould into alignment with the reaction tube. The mould itself was raised into the reaction tube, the power was switched off and the droplet quenched. The reaction chamber was then purged with

helium and the sample subsequently collected for sulphur analysis.

In a daily series of runs, the pyrometer calibration curve was checked against the melting point of pure iron. For this purpose the sample was slightly super cooled and upon freezing, the pyrometer deflected rapidly back to the melting point. Since supercooling can be very high in levitation melting techniques⁽³¹⁾, freezing was generally induced by tapping the reaction chamber, thus allowing some condensed fumes to fall upon the droplet and nucleate solidification.

2.4.2. Temperature Control

The heat in a levitated droplet is generated by the I^2R losses of the current induced in it. The amount of heat produced depends therefore, on the induction field, the position of the specimen in this field, and on the nature of the specimen itself. Heat is lost by the specimen through radiation and convective conduction of the gas stream.

The temperature of the levitated droplet therefore results from a heat balance, the elements of which are:

- 1) coil current and geometry,
- 2) weight, size and electrical properties of the sample,
- and 3) composition, flow rate and conductive properties of the gas stream.

In the present work, special effort was made to keep the flow rate of H_2-H_2S mixtures constant. For practical purposes, the weight of iron and iron-chromium samples was kept between 0.85 and 1.25 g and it follows that the temperature could be controlled only by the coil current and geometry (see 2.2.2.).

2.4.3. Method of Temperature Reading

As already mentioned, the temperature was measured by sighting

the pyrometer at the bottom of the levitated droplet. The reason for this was that at high temperatures, fumes of iron sulphide and/or chromium sulphide interfered with temperature reading made from the top. The gas stream was not inverted since its upward flow at high rates aided levitation slightly.

As shown in the following table, no difference in the steady state sulphur content of the droplet was observed when sighting the pyrometer at the top or at the bottom of the levitated droplet, while using the same gas mixture and the same pyrometer reading (1590°C).

<u>%S Observed in Top Measurement</u>	<u>%S Observed in Bottom Measurement</u>
0.201	0.204
0.203	0.199
0.188	0.205
0.194	0.203

2.4.4. Use of Prepared Gas Mixtures

In the prepared gas mixtures, the hydrogen sulphide content was found to decrease over a period of about one to two weeks. The rate of deterioration depended on the initial H₂S concentration and on the initial state of sulphur absorption of the gas cylinder walls. Hence, it was necessary to check the gas composition for each series of runs, and the gas sampling device (Fig. 4) was therefore designed. In general, the gas analysis showed no noticeable change in H₂S content over periods of up to four days.

2.5 Analysis

2.5.1 Droplet Sulphur Analysis

The sulphur analyses of the levitated samples were carried out in

a Leco 518 titrator according to the combustion iodometric procedure, (A. S. T. M. method E 30-47). For each series of runs, the titrator was calibrated by means of the NBS standard 133a⁽³³⁾.

2.5.2. Chromium Analysis

Since the prepared samples contained only iron and chromium, a simple volumetric method of titration was used⁽³⁴⁾. Oxidation with perchloric acid was followed by reduction with ferrous ammonium sulphate, the latter being compared with a standardized potassium permanganate solution.

2.5.3. Gas Analysis

For determining the hydrogen sulphide content, an improved volumetric method was used⁽³⁵⁾. Alkaline sodium hypochlorite was used as a combined absorbing and oxidizing reagent of hydrogen sulphide. The resulting sulphate was titrated by the usual iodometric method.

Efforts were made to get reproducible analyses from a given gas mixture. It was found that maximum reproducibility was achieved when passing the H_2-H_2S gas mixture through the sampling bulb for about thirty minutes and by flushing the sampling bulb for forty to fifty minutes with a very low helium flow. During bubbling of the $He-H_2-H_2S$ mixture into the reagent, absorption of hydrogen sulphide was enhanced by stirring the reagent with a magnetic stirrer. Boiling was found to have no influence on the degree of oxidation of H_2S to sulphate.

2.6 Pyrometer Calibration

For the reliable use of the pyrometer, calibration of this instrument was necessary. Armco iron, held in an alumina crucible under

an atmosphere of hydrogen, was heated by induction. The pyrometer lens was sighted on to the melt via a 45° prism and the true temperature was obtained with a Pt-5% Rh/Pt-20% Rh thermocouple. In order to eliminate any interaction of the induction field with the thermocouple voltage, the potentiometer was grounded and the alumina crucible was surrounded by a graphite susceptor. A more thorough description of the calibration apparatus is given in Fig. 5 and the calibration curve is shown in Fig. 6. It can be noticed that a slight supercooling was observed before freezing.

CHAPTER III

EXPERIMENTAL RESULTS

All experimental results obtained from gas, sulphur and chromium analysis are given in form of tables and figures. This chapter will collect all data and refer to both tables and figures.

3.1 Binary System Fe-S

3.1.1. Gas Analysis Results

For determining the hydrogen sulphide content of a H_2 - H_2S gas mixture, the following information was used:

- 1) volume of the sampling bulb ($V=136.8$ ml at $25^\circ C$),
- 2) volume A of titration solution (ml of thiosulphate 0.01 N),
- 3) barometric pressure and
- 4) room temperature

The H_2S content of the gas mixture was then derived in terms of the ratios B and R:

$$B = \frac{\text{atoms of hydrogen}}{\text{atoms of sulphur}}$$

$$R = \frac{X_{H_2S}}{X_{H_2}} = \frac{P_{H_2S}}{P_{H_2}} = \frac{V_{H_2S}}{V_{H_2}}$$

is the ratio of moles of hydrogen sulphide and hydrogen. R is also

equal to the ratio of partial pressures and partial volumes. The ratios B and R were obtained with a small computer program, which is shown in Appendix 2, together with an example of input and output data.

The analysis results of all gas mixtures used in this work are reported in Table 7(b), 8(b) and 9(b) in terms of the following quantities:

- 1) B_m - mean value of ratio B
- 2) R_m - mean value of the ratio of moles of H_2S and H_2
- 3) N - number of analyses of which B_m and R_m are the means
- 4) s - standard deviation of R_m for this set of analyses, and
- 5) RSD - relative standard deviation, which is $100 \cdot s/R_m$ and thus expressed in %.

As seen from these tables, the accuracy of the analysis increased with the content of hydrogen sulphide in the gas mixture. The exchange of oxygen between the alkaline solution and the atmosphere, occurring mainly in the stirred reagent, may account for this phenomenon. Its effect is naturally more sensitive when dealing with low H_2S contents.

3.1.2. Kinetic Runs

Before deriving equilibrium data in a certain experimental apparatus, the approach to equilibrium, particularly in a levitation melting technique, always needs to be investigated. For a gas-metal reaction, this investigation generally involves the study of the effect of gas composition and temperature. Since thermal diffusion was inevitably present in the levitation apparatus, the effect of gas flow rate was also examined. Thus, in the present kinetic study, the amount

of dissolved sulphur was experimentally determined as a function of levitation time for different values of the following variables:

- 1) gas flow rate,
 - 2) gas composition,
- and
- 3) temperature.

In a first series of experiments, the gas flow rate took the following three values:

Flow rate 1	0.9 l/min.
Flow rate 2	2.6 l/min.
Flow rate 3	5.1 l/min.

The effect of flow rate on the approach to equilibrium was examined for three combinations of temperature and gas composition.

t °C	$\frac{P_{H_2S}}{P_{H_2}}$	Reference	
		Table	Figure
1600	0.00156 ± 0.00002	2	7
1755	0.00148 ± 0.00006	3	8
1755	0.00896 ± 0.00011	4	9

In the last case, only flow rates 1 and 2 could be used because of mechanical instabilities arising from the combination of high flow rate and a low surface tension (high S content).

In a second series of experiments, the gas flow rate was kept constant (2.6 l/min.) and the amount of dissolved sulphur was

determined as a function of levitation time for different gas compositions at two temperatures.

P_{H_2S}/P_{H_2}	Temp. °C	Table	Figure
0.00090 ± 0.00003	1590 1755	5	10
0.00184 ± 0.00008	1590 1755	5	11
0.00501 ± 0.00014	1590		
0.00472 ± 0.00009	1755	6	12
0.00894 ± 0.00003	1590 1750	6	13
0.01405 ± 0.0015	1590 1755	6	14

It should be noticed that for the very high H_2S/H_2 ratio of 0.01405, a steady state was not reached even after 60 minutes of levitation. It also may be noticed that samples with a sulphur content as high as 12 weight percent, could be levitated using an appropriate coil.

3.1.3. <Equilibrium>Results*

The <equilibrium>* sulphur contents at different temperatures and gas compositions were taken from the above kinetic runs and from other specific equilibration runs, (mainly at 1525°C). The sulphur contents for each temperature are reported in the following tables:

* The nature of this <equilibrium> will be discussed in 5.1.

1525°C	Table 7(a)
1600°C	Table 8(a)
1755°C	Table 9(a)

The number of a run consists of five digits. The first digit indicates the temperature:

1	for	1525°C
2	for	1600°C or 1590°C
3	for	1690°C and
4	for	1755°C

The next two digits indicate the chronological order in which these runs were carried out and the last two digits indicate the number of experiments, of which the given run is the mean.

The analysis results are reported as:

$(\%S)_m$: mean value of sulphur content,

N : number of experiments of which $(\%S)_m$ is the mean,

s : standard deviation and

RSD : relative standard deviation i. e. $100 \times s / (\%S)_m$

As shown in these tables, the accuracy of the analysed sulphur content, (RSD is generally less than 2%), indicates the good reproducibility of both the Leco sulphur titrator and the levitation apparatus.

3.2 Ternary System Fe-S-Cr

3.2.1. Gas Analysis

The analysis of the gas mixture used for ternary Fe-S-Cr runs have already been reported in the section concerning the binary

system (3.1.1.).

3.2.2. Chromium Analyses

As indicated in 2.3.2., the prepared Fe-Cr rods were checked for homogeneity in chromium content. For that purpose, samples for Cr analysis were taken as shown in the diagram below.

A 1	Section 1	A 2	Section 2	A 3	Section 3	A 4	Section 4
-----	-----------	-----	-----------	-----	-----------	-----	-----------

Each section provided five or six samples for levitation. The results of Cr analysis are reported in Table 10 and as seen from this table, the relative maximum deviation

$$\text{RMD} = \frac{\text{max. deviation}}{\text{mean Cr content}} \times 100$$

only once exceeded 2% and was generally found to be less than 1%.

This degree of homogeneity was considered satisfactory. The chromium content of a levitation sample was taken to be the mean of the analysis of both ends of its section.

3.2.3. Kinetic Results

3.2.3.1. Chromium Content as a Function of Time

Due to the difference in the vapour pressures of iron and chromium at any given temperature⁽³⁶⁾, the chromium content of Fe-Cr samples was expected to decrease with increasing levitation time and temperature. No equilibrium vapour pressure data could be applied successfully, since vapour saturation was not achieved with the flow rates used and hence the rate of chromium loss needed to be determined experimentally. For that purpose, Fe-Cr samples were

levitated in a gas stream of hydrogen at the same flow rate of 2.6 l/min. at 1590°C and 1755°C for different periods. The experimental results, shown in Fig. 15, are expressed in terms of a relative percent loss in ten minutes.

$$\text{RPL} = \frac{\% \text{Cr}_{\text{initial}} - \% \text{Cr}_{(10 \text{ min.})}}{\% \text{Cr}_{\text{initial}}} \times 100$$

see Table 11

3.2.3.2. Sulphur Content as a Function of Time

Previous studies have shown that chromium contents of 20 wt. % in the ternary system Fe-S-Cr raised the equilibrium sulphur content up to three times its value in the binary system Fe-S, obtained at the same temperature and for the same H₂-H₂S composition. The time required to reach equilibrium was thus expected to increase at a similar rate and needed to be determined experimentally. For that purpose, before each new series of ternary runs, some Fe-Cr samples of the highest chromium content were levitated in the given gas mixture and at the desired temperature for increasing periods of time. Equilibrium was considered to be reached when the analysed sulphur content started to decrease with increasing levitation time. This decrease of the sulphur content resulted from a decrease of the chromium content owing to its higher evaporation rate as compared to that of iron. In Table 12 is shown the analysed sulphur content as a function of levitation time, for the temperatures and gas compositions used.

3.2.4. <Equilibrium>Results

The experimental results of levitation runs with Fe-Cr samples were carried out at four temperatures and are shown in terms of initial Cr content, levitation time and analysed sulphur content in the following tables:

1525°C

Table 13

1600°C

Table 14

1690°C

Table 15

1755°C

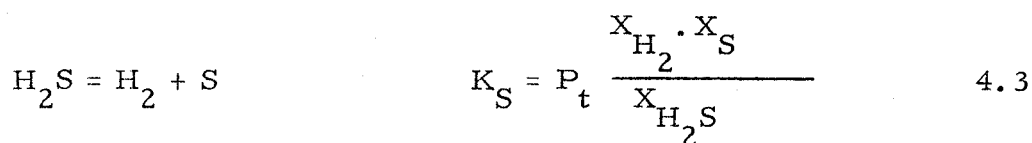
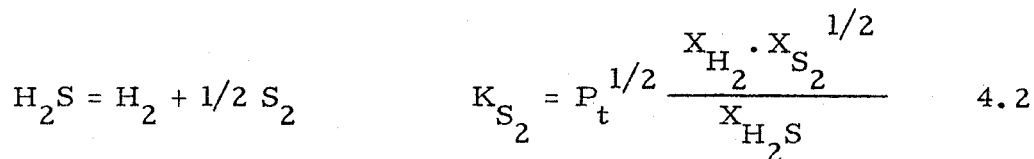
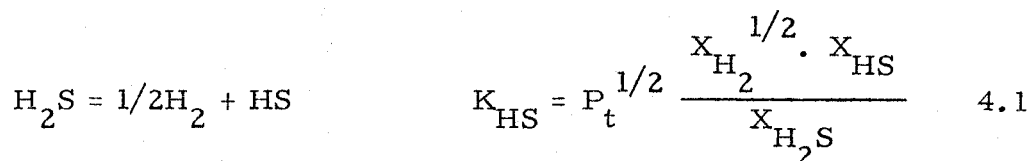
Table 16

CHAPTER IV

METHODS OF CALCULATION

4.1 Hydrogen Sulphide Dissociation

At high temperatures, hydrogen sulphide is unstable and partially dissociates into HS, H₂S, S₂ and S, the relative amounts of which are controlled by the following equilibrium equations, corresponding to three significant types of dissociation of H₂S.



where P_t is the total pressure in the reaction tube and X_{H_2} , $X_{\text{H}_2\text{S}}$, X_{S_2} , and X_{S} are the mole fractions of the different gas components. These mole fractions are naturally related by:

$$1 = X_{\text{H}_2} + X_{\text{H}_2\text{S}} + X_{\text{HS}} + X_{\text{S}_2} + X_{\text{S}} \quad 4.4$$

Furthermore, the value of the ratio of hydrogen and sulphur atoms in the inlet gas is given by chemical analysis B of the H_2-H_2S gas mixture and can be expressed in terms of the mole fractions as follows:

$$B = \frac{\text{atoms hydrogen}}{\text{atoms sulphur}} = \frac{2X_{H_2S} + 2X_{H_2} + X_{HS}}{X_{H_2S} + X_{HS} + 2X_{S_2} + X_S} \quad 4.5$$

For given values of the equilibrium constants, the chemical gas analysis and the total pressure, this set of five equations gives the equilibrium values of all five mole fractions at a certain temperature. For this purpose, a computer programme was used, which is shown in Appendix 2, together with an example of input and output data, giving an idea of the degree of dissociation at high temperature.

The above method of calculation for H_2S dissociation, as well as the thermodynamic data of the three free energies of H_2S dissociation were taken from Ref. 20.

4.2 Chromium Loss

In 3.2.3.1., the chromium loss was determined experimentally for two temperatures $1590^\circ C$ and $1755^\circ C$. These experimental results needed to be extrapolated for $1525^\circ C$, $1600^\circ C$ and $1690^\circ C$, at which temperatures Fe-Cr alloys were levitated. Since the temperature dependence of chromium vapour pressure is expressed by

$$\log p = \frac{-\Delta H_v^\circ}{4.576 T} + b \quad 4.6$$

where ΔH_v° is the enthalpy of vaporization and b is a constant, the chromium loss was considered to be proportional to the chromium vapour pressure and subject to the same temperature dependence.

$$\log (\text{Cr loss}) = \frac{A}{T} + B \quad 4.7$$

A linear relationship with reciprocal temperature gave the following chromium losses, expressed in % of the initial chromium percentage per 10 minutes:

$t^{\circ}\text{C}$	Cr loss
1525	0.41
1600	0.81
1690	1.7
1755	2.9

(see Fig. 16)

4.3 Thermodynamic Derivations

4.3.1. Binary System

When passing a stream of H_2 - H_2S gas mixture over liquid iron, one investigates the reaction:



with an equilibrium constant

$$K = \frac{P_{\text{H}_2\text{S}}}{P_{\text{H}_2} \cdot a_{\text{S}}} \quad 4.9$$

Adopting the infinite dilute solution as reference state and defining the Henrian activity as proportional to the concentration,

$$a_{\text{S}} = f_{\text{S}} \cdot \% \text{S in a Henrian wt. \% scale} \quad 4.10$$

$$a_S = \gamma_S \cdot X_S \text{ in a Henrian mole fraction scale} \quad 4.11$$

$$a_S = \Psi_S \cdot Z_S \text{ in a Henrian lattice ratio scale} \quad 4.12$$

where f_S , γ_S , Ψ_S , are the activity coefficients in the different scales and measure the deviation from Henry's law at finite concentrations.

In the reference state of infinite dilute solution,

$$f_S \rightarrow 1 \quad \text{when } \%S \rightarrow 0$$

$$\gamma_S \rightarrow 1 \quad \text{when } X_S \rightarrow 0$$

$$\Psi_S \rightarrow 1 \quad \text{when } Z_S \rightarrow 0$$

For the different scales, apparent equilibrium constants K' may be expressed as follows:

$$K'(\%) = \frac{P_{H_2S}}{P_{H_2} \cdot \%S} \quad 4.13$$

$$K'(X) = \frac{P_{H_2S}}{P_{H_2} \cdot X_S} \quad 4.14$$

$$K'(Z) = \frac{P_{H_2S}}{P_{H_2} \cdot Z_S} \quad 4.15$$

Thus, the logarithms of the true equilibrium constants K can be expressed in terms of the apparent equilibrium constants and the activity coefficients:

$$\log K(\%) = \log K'(\%) - \log f_S \quad 4.16$$

$$\log K(X) = \log K'(X) - \log \gamma_S \quad 4.17$$

$$\log K(Z) = \log K'(Z) - \log \Psi_S \quad 4.18$$

As the sulphur concentrations tend to 0, the value of the apparent equilibrium constants K' tend to the true equilibrium constants K .

At finite sulphur contents, the logarithms of the activity coefficients can be expressed as a function of the sulphur concentrations:

$$\log f_S = e_S^S (\%S) + r_S^{S,S} (\%S)^2 + \dots \quad 4.19$$

$$2.3 \log \gamma_S = \epsilon_S^S \cdot X_S + p_S^{S,S} \cdot (X_S)^2 + \dots \quad 4.20$$

$$2.3 \log \Psi_S = \theta_S^S \cdot Z_S + \dots \quad 4.21$$

where e_S^S , ϵ_S^S , θ_S^S and $r_S^{S,S}$, $p_S^{S,S}$ are the first order and second order interaction coefficients respectively, sometimes called self interaction coefficients.

The study of the temperature dependence of reaction 4.8 gives the free energy,

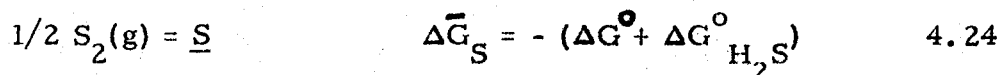
$$\Delta G^\circ = -RT \ln K = A + BT \quad 4.22$$

Combining equation 4.22 with the free energy change associated to the reaction of H_2S dissociation:



one obtains the free energy of solution of sulphur in iron, associated to

the reaction:



4.3.2. Ternary System Fe-S-Cr

As shown in 4.3.1., the experimental study of reaction 4.8 in the binary system Fe-S led to the apparent equilibrium constant K' , and the true equilibrium constant K , related by the equation 4.16. When equilibrating Fe-S-Cr alloys, an apparent equilibrium constant K'' is used,

$$K''(\%) = \frac{P_{H_2S}}{P_{H_2} \cdot \%S} \quad 4.25$$

which is related to the true equilibrium constant $K(\%)$,

$$K(\%) = \frac{P_{H_2S}}{P_{H_2} \cdot f_S \cdot \%S} = \frac{P_{H_2S}}{P_{H_2} \cdot f_S^S \cdot f_S^{Cr} \cdot \%S} \quad 4.26$$

by the relation:

$$\log K(\%) = \log K''(\%) - \log f_S^S - \log f_S^{Cr} \quad 4.27$$

Combining equation 4.27 with equation 4.16 obtained for the binary system, the former equation becomes:

$$\log f_S^{Cr} = \log K''(\%) - \log K'(\%) \quad 4.28$$

This latter equation expresses the effect of chromium on the activity coefficient of S in Fe-S-Cr alloys in terms of the binary and ternary

apparent equilibrium constants $K'(\%)$ and $K''(\%)$, taken for the same value of sulphur concentration and at the same temperature.

Expressed in terms of chromium concentrations

$$\log f_S^{\text{Cr}} = e_S^{\text{Cr}}(\% \text{Cr}) + r_S^{\text{Cr, Cr}}(\% \text{Cr})^2 + r_S^{\text{S, Cr}}(\% \text{S})(\% \text{Cr}) + \dots \quad 4.29$$

First order and higher order interaction coefficients of chromium upon the sulphur activity are thus derived.

The study of the temperature dependence upon, say, the first order free energy interaction coefficient e_S^{Cr} gives the first order enthalpy and entropy interaction coefficients h_S^{S} and s_S^{S} related by:

$$e_S^{\text{Cr}} = \frac{h_S^{\text{S}}}{2.3 RT} - \frac{s_S^{\text{S}}}{2.3 R} \quad 4.30$$

CHAPTER V

DISCUSSION

5.1 Thermal Diffusion

5.1.1. Effect of Thermal Diffusion

The methods of calculation described in the preceding chapter were used to derive:

- 1) <equilibrium constants> and <first order free energy interaction coefficients> for the binary system Fe-S;
- 2) first order free energy, enthalpy and entropy interaction coefficients of chromium in the ternary system Fe-S-Cr.

However, the nature of the <equilibrium> established in this work needs further discussion since thermal diffusion effects are inevitably present in a levitation-melting technique, where a cold gas mixture flows past a levitated high temperature droplet. In the gas phase surrounding the droplet a temperature gradient is created which causes the heavier molecules of the gas mixture, i. e. hydrogen sulphide, to concentrate in the cooler regions of the gas phase, thus lowering the H_2S/H_2 ratio at the gas-metal interface to an unknown extent. Hence the <apparent equilibrium constant> <K'>, derived from gas composition and droplet sulphur content are not true apparent equilibrium constants but rather steady state values, obtained under certain conditions of temperature gradient

and gas composition. Assuming that strong stirring due to the induction field gives a homogenous sulphur concentration and a uniform temperature in the levitated droplet, one may represent the droplet sulphur content, the temperature and sulphur activity profiles as shown in Fig. 17.

The same observation is valid for the < apparent equilibrium constant >, $K''>$, obtained from ternary results. However, when deriving the effect of Cr upon the sulphur activity coefficient, one uses the relationship:

$$\log f_S^{Cr} = \log K''(\%) - \log K'(\%) \quad 5.1$$

or

$$\log f_S^{Cr} = \log \frac{f_S^{\% S_{bin}}}{f_S^{\% S_{ter}}} \quad 5.2$$

also

$$\log f_S^{Cr} = \left\langle e_S^S \right\rangle (\% S_{bin} - \% S_{ter}) + \log \frac{\% S_{bin}}{\% S_{ter}} \quad 5.3$$

where $\% S_{ter}$ is the analysed sulphur content in the ternary system, and $\% S_{bin}$ the sulphur content obtained in the binary system with the same gas composition. The errors due to thermal diffusion are cancelled out provided its effect is kept constant. It follows that binary and ternary results do not constitute in themselves true thermodynamic data but their comparison gives accurate data for interaction coefficients.

5.1.2. Control of Thermal Diffusion

A brief review of the literature ⁽³⁷⁻⁴⁰⁾ shows that the degree of thermal diffusion in a gas mixture depends on

- 1) the temperature gradient in the gaseous phase and
- 2) the nature of the gas mixture.

5.1.2.1. Temperature Gradient

The temperature gradient depends upon the droplet temperature, the gas flow dynamics and the physical properties of the gas mixture. Thus for a given gas mixture, temperature, droplet size and reaction tube diameter, the temperature gradient only depends on the gas flow rate. Therefore, runs with different flow rates were carried out. As seen from Fig. 7, 8, and 9, the steady state droplet sulphur contents generally decreased with increasing flow rate. This effect is caused by enhanced thermal diffusion resulting from the increased temperature gradient with increasing flow rate. It can also be noticed that the effect of flow rate is more pronounced at higher temperatures. This study showed that the thermal diffusion effect could be minimized by using very low gas flow rates. However, the use of very low flow rates markedly increased the time required to reach a steady state and therefore flow rate 2 of 2.6 l/min. was chosen. This permitted a fast attainment of a steady state, and also did not cause insurmountable problems in levitation stability.

5.1.2.2. Nature of the Gas Mixture

Thermal diffusion in gas mixtures was described by Chapman⁽³⁷⁾ in terms of intermolecular force fields, relative molecular weights, sizes and concentrations of the gaseous components. Gillepsie's⁽³⁸⁾ theory, based solely on molecular weight, expressed the thermal diffusion ratio k_T , of the binary gas mixture of species 1 and 2:

$$k_T = \frac{d \ln x_1}{d \ln T} = \frac{x_2 (m_2 - m_1)}{2 (m_1 x_1 + m_2 x_2)} \quad 5.4$$

where x denotes mole fraction and m the square root of the molecular weight. Equation 5.4 expressed in terms of the heavier gas 1 can be written:

$$k_T = \frac{m_2 - m_1}{2 \left(m_1 \frac{x_1}{1-x_1} + m_2 \right)} \quad 5.5$$

It follows that k_T decreases with increasing content of the heavier gas 1 and hence a decrease of the thermal diffusion effect when using gas mixtures with increasing H_2S/H_2 ratio can be expected, see 5.2.2. For a multicomponent gas mixture Gillepsie derived a thermal diffusion ratio:

$$k_T = \frac{d \ln x_1}{d \ln T} = \frac{1 - m_1}{2 \sum m_i x_i} \quad 5.6$$

It follows that the use of a heavy inert carrier gas reduces the thermal diffusion effect. This has been successfully applied by Dastur and Chipman⁽⁴¹⁾. However, this method was not used in the present work because a heavy inert gas such as argon was found to decrease the rate of attainment of a steady state.

The variation of thermal diffusion with H_2S/H_2 ratio will be discussed more thoroughly in the section on ternary results, see 5.3.2.

5.2 Binary System Fe-S

5.2.1 <Apparent Equilibrium Constant> and <Self Interaction Parameter> .

Using the results of gas and sulphur analyses reported in

Tables 7, 8 and 9 the H_2S/H_2 ratio of the gas mixture was corrected for the hydrogen sulphide dissociation (see 4.1) and the < apparent equilibrium constant >, <K'> was derived. Table 17 shows the following results for 1525^o, 1600^o and 1755^oC:

1) the analysed $\frac{P_{H_2S}}{P_{H_2}}$ ratio,

2) the corrected $\frac{P_{H_2S}}{P_{H_2}}$ ratio for H_2S dissociation,

3) the mean of the analysed sulphur content,

4) the logarithm of the < apparent equilibrium constant > <K'> , using the corrected P_{H_2S}/P_{H_2} ratio,

and

5) the error in <log K'> due to the standard deviations of both gas and sulphur analysis results.

In Table 18 the same results are expressed using mole fraction and z_S as concentration variables.

No significant curvature is apparent in the plots of <log K'> versus S content, given in Fig. 18, 19, 20 and for each temperature the experimental points were fitted by a least square line with a 68% confidence limit, thus giving: (see Fig. 21)

$$\langle \log K(\%) \rangle = \langle \log K'(\%) \rangle - \langle e_S^S \rangle \cdot (\%S) \quad 5.7$$

1525° C	$\langle \log K(\%) \rangle$	=	-2.467 ± 0.015
	$\langle e_S^S \rangle$	=	-0.052 ± 0.002
1600° C	$\langle \log K(\%) \rangle$	=	-2.463 ± 0.008
	$\langle e_S^S \rangle$	=	-0.052 ± 0.002
1755° C	$\langle \log K(\%) \rangle$	=	-2.453 ± 0.014
	$\langle e_S^S \rangle$	=	-0.044 ± 0.002

The results were also processed in terms of the lattice ratio variable z:

1525° C	$\langle \log K(Z) \rangle$	=	-0.715 ± 0.014
	$\langle E_S^S \rangle$	=	-3.20 ± 0.11
1600° C	$\langle \log K(Z) \rangle$	=	-0.716 ± 0.014
	$\langle E_S^S \rangle$	=	-3.14 ± 0.12
1755° C	$\langle \log K(Z) \rangle$	=	-0.707 ± 0.008
	$\langle E_S^S \rangle$	=	-3.28 ± 0.10

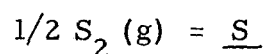
$$\langle \Theta_S^S \rangle = 2.303 \cdot \langle E_S^S \rangle \quad 5.8$$

A least square line was used to express the temperature dependence of both the $\langle \text{equilibrium constant} \rangle$, $\langle K \rangle$, and the $\langle \text{self interaction}$

coefficients (Fig. 22 and 23).

5.2.2. Discussion

It should be repeated again that the results obtained for the binary system do not give accurate thermodynamic data and have been processed for comparison purposes with ternary results only. Therefore, no attempt has been made here to give values for the free energy, enthalpy and entropy of sulphur solution into liquid iron according to the reaction 4.24



From Fig. 21, 22, 23, the effect of thermal diffusion can be observed as follows:

- 1) All values of $\langle \log K \rangle$ or $\langle \log K' \rangle$ obtained in this work are larger than those found by any other worker. This is due to the overestimation of the P_{H_2S}/P_{H_2} ratio at the gas-metal interface when using the analysed bulk gas ratio.
- 2) All values of $\langle e_S^S \rangle$ obtained in the present work are lower than those found by any other worker, thus giving steeper slopes in the plots of $\langle \log K'(\%) \rangle$ versus %S. It follows that the overestimation of the P_{H_2S}/P_{H_2} ratio and hence of $\langle \log K'(\%) \rangle$ decreases when using gas mixtures with increasing H_2S contents. This observation agrees with Gillepsie's theory reported in 5.1.2.

5.3 Ternary System Fe-S-Cr

5.3.1. Temperature Dependence of e_{S-Cr}^{Cr}

According to the method described in 4.3.2. an < apparent equilibrium constant > , $\langle K'' \rangle$, which was derived from the corrected P_{H_2S}/P_{H_2} ratio and the analysed sulphur content, was compared to the < apparent equilibrium constant > , $\langle K' \rangle$, corresponding to the same sulphur content in the binary system.

Tables 19-22 show:

- 1) the analysed S content
- 2) $\langle \log K''(\%) \rangle$
- 3) $\langle \log K'(\%) \rangle$
- 4) $\log f_S^{Cr} = \langle \log K''(\%) \rangle - \langle \log K'(\%) \rangle$ and
- 5) the corrected Cr content

for temperatures of 1525°, 1600°, 1690° and 1755°C. These results are shown in Fig. 24-28 on a weight percent and mole fraction basis. Tables 23-26 and Fig. 29, 30 show the effect of Cr on the sulphur activity coefficient on a lattice ratio basis.

Since no significant curvature was observed in the plots of $\log f_S^{Cr}$ versus %Cr or $\log \psi_S^{Cr}$ versus z_{Cr} , the experimental points were fitted by a least square line with a 95% confidence limit, passing through the origin. For the different temperatures the first order free energy interaction coefficients, e_S^{Cr} , on a weight percent basis are:

$t^{\circ}C$	e_S^{Cr}	95% Confidence Interval	Correlation Coefficient
1525	-0.0120	± 0.0004	0.997
1600	-0.0105	± 0.0005	0.996
1690	-0.0088	± 0.0007	0.985
1755	-0.0057	± 0.0005	0.983

The corresponding values on a lattice ratio basis are:

$t^{\circ}\text{C}$	θ_S^{Cr}	95% Confidence Interval	Correlation Coefficient
1525	-2.50	± 0.08	0.998
1600	-2.18	± 0.10	0.996
1690	-1.82	± 0.14	0.985
1755	-1.15	± 0.10	0.983

The relationship between e_S^{Cr} and reciprocal temperature was fitted to a least square line with a 68% confidence limit,

$$e_S^{\text{Cr}} = (94.2/T + 0.040) \quad 5.9$$

from which the first order enthalpy and entropy interaction coefficients were derived:

$$h_S^{\text{Cr}} = -430 \pm 70 \quad 5.10$$

$$s_S^{\text{Cr}} = -0.183 \pm 0.007 \quad 5.11$$

On a lattice ratio basis the temperature and concentration dependence can be expressed by:

$$E_S^{\text{Cr}} = -8365/T + 35.27 \quad 5.12$$

or

$$\theta_S^{\text{Cr}} = -19240/T + 81.11 \quad 5.13$$

5.3.2 Discussion

As shown in Fig. 29 and 31 the results of the present work agree very well with the data of Ban-ya and Chipman⁽²⁷⁾

$e_S^{Cr} = -0.0107$, at 1550°C , and disagree with those of Griffing and Healy⁽²³⁾ and Adachi and Morita⁽²⁶⁾. As shown in the tables of

5.3.1 a least square line fits the data points of the present work reasonably well in both the weight percent and lattice ratio scale. It should be noticed, that the lattice ratio scale gives no better linear relationship.

It is remarkable that the first order free energy interaction coefficients, e_S^{Cr} or θ_S^{Cr} , are valid up to Cr concentrations of 40 wt.%. It can hardly be said that the method used was insensitive to higher orders of the activity coefficient, for the data points show little scattering. The similar chemical and physical properties of iron and chromium may account for the observed constancy of the interaction coefficient e_S^{Cr} up to 40 wt.%. The experimental results lead one to think that e_S^{Cr} may stay constant for higher Cr contents and even up to pure Cr. In this respect it may be noticed that Griffing and Healy⁽²³⁾ found

$$\text{for } \%Cr = 0 \quad \log f_S^{Cr} = -0.06 \quad \text{at } 1600^\circ\text{C}$$

$$\text{for } \%Cr = 100 \quad \log f_S^{Cr} = -1.34 \quad \text{at } 1760^\circ\text{C} .$$

Disregarding the temperature difference a constant first order interaction coefficient of 0.0128 can be derived, which is similar to the values of e_S^{Cr} found in the present work.

The fact that the interaction coefficients e_S^{Cr} of Ban-ya and Chipman⁽²⁷⁾ and those of the present study are identical, leads to

the conclusion that in comparative levitation-melting studies of binary and ternary systems the effect of thermal diffusion due to a temperature gradient (5.1.2.1) can be cancelled out to a great extent by keeping the gas flow rate constant. However, the thermal diffusion effect due to a variation in gas compositions (5.1.2.2) needs further examination.

In this respect, consider Fig. 32. Let $1'$ be the value of $\langle \log K' \rangle$ obtained when levitating a pure iron sample in a given gas mixture of P_{H_2S}/P_{H_2} ratio equal to R_1 . Using the same gas mixture R_1 , the points $2''$, $3''$, $4''$ represent the values of $\langle \log K'' \rangle$ when levitating Fe-Cr samples of increasing chromium content. The corresponding $\log f_S^{Cr}$ are derived from $\langle \log K'' \rangle - \langle \log K' \rangle$ where the values of $\langle \log K' \rangle$, represented by $2'$, $3'$, $4'$, correspond to the sulphur contents S_2 , S_3 , S_4 respectively in the binary system Fe-S. Thus the ternary points $2''$, $3''$, $4''$, obtained with a gas composition R_1 are compared to the binary points $2'$, $3'$, $4'$ obtained with gas mixtures R_2 , R_3 , R_4 of increasing H_2S content for which the thermal diffusion effect is gradually attenuated according to Gillepsie's theory, see 5.1.2.2. To estimate the effect of thermal diffusion due to the variation in gas composition, the ternary values $2''$, $3''$, $4''$ need to be compared to the binary values $2'''$, $3'''$, $4'''$, which have the same thermal diffusion error as point $1'$. The ratios $\frac{2''' - 2'}{2' - 2''}$, $\frac{3''' - 3'}{3' - 3''}$ etc. measure the variation in thermal diffusion that results from a change in gas composition.

This effect was examined for the ternary runs carried out at 1525° and 1755° C, see Fig. 33. At each temperature a line was drawn through the point of 0.0% Cr. Its slope was taken to be equal to the corresponding value of e_S^S given by Ban-ya and Chipman⁽²⁷⁾, as these values were determined in the absence of thermal diffusion. For 1755° C the value of e_S^S used was obtained by extrapolation of their data. Thus the change in interaction coefficient, due to the variation of thermal

diffusion with gas composition, was found to be within the 95% confidence limit.

SUMMARY

The effect of chromium on the activity coefficient of sulphur in the ternary system Fe-S-Cr has been investigated over the temperature range 1525°C to 1755°C for chromium concentrations up to 40 weight percent, using a levitation-melting technique in H₂-H₂S atmosphere. The effect of thermal diffusion in the gas mixtures could be controlled and was cancelled out in the derivation of interaction coefficients of the ternary system Fe-S-Cr. On a weight percent basis the temperature and composition dependence of the chromium interaction is given by the relationship:

$$\log f_S^{\text{Cr}} = (-94.2/T + 0.040) (\% \text{ Cr})$$

where $e_S^{\text{Cr}} = -94.2/T + 0.040$

is the first order free energy interaction coefficient. The first order enthalpy and entropy interaction coefficients are found to be

$$h_S^{\text{Cr}} = -430 \pm 70 \text{ and}$$

$$s_S^{\text{Cr}} = -0.183 \pm 0.007 \text{ respectively}$$

In terms of concentration variable z :

$$\log \Psi_S^{\text{Cr}} = (-8365/T + 35.27) z_{\text{Cr}}$$

$$\theta_S^{\text{Cr}} = -19240/T + 81.11$$

APPENDIX I

In a non-ideal solution:

activity of i = activity coefficient of i x concentration of i

1) On a mole fraction basis

$$a_i = \gamma_i X_i \quad \text{A.1}$$

where X_i is the mole fraction.

The Taylor expansion of $\ln \gamma_i$ in a multicomponent solution of solutes 2, ..., i, j, k, \dots, m in solvent 1 gives for the reference state of infinitely dilute solution:

$$\ln \gamma_i = \sum_{j=2}^m \frac{\partial \ln \gamma_i}{\partial X_j} X_j + \sum_{j=2}^m \sum_{k=2}^m \frac{1}{2} \frac{\partial^2 \ln \gamma_i}{\partial X_j \partial X_k} X_j X_k + O(X^3) \quad \text{A.2}$$

where the derivations are to be taken for $X \rightarrow 1$.

Multiplication by RT gives the Taylor expansion of excess partial molar free energy of mixing for component i :

$$F_i^E = RT \ln \gamma_i \quad \text{A.3}$$

$$F_i^E = H_i^M - TS_i^E \quad \text{A.4}$$

where H_i^M is partial molar enthalpy of mixing and S_i^M is excess partial molar entropy of mixing. When limiting the Taylor expansion of the excess partial molar free energy of mixing to the first order

terms, one obtains:

$$F_i^E = RT \ln \gamma_i = \sum_{j=2}^m \left(\frac{\partial \ln \gamma_i}{\partial X_j} \right) X_j + O(X^2) . \quad \text{A.5}$$

$$RT \epsilon_i^j = \left(\frac{\partial F_i^E}{\partial X_j} \right)_{X_1 \rightarrow 1} = RT \left(\frac{\partial \ln \gamma_i}{\partial X_j} \right)_{X_1 \rightarrow 1} \quad \text{A.6}$$

is the first order free energy interaction coefficient of component j on the activity coefficient of component i , γ_i . ϵ_i^j is sometimes called first order self interaction parameter.

$$\eta_i^j = \left(\frac{\partial H_i^M}{\partial X_j} \right)_{X_1 \rightarrow 1} \quad \text{A.7}$$

is the first order enthalpy interaction coefficient and

$$\sigma_i^j = \left(\frac{\partial S_i^E}{\partial X_j} \right)_{X_1 \rightarrow 1} \quad \text{A.8}$$

is the first order entropy interaction coefficient. ϵ_i^j , η_i^j and σ_i^j are related by the relationship:

$$\epsilon_i^j = \frac{\eta_i^j}{RT} - \frac{\sigma_i^j}{R} \quad \text{A.9}$$

A similar formalism is derived for higher orders of the Taylor expression,

$$\text{e.g. } \rho_i^{j,k} = \frac{\partial^2 \ln \gamma_i}{\partial X_j \partial X_k} \quad \text{A.10}$$

where $\rho_i^{j,k}$ is the second order free energy interaction coefficient of both components j and k upon the activity coefficient of i.

$\rho_i^{i,i}$ would also be called second order self interaction parameter of component i.

2) On a weight percent basis

$$a_i = f_i \times (\%i) \quad \text{A. 11}$$

$\ln \gamma_i$ becomes $\log f_i$

$$F_i^E \quad " \quad \mathcal{F}_i^E$$

$$H_i^M \quad " \quad \mathcal{H}_i^M$$

$$S_i^M \quad " \quad \mathcal{S}_i^E$$

$$\epsilon_i^j \quad " \quad e_i^j = \left(\frac{\partial \log f_i}{\partial (\%j)} \right) \%1 \rightarrow 100 \quad \text{A. 12}$$

$$\eta_i^j \quad " \quad h_i^j = \left(\frac{\partial \mathcal{H}_i^M}{\partial (\%j)} \right) \%1 \rightarrow 100 \quad \text{A. 13}$$

$$\sigma_i^j \quad " \quad s_i^j = \left(\frac{\partial \mathcal{S}_i^E}{\partial (\%j)} \right) \%1 \rightarrow 100 \quad \text{A. 14}$$

$$\rho_i^{j,k} \quad " \quad r_i^{j,k}$$

Eqn. A. 8 becomes

$$e_i^j = \frac{h_i^j}{2.303 RT} - \frac{s_i^j}{2.303} \quad \text{A. 15}$$

3) Using the concentration variable z_i

$$z_i = \frac{n_i}{n_1 + \sum v_j n_j} \quad \text{A.16}$$

where n is the number of moles

$v_j = +1$ for a substitutional solute 1

$v_j = -1/b$ for an interstitial solute

and

b is the number of interstitial sites per lattice atom.

The activity of i is expressed as follows:

$$a_i = \Psi_i \times z_i \quad \text{and} \quad \text{A.17}$$

$$\ln \gamma_i \text{ becomes } \ln \Psi_i$$

$$\epsilon_i^j \text{ becomes } \theta_i^j$$

4) Conversion formulas

$$\epsilon_i^j = 230 \frac{M_j}{M_1} e_i^j + \frac{M_1 - M_j}{M_1} \quad \text{A.18}$$

$$\sigma_i^j = 100 \frac{M_j}{M_1} s_i^j - R \frac{M_1 - M_j}{M_1} \quad \text{A.19}$$

$$h_i^j = 100 \frac{M_j}{M_1} h_i^j \quad \text{A.20}$$

$$\epsilon_i^j = \theta_i^j + (1 - v_j) \quad \text{A.21}$$

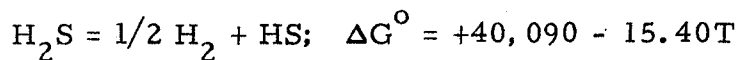
see references: 2, 8, 9, 42.

APPENDIX 2

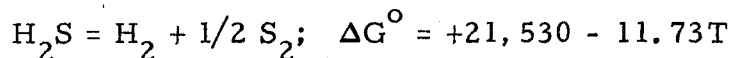
Two short computer programmes were applied to the gas analysis results to derive:

- 1) the ratio $B = \frac{\text{atoms hydrogen}}{\text{atoms sulphur}}$ of the gas mixture
- 2) the ratio $R = P_{\text{H}_2\text{S}}/P_{\text{H}_2}$ at room temperature
- 3) the corrected $P_{\text{H}_2\text{S}}/P_{\text{H}_2}$ ratio, R CORR., for H_2S dissociation at high temperature.

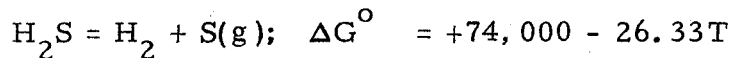
B and R were derived from calculation 1 and R CORR. from calculation 2. In the latter the following thermodynamic data^(21, 22) were used.



$$\log K_{\text{HS}} = -8763/T + 3.367$$



$$\log K_{\text{S}_2} = -4706/T + 2.564$$



$$\log K_{\text{S}} = -16,175/T + 5.760$$

1) Calculation of B and R

PROGRAM TST (INPUT,OUTPUT,TAPE5=INPUT,TAPE6=OUTPUT)

C A =NUMBER OF ML. THIOSULPHATE 0.01N USED IN THE TITRATION
 C PMB =BAROMETRIC PRESSURE IN
 C PL =PRESSURE IN ATMOSPHERE
 C TL =ROOM TEMPERATURE
 C VOLUME OF SAMPLING BULB = 136.8 ML
 C 1 ML. THIOSULPHATE CORRESPONDS TO 0.00004.G OF SULPHUR
 C B =RATIO OF HYDROGEN ATOMS AND SULPHUR ATOMS IN THE GAS
 C R = H2S/H2 RATIO

INTEGER RUN

101 FORMAT (I5,3F9.2)

102 FORMAT (1H0,16,6X,F5.2,6X,F6.1,6X,F7.3,E16.3)

2 READ (5,101) RUN,A,PMB,TL

IF (RUN.EQ.0) STOP

PL=PMB/760.0

3 AS=A*4.E-05/32.066

PH2S=AS*0.08206*TL/0.1368

PH2=PL-PH2S

R=PH2S/PH2

AH2=PH2*0.1368/(0.08206*TL)

AH=2.0*(AS+AH2)

B=AH/AS

WRITE (6,102) RUN,A,B,PL,R

GO TO 2

END

RUN	Data Input			Data Output		
	A	PMB	TL	B	PL	R
275	39.2	760.2	298.0	228.9	1.000	8.816E-03
276	38.6	759.8	298.0	232.3	1.000	8.684E-03
277	40.0	759.4	299.0	223.3	0.999	9.037E-03
278	39.4	758.6	297.0	228.0	0.996	9.029E-03
279	40.1	756.9	297.0	223.5	0.995	9.012E-03
280	40.0	756.4	297.0	223.9	0.995	9.012E-03

2) Calculation of R_{CORR} .

This has been done for the gas mixture described in calculation 1 for which $B_m = 226.7$ and $R_m = 0.008905$ by solving a system of five equations and the five unknowns X_{H_2} , X_{H_2S} , X_{HS} , X_{S_2} , X_S

```

PROGRAM TST (INPUT,OUTPUT,TAPE5=INPUT,TAPE6=OUTPUT)
C      THE DISSOCIATION IS CORRECTED FOR 1525 AND 1755 C
C      PT =MEAN BAROMETRIC PRESSURE IN ATMOSPHERES
DIMENSION TTC(30)
104 FORMAT (2F8.1)
66  FORMAT (2F8.1)
70  FORMAT (1H1,71HH2S DISSOCIATION CORRECTED PH2S/PH2 RATIO AT GIVEN
1    TEMPERATURES FOR B=    ,F6.1//)
208 FORMAT (1H--,13X,1HT,18X,4HRCOR,11X,3HXH2,11X,4HXH2S,10X,3HXHS,
211X,3HXS2,11X,2HXS,8X,4HITER )
209 FORMAT (1H ,10X,F6.0,10X,6E14.4,16  )
EPS=1.E-07
MAX=20
DO 25 I=1,2
READ (5,104) (TTC(I),I=1,2)
1 READ (5,66) B,PT
IF (B.EQ.0.0) STOP
WRITE (6,70) B
WRITE (6,208)
DO 25 I=1,2
TC=TTC(I)
T=TC+273.0
PT2=SQRT(PT)
TKHS=-8763.0/T+3.367
AKHS=10.0**TKHS
TKS2=-4706.0/T+2.564
AKS2=10.0**TKS2
TKS=-16175.0/T+5.760
AKS=10.0**TKS
ITER=1
XH2S=0.0
XHS=0.0
XS2=0.0
XS=0.0
10 BIG=0.0

```

```

C      COMPUTE XH2
      TEMP=1.0-XH2S-XHS-XS2-XS
      IF (ABS(TEMP-XH2).GT.BIG)   BIG=ABS(TEMP-XH2)
      XH2=TEMP
C      COMPUTE XH2S
      TEMP=(2.0*XH2-(B-1.0)*XHS-2.0*B*XS2-B*XS)/(B-2.0)
      IF (ABS(TEMP-XH2S).GT.BIG)   BIG=ABS(TEMP-XH2S)
      XH2S=TEMP
C      COMPUTE XHS
      TEMP=AKHS*XH2S/(PT2*SQRT(XH2))
      IF (ABS(TEMP-XHS).GT.BIG)   BIG=ABS(TEMP-XHS)
      XHS=TEMP
C      COMPUTE XS2
      TEMP=(AKS2*XH2S/(PT2*XH2))**2
      IF (ABS(TEMP-XS2).GT.BIG)   BIG=ABS(TEMP-XS2)
      XS2=TEMP
C      COMPUTE XS
      TEMP=AKS*XH2S/(PT*XH2)
      IF (ABS(TEMP-XS).GT.BIG)   BIG=ABS(TEMP-XS)
      XS=TEMP
      IF (BIG.LT.EPS) GO TO 20
      IF (ITER.GE.MAX) GO TO 20
      ITER=ITER+1
      GO TO 10
20 RCOR=XH2S/XH2
   WRITE (6,209) TC,RCOR,XH2,XH2S,XHS,XS2,XS,ITER
25 CONTINUE
   GO TO 1
   END
'      6400 END OF RECORD
1525.0  1755.0
226.7   0.998
0.0

```

Data Output

	1525°C	1755°C
$(P_{H_2S}/P_{H_2})_{CORR.}$	8.513E-03	7.633E-03
X_{H_2}	9.912E-01	9.914E-01
X_{H_2S}	8.438E-01	7.568E-03
X_{HS}	2.639E-04	8.450E-04
X_{S_2}	5.668E-05	1.788E-04
X_S	4.943E-06	4.644E-05
	AFTER 7 ITERATIONS	AFTER 10 ITERATIONS

REFERENCES

1. J. Chipman: Discussions, Faraday Soc. 1948, No. 4, 23-49.
2. C. Wagner: Thermodynamics of Alloys, Addison Wesley Publ. Company, Reading, Mass., 1952, 53.
3. R.P. Smith: J. Am. Chem. Soc., 1946, 68, 1163-75.
4. L.S. Darken and R.P. Smith: J. Am. Chem. Soc., 1946, 68, 1172-75.
5. J. Chipman, Trans. AIME, 1967, 239, 1332-1336.
6. L.S. Darken and R.W. Gurry: Physical Chemistry of Metals, McGraw-Hill Book Company, Inc., 1953.
7. J. Chipman, J. Iron and Steel Inst., 180, 97 (1955).
8. C.H.P. Lupis and J.F. Elliott, Trans. AIME, 1965, 233, 829-830.
9. C.H.P. Lupis and J.F. Elliott, Acta. Met. 1966, 14, 529-538.
10. J. Chipman and Ta Li, Trans. ASM, 1937, 25, 435.
11. E. Maurer, G. Hammer and H. Mobius, Arch. Eisenhüttenw, 1942, 16, 159.
12. J. White and H. Skelly, J. Iron and Steel Inst. 1947, 155, 201.
13. J.A. Kitchener, J. O' M. Bockris and A. Liberman, Discussions, Faraday Soc., No. 4, 1948, 49-59.
14. J.P. Morris and A.J. Williams, Trans. ASM, 1949, 41, 1425-1439.
15. C.W. Sherman, H.I. Elvander and J. Chipman, Trans. AIME, 1950, 188, 334-340.
16. J.A. Cordier and J. Chipman, Trans. TMS-AIME, 1955, 202, 905-907.

17. A. Adachi and Z. Morita, Techn. Reports Osaka University, 1958, 8, 385-394.
18. C. Yoshii and K. Sasaki, Japan Soc. Sci. Promotion 19th Tech. Com. Rept., 1966, 8131-8206.
19. T. Fuwa, S. Ban-ya and K. Yoshida, Japan Soc. Sci. Promotion 19th Tech. Com. Rept., 1966, 8130-8205.
20. S. Ban-ya and J. Chipman, Trans. AIME, 1968, 242, 940-946.
21. Nat. Bur. St. (U.S.) Tech. Note No. 270-1, 1965.
22. K.K. Kelley, U.S. Bur. Mines, Bull. No. 584, 1960.
23. N.R. Griffing and G.W. Healy, Trans. AIME, 1960, 218, 849-854.
24. J.F. Elliott et al: Thermochemistry for Steelmaking, Vol. II, Addison-Wesley Publish. Co. Inc. 1963, 368.
25. R. Vogel and R. Reinbach, Archiv. Eisenhüttenw., 1938, 11, 457.
26. A. Adachi, Z. Morita, Techn. Rept. Osaka University, 1963, 13, No. 551, 131-7.
27. S. Ban-ya, J. Chipman, Trans. AIME, 1969, 245, 133-143.
28. P. Kershaw, Ph.D. thesis, 1968, McMaster University.
29. A.E. Jenkins et al: Symposium on Metallurgy at High Press. and High Temp. AIME Conf., 1963, 22, 23-43.
30. F.C. Larche, M.Sc. Thesis, 1968, McMaster University.
31. A. McLean, J. Met. Club, University of Strathclyde, 1966, 18, 37.
32. J.F. Elliott et al: Thermochemistry for Steelmaking, Vol. II, Addison-Wesley Publishing Co., Inc., 1963, 634.
33. NBS Misc. Publ., 260, 1968.

34. Industrial Method, Styria Steel, Austria.
35. J. A. Kitchener, A. Liberman and D. A. Sprott, *Analyst*, 1951, 76, 509-516.
36. J. F. Elliott et al: *Thermochemistry for Steelmaking*, Vol. II, Addison-Wesley Publishing Co. Inc., 1963, 264.
37. S. Chapman, *Phil. Trans. Roy Soc. A.*, 1916, 216, 279, 1917, 217, 115.
38. L. J. Gillepsie, *J. Chem. Phys.*, 1939, 7, 530.
39. J. O. Hirschfelder, C. F. Curtiss and R. B. Bird: *Molecular Theory of Gases and Liquids*, John Wiley and Sons, Inc. New York, 1954.
40. R. D. Present: *Kinetic Theory of Gases*, McGraw-Hill Book Company Inc., New York, Toronto, London, 1958.
41. M. N. Dastur and J. Chipman: *Discussions of the Faraday Society*, Butterworths, London, 1961, 100-108.
42. J. F. Elliott: *Thermodynamic Aspects of Vacuum Metallurgy*, Le Vide, France, 1968.

Table 1. Comparison of Systems Used for Expressing Concentrations, Activities and Interaction Coefficients

Type	I Practical	II Atom Fraction	III Quadratic	IV Atom Ratio	V Interstitial
		Binary Solutions			
a. Concentration	$(\%2) = \frac{100 w_2}{w_1 + w_2}$	$x_2 = \frac{n_2}{n_1 + n_2}$	$x_2 = \frac{n_2}{n_1 + n_2}$	$y_2 = \frac{n_2}{n_1}$	$z_2 = \frac{n_2}{n_1 - n_2/b}$
b. Activity Coefficient	$f_2 = a_2/(\%2)$	$y_2 = a_2/x_2$	$y_2 = a_2/x_2$	$\varphi_2 = a_2/y_2$	$\Psi_2 = a_2/z_2$
c. Deviation Coefficient	$e_2^2 = \frac{d \log f_2}{d(\%2)}$	$\epsilon_2^2 = \frac{d \ln \gamma_2}{dx_2}$	$a_{12} = \frac{d \ln \gamma_2}{d(1 - x_2)^2}$	$\zeta_2^2 = \frac{d \ln \varphi_2}{dy_2}$	$\theta_2^2 = \frac{d \ln \Psi_2}{dz_2}$
		Multicomponent Solutions			
d. Concentration	$(\%2) = \frac{100w_2}{\Sigma w_i}$	$x_2 = \frac{n_2}{\Sigma n_i}$	$x_2 = \frac{n_2}{\Sigma n_i}$	$y_2 = \frac{n_2}{n_1}$ or $y'_2 = \frac{n_2}{n_1 + n_3}$	$z_2 = \frac{n_2}{n_1 + \Sigma v_j n_j}$
e. Interaction Coefficient	$e_2^j = \frac{\partial \log f_2}{\partial (\%_j)}$	$\epsilon_2^j = \frac{\partial \ln \gamma_2}{\partial x_j}$	-	$\zeta_2^j = \frac{\partial \ln \varphi_2}{\partial y_j}$	$\theta_2^j = \frac{\partial \ln \Psi_2}{\partial z_j}$

Derivatives are to be taken at infinite dilution. w_i signifies the mass, n_i the number of moles of any component including 1, the solvent, and 2, j, k, solutes. b is the number of interstitial sites per lattice atom. For a substitutional solute $v_j = 1$, for interstitial $v_j = -1/b$.

TABLE 2
 ATTAINMENT OF <EQUILIBRIUM> AT 1600°C

EFFECT OF FLOW RATE

1600°C

$$P_{H_2S}/P_{H_2} = 0.00156 \pm 0.00002$$

	FLOW 1 0.9 l/min.	FLOW 2 2.6 l/min.	FLOW 3 5.1 l/min.
TIME	wt. %S	wt. %S	wt. %S
0.5	0.034	0.074	0.107
1	0.078	0.122	0.150
2	0.136	0.211	0.241
3	0.194	0.276	0.306
4	0.239	0.317	0.339
5	0.278	0.347	0.364
6	0.301	0.381	0.382
8	0.345	0.409	0.396
10	0.352	0.422	0.415
10		0.414	
12.5		0.442	0.408
15	0.424	0.439	0.400
17.5		0.447	
20		0.438	
25		0.441	
30		0.441	
40		0.439	

SEE ALSO FIG. 7

TABLE 3
 ATTAINMENT OF <EQUILIBRIUM> AT 1755° C
 EFFECT OF FLOW RATE
 1755° C

$$P_{H_2S}/P_{H_2} = 0.00148 \pm 0.00006$$

	FLOW 1 0.9 l/min.	FLOW 2 2.6 l/min.	FLOW 3 5.1 l/min.
TIME min.	wt. %S	wt. %S	wt. %S
0.5	0.029	0.079	0.076
1	0.066	0.122	
1.5			0.188
2	0.121	0.216	
3	0.184	0.262	
4	0.222	0.307	0.306
5	0.255	0.323	
6	0.293	0.336	0.322
8	0.328	0.349	
10	0.345	0.353	0.334
12.5	0.363	0.366	
15	0.380	0.359	

SEE ALSO FIG. 8

TABLE 4

ATTAINMENT OF <EQUILIBRIUM> AT 1755°C

EFFECT OF FLOW RATE

1755°C

$$P_{\text{H}_2\text{S}}/P_{\text{H}_2} = 0.00895 \pm 0.00011$$

	FLOW 1 0.9 l/min	FLOW 2 2.6 l/min
TIME min.	wt. %S	wt. %S
0.5	0.167	0.422
1	0.440	0.746
2	0.864	1.27
3	1.18	1.63
4	1.40	1.95
5	1.62	2.19
5		2.20
6	1.89	2.36
8	2.18	2.60
10	2.44	2.67
10		2.70
12.5	2.54	2.76
15		2.83
15	2.62	2.85
17.5	2.75	2.86
20	2.69	2.94
25	2.70	
30	2.70	
40	2.80	
50	2.90	

SEE ALSO FIG. 9

TABLE 5

ATTAINMENT OF <EQUILIBRIUM>

FOR VERY LOW AND LOW VALUES OF

$$P_{\text{H}_2\text{S}}/P_{\text{H}_2}$$

EFFECT OF TEMPERATURE

TIME min.	$P_{\text{H}_2\text{S}}/P_{\text{H}_2} = 0.00090$		$P_{\text{H}_2\text{S}}/P_{\text{H}_2} = 0.00184$	
	1590°C	1755°C	1590°C	1755°C
	wt. %S	wt. %S	wt. %S	wt. %S
3				0.413
5	0.226		0.446	0.449
7.5	0.245	0.232	0.512	0.460
10	0.255	0.235	0.531	0.477
12.5	0.262	0.243	0.548	0.471
15	0.263	0.259	0.532	0.471
17.5	0.265	0.235	0.532	0.473
20	0.265	0.238	0.540	0.479
25	0.261	0.237	0.540	0.486
30	0.263	0.229	0.528	0.475
40	0.265	0.243	0.542	0.473
50	0.264		0.532	

SEE ALSO FIG. 10 AND 11

TABLE 6

ATTAINMENT OF <EQUILIBRIUM>
 FOR MEDIUM, HIGH AND VERY HIGH VALUES OF
 $\frac{P_{H_2S}}{P_{H_2}}$
 EFFECT OF TEMPERATURE

	$\frac{P_{H_2S}}{P_{H_2}} =$ 0.00501 0.00472		$\frac{P_{H_2S}}{P_{H_2}} =$ 0.00894		$\frac{P_{H_2S}}{P_{H_2}} =$ 0.01405	
	1590°C	1755°C	1590°C	1755°C	1590°C	1755°C
TIME min.	wt. %S	wt. %S	wt. %S	wt. %S	wt. %S	wt. %S
0.5			0.429			
1			0.825			
2			1.36		4.71	
3			1.79			3.43
4			2.12			
5	1.48	1.25				4.06
6			2.65			
7.5	1.62	1.38			5.64	4.88
8			2.99			
10	1.66	1.45	3.26	2.74	5.98	4.95
12.5	1.72	1.43	3.41		6.91	5.47
15	1.76	1.43	3.55		7.80	5.76
15						5.76
17.5	1.77	1.43	3.61	2.90	8.20	5.99
20	1.73	1.48	3.84		8.27	6.25
25	1.76	1.47	3.81		9.16	6.53
30	1.67	1.48	3.76		9.53	6.72
35	1.72				10.8	
40	1.72	1.47			11.1	6.58
45			3.76			
50	1.78				12.4	
60	1.71		3.93		12.6	
75			3.79			

SEE ALSO FIG. 12, 13 AND 14

TABLE 7

<EQUILIBRIUM> RESULTS AT 1525°C

RUN	(a) DROPLET ANALYSIS				(b) GAS ANALYSIS				
	(%S) _m	N	S	RSD	B _m	R _m x1000	N	S x1000	RSD
10106	0.581	6	0.023	3.9	1096	1.83	13	0.05	2.7
10205	0.646	5	0.013	2.0	984	2.04	6	0.07	3.4
10305	0.819	5	0.008	1.0	777	2.58	9	0.05	1.9
10404	3.96	4	0.06	1.4	221	9.15	5	0.17	1.9
10505	2.63	5	0.04	1.6	290	6.95	3	0.08	1.2
10605	0.633	5	0.009	1.4	902	2.22	3	0.07	2.9
10701	4.76	1			215	9.38	1		
10804	2.52	4	0.05	2.1	296	6.81	6	0.13	1.9
10904	2.410	4	0.002	0.1	314	6.42	2	0.03	0.5
11004	4.24	4	0.08	1.8	226	8.92	4	0.12	1.3

TABLE 8

<EQUILIBRIUM> RESULTS AT 1600°C

RUN	(a) DROPLET ANALYSIS				(b) GAS ANALYSIS				
	(%S) _m	N	S	RSD	B _m	R _m x1000	N	S x1000	RSD
20110*	1.73	10	0.03	1.7	401	5.01	5	0.14	2.8
20207	0.264	7	0.002	0.8	2237	0.90	7	0.03	3.0
20309*	0.536	9	0.006	1.1	1085	1.84	5	0.08	4.0
20406*	3.81	6	0.06	1.7	227	8.94	5	0.03	0.3
20507	0.441	7	0.003	0.7	1287	1.56	7	0.02	1.3
20603	0.633	3	0.003	0.5	932	2.12	10	0.13	6.1
20708	1.25	8	0.01	0.9	503	3.99	4	0.03	0.8
20809	2.88	9	0.04	1.5	264	7.64	4	0.08	1.0

* RUNS CARRIED OUT AT 1590 C

TABLE 9

<EQUILIBRIUM> RESULTS AT 1755°C

RUN	(a) DROPLET ANALYSIS				(b) GAS ANALYSIS				
	(%S) _m	N	S	RSD	B _m	R _m x1000	N	S x1000	RSD
40108	0.476	8	0.005	1.0	1085	1.84	5	0.08	4.1
40208	0.240	8	0.009	3.7	2237	0.90	7	0.03	3.0
40303	1.430	3	0.002	0.1	426	4.72	4	0.09	2.1
40403	6.61	3	0.10	1.5	144	14.05	9	0.15	1.1
40503	0.355	3	0.002	0.6	1549	1.30	10	0.06	4.6
40602	2.82	2	0.12	4.1	227	8.94	5	0.03	0.3
40704	0.367	4	0.009	2.4	1354	1.48	3	0.06	4.1
40805	2.86	5	0.07	2.5	224	9.00	2	0.26	2.9
40905	0.908	5	0.007	0.8	598	3.36	2	0.01	0.3
41005	2.26	5	0.04	1.8	271	7.44	3	0.08	1.1

TABLE 10
CHROMIUM CONTENT OF IRON-CHROMIUM ALLOYS

MELT	ANALYSIS (wt. %Cr)				
	A 1	A 2	A 3	A 4	MRD
1	1.99	1.97	2.00		0.8
2	2.00	1.97	1.94		1.5
3	4.18	4.93	4.85	4.78	7.5
4	4.93	4.89	4.91	5.05	1.6
5	9.87	9.74		9.74	0.7
6	9.92	9.59	9.96	9.98	1.9
7		14.9		14.9	0.0
8		14.9		14.8	0.4
9	19.8		19.5	19.7	0.8
10	19.8	19.7	19.8		0.3
11		19.5			
12	24.6	24.3		24.6	0.6
13	24.3	24.4		24.5	0.4
14	29.2	29.2	29.5		0.5
15	29.4	29.4	29.6		0.4
16	32.4	32.4	32.6		0.3
17	34.8	34.4	34.6		0.6
18	39.8	39.4	39.3		0.7
19	41.4	41.3	41.3		0.2
20	39.2	38.3	39.7		1.8

TABLE 11

CHROMIUM LOSS DURING LEVITATION

EFFECT OF TEMPERATURE

	RUN	wt. %Cr INIT.	TIME	wt. %Cr FIN.	CHROMIUM LOSS	
1590°C FLOW OF HYD. 2.6 l/min.	734	34.6	15	34.1	0.60	
	733	34.6	30	34.1		
	732	34.6	45	33.7		
	729	24.6	15	24.4	0.74	
	730	24.6	30	24.2		
	731	24.6	45	23.7		
	726	14.9	15	14.7	0.78	
	727	14.9	30	14.6		
	728	14.9	45	14.4		
Cr LOSS IN % OF INIT. CONTENT PER 10 MINUTES:					0.74	
1755°C FLOW OF HYD. 2.6 l/min.	720	34.6	18	32.5	3.2	
	721	34.6	30	32.0		
	724	24.6	15	23.7	2.9	
	725	24.6	30	22.7		
	722	14.9	15	14.3	3.4	
	723	14.9	30	13.5		
	Cr LOSS IN % OF INIT. CONTENT PER 10 MINUTES:					2.9

SEE ALSO FIG. 15 AND 16

TABLE 12

 ATTAINMENT OF <EQUILIBRIUM>
 IN IRON-CHROMIUM ALLOYS

	RUN	wt. %Cr	TIME	wt. %S
1525°C $P_{H_2S}/P_{H_2} =$ 0.00204	807	41.3	45	2.39
	804	41.3	50	2.41
	808*	41.3	60	2.55
	809	41.3	75	2.37
1600°C $P_{H_2S}/P_{H_2} =$ 0.00212	965	39.3	30	1.86
	961	39.4	45	1.90
	962	39.4	60	1.93
	963	39.3	75	1.89
	964	39.3	90	1.82
1690°C $P_{H_2S}/P_{H_2} =$ 0.00299	1006	39.3	20	1.68
	1007	39.3	30	1.76
	1008	39.3	40	1.97
	1010	32.4	30	1.68
	1011	32.4	45	1.56
	1012	32.4	60	1.44
1755°C $P_{H_2S}/P_{H_2} =$ 0.00130	711	41.3	12.5	0.592
	712	41.3	15	0.586
	713	41.3	20	0.611
	714	41.3	25	0.608
	715	34.4	12.5	0.503
	716	34.4	15	0.505
	717	34.4	20	0.519
	718	34.4	25	0.515

*RUN AT 1515 C

TABLE 13

TERNARY SYSTEM

IRON - SULPHUR - CHROMIUM

<EQUILIBRIUM> RESULTS AT 1525°C

RUN	wt. %S	wt. %Cr INIT.	TIME min.	wt. %Cr FIN.
824	0.783	1.96	45	1.92
825	0.788	1.96	35	1.93
823	0.583	1.98	40	1.90
820	0.644	4.90	45	4.81
821	0.659	4.90	45	4.81
822	0.665	4.90	45	4.81
827	1.02	9.74	50	9.54
828	1.01	9.74	60	9.50
829	1.03	9.74	50	9.54
816	0.897	14.9	50	14.6
817	0.886	14.9	50	14.6
818	0.898	14.9	50	14.6
833	1.42	19.5	50	19.1
834	1.42	19.5	50	19.1
814	1.19	24.6	50	24.1
815	1.23	24.6	50	24.1
830	2.03	29.5	60	28.8
831	2.05	29.5	60	28.8
832	2.08	29.5	50	28.9
810	1.70	34.6	55	33.8
811	1.73	34.6	55	33.8
812	1.68	34.6	60	33.7
813	1.21	34.6	50	24.1
804	2.19	41.3	50	40.5
807	2.17	41.3	45	40.5
808	2.31	41.3	60	40.3
809	2.16	41.3	75	40.0

TABLE 14

TERNARY SYSTEM

IRON - SULPHUR - CHROMIUM

<EQUILIBRIUM> RESULTS AT 1600°C

RUN	wt. %S	wt. %Cr INIT.	TIME min.	wt. %Cr FIN.
975	0.595	1.96	30	1.91
976	0.582	1.96	40	1.90
977	0.589	1.96	40	1.90
973	0.651	4.90	45	4.72
974	0.647	4.90	45	4.72
978	0.739	9.75	50	9.36
980	0.721	9.75	50	9.36
981	0.732	9.75	50	9.36
971	0.838	14.9	50	14.3
972	0.845	14.9	50	14.3
982	0.920	19.7	60	18.8
983	0.888	19.7	60	18.8
968	1.03	24.4	60	23.2
969	1.05	24.4	60	23.2
966	1.25	32.5	60	30.9
967	1.27	32.5	60	30.9
963	1.72	39.3	75	36.9
964	1.66	39.3	90	36.5
961	1.73	39.4	45	37.9
962	1.75	39.4	60	37.5

TABLE 15

TERNARY SYSTEM

IRON - SULPHUR - CHROMIUM

<EQUILIBRIUM> RESULTS AT 1690°C

RUN	wt. %S	wt. %Cr INIT.	TIME min.	wt. %Cr FIN.
1024	0.785	1.96	25	1.87
1025	0.791	1.96	25	1.87
1033	0.784	1.94	20	1.87
1022	0.864	4.92	30	4.66
1023	0.870	4.92	30	4.66
1032	0.874	4.92	25	4.71
1020	0.984	9.75	30	9.24
1021	0.928	9.75	30	9.24
1031	0.983	9.78	25	9.34
1018	1.11	14.9	30	14.1
1019	1.10	14.9	30	14.1
1030	1.06	14.9	40	13.8
1016	1.22	19.7	30	18.7
1017	1.20	19.7	30	18.7
1029	1.20	19.7	40	18.4
1013	1.34	24.4	30	23.1
1014	1.29	24.4	40	22.7
1028	1.28	24.4	40	22.7
1010	1.53	32.5	30	30.8
1011	1.42	32.5	45	30.0
1012	1.31	32.5	60	29.1
1008	1.79	39.3	40	36.6

TABLE 16

TERNARY SYSTEM

IRON - SULPHUR - CHROMIUM

<EQUILIBRIUM> RESULTS AT 1755°C

RUN	wt. %S	wt. %Cr INIT.	TIME min.	wt. %Cr FIN.
680	0.333	1.98	12.5	1.91
684	0.333	1.98	12.5	1.91
685	0.346	1.98	17.5	1.88
686	0.321	1.98	20.5	1.86
687	0.352	4.82	12.5	4.65
688	0.353	4.82	15	4.61
689	0.356	4.82	17.5	4.58
690	0.364	4.82	20	4.54
693	0.390	9.74	17.5	9.25
694	0.380	9.74	20	9.18
697	0.388	14.9	17.5	14.2
698	0.396	14.9	20	14.1
701	0.425	19.6	17.5	18.6
702	0.415	19.6	20	18.5
705	0.441	24.5	17.5	23.3
706	0.440	24.5	20	23.1
709	0.481	29.2	17.5	27.7
710	0.475	29.2	20	27.5
717	0.472	34.5	20	32.5
718	0.468	34.5	25	32.0
713	0.555	41.3	20	38.9
714	0.553	41.3	25	38.3

TABLE 17
 BINARY SYSTEM
 TEMPERATURE DEPENDENCE OF
 LOG K' (%)

RUN	P_{H_2S}/P_{H_2} ANAL.	P_{H_2S}/P_{H_2} CORR.	wt. %S	$\langle \text{LOG K}' (\%) \rangle$	$\Delta \text{LOG K}'$ in %
----- 1525 C -----					
10106	1.83	1.77	.581	-2.517	2.9
10205	2.04	1.97	.646	-2.516	2.4
10305	2.58	2.49	.819	-2.517	1.3
10404	9.15	8.75	3.96	-2.656	1.5
10505	6.95	6.67	2.63	-2.595	1.2
10605	2.22	2.15	.634	-2.470	1.9
10701	9.38	8.97	4.76	-2.725	
10804	6.81	6.53	2.52	-2.586	1.7
10904	6.42	6.16	2.41	-2.592	0.2
11004	8.92	8.53	4.24	-2.697	1.4
----- 1600 C -----					
20110	5.01	4.73	1.73	-2.564	2.0
20207	0.90	.85	.264	-2.491	1.6
20309	1.84	1.76	.537	-2.485	2.3
20406	8.94	8.33	3.81	-2.660	1.4
20507	1.56	1.47	.441	-2.476	0.9
20603	2.12	2.04	.632	-2.492	2.9
20708	3.99	3.76	1.25	-2.522	0.7
20809	7.64	7.13	2.88	-2.606	1.1
----- 1755 C -----					
40108	1.84	1.64	.475	-2.462	2.2
40208	0.90	.80	.240	-2.478	2.9
40303	4.72	4.13	1.43	-2.540	0.8
40403	14.05	11.8	6.61	-2.74	
40503	1.30	1.15	.354	-2.489	2.2
40602	8.94	7.63	2.82	-2.568	2.5
40704	1.48	1.31	.367	-2.446	2.8
40805	9.00	7.72	2.86	-2.569	2.3
40905	3.36	2.95	.909	-2.488	0.5
41005	7.44	6.42	2.26	-2.546	1.2

SEE ALSO FIG. 18, 19, 20, AND 21

TABLE 18

BINARY SYSTEM

TEMPERATURE DEPENDENCE OF
<LOG K'(X)> AND <LOG K'(Z)>

RUN	P_{H_2S}/P_{H_2} CORR.	x_S	<LOG K'(X)>	z_S	<LOG K'(Z)>
----- 1525 C -----					
10106	1.77	.0101	-.756	.0103	-.765
10205	1.97	.0112	-.755	.0114	-.765
10305	2.49	.0142	-.755	.0146	-.768
10404	8.75	.0670	-.884	.0774	-.947
10505	6.67	.0449	-.828	.0493	-.869
10605	2.15	.0110	-.709	.0112	-.719
10701	8.97	.0801	-.951	.0953	-1.027
10804	6.53	.0431	-.819	.0472	-.858
10904	6.16	.0412	-.825	.0449	-.863
11004	8.53	.0717	-.924	.0836	-.991
----- 1600 C -----					
20110	4.73	.0298	-.799	.0317	-.826
20207	.85	.0046	-.731	.0046	-.735
20309	1.76	.0093	-.724	.0095	-.732
20406	8.33	.0646	-.889	.0742	-.949
20507	1.47	.0077	-.716	.0078	-.722
20603	2.04	.0110	-.731	.0112	-.740
20708	3.76	.0216	-.758	.0226	-.778
20809	7.13	.0491	-.838	.0545	-.883
----- 1755 C -----					
40108	1.64	.0082	-.702	.0084	-.709
40208	.80	.0042	-.718	.0042	-.722
40303	4.13	.0247	-.777	.0259	-.799
40403	11.77	.1098	-.970	.1406	-1.077
40503	1.15	.0062	-.728	.0062	-.734
40602	7.63	.0481	-.800	.0533	-.844
40704	1.31	.0064	-.686	.0065	-.692
40805	7.72	.0488	-.801	.0540	-.845
40905	2.95	.0157	-.726	.0162	-.740
41005	6.42	.0387	-.780	.0420	-.815

TABLE 19

 TERNARY SYSTEM
 IRON - SULPHUR - CHROMIUM

 EFFECT OF CHROMIUM ON THE
 ACTIVITY COEFFICIENT OF SULPHUR AT

1525°C

$$\left(\frac{P_{H_2S}}{P_{H_2}} \right) = 0.00204 \quad \text{OR}$$

$$CORR. 0.00253$$

WEIGHT PERCENT SCALE

RUN	wt. %S	<LOG K'>	<LOG K'>	LOG f _S ^{Cr}	wt. %Cr CORR.
824*	.861	-2.532	-2.513	-.019	1.92
825*	.867	-2.535	-2.513	-.022	1.93
823	.641	-2.498	-2.501	.003	1.90
820	.708	-2.541	-2.505	-.037	4.81
821	.725	-2.551	-2.506	-.046	4.81
822	.731	-2.555	-2.506	-.049	4.81
827*	1.12	-2.646	-2.526	-.120	9.54
828*	1.11	-2.643	-2.526	-.117	9.50
829*	1.14	-2.652	-2.527	-.125	9.54
816	.987	-2.685	-2.519	-.166	14.6
817	.975	-2.680	-2.519	-.161	14.6
818	.988	-2.686	-2.519	-.166	14.6
833*	1.57	-2.791	-2.550	-.241	19.1
834*	1.57	-2.792	-2.550	-.242	19.1
814	1.31	-2.810	-2.537	-.273	24.1
815	1.36	-2.824	-2.539	-.285	24.1
830*	2.23	-2.946	-2.585	-.361	28.8
831*	2.25	-2.950	-2.586	-.364	28.8
832*	2.29	-2.956	-2.588	-.368	28.9
810	1.87	-2.963	-2.566	-.397	33.8
811	1.90	-2.970	-2.567	-.402	33.8
812	1.84	-2.957	-2.565	-.392	33.7
813	1.33	-2.816	-2.538	-.278	24.1
804	2.41	-3.073	-2.594	-.478	40.5
807	2.39	-3.069	-2.593	-.476	40.5
808	2.55	-3.097	-2.602	-.495	40.3
809	2.37	-3.066	-2.592	-.474	40.0

SEE ALSO FIG. 24

 * Runs carried out with $\left(\frac{P_{H_2S}}{P_{H_2}} \right) CORR. = 0.00253$

TABLE 20

TERNARY SYSTEM
IRON - SULPHUR - CHROMIUM

EFFECT OF CHROMIUM ON THE
ACTIVITY COEFFICIENT OF SULPHUR AT

1600°C

$$(P_{H_2S}/P_{H_2})_{CORR.} = 0.00203$$

WEIGHT PERCENT SCALE

RUN	wt. %S	<LOG K'>	<LOG K'>	LOG f _S ^{Cr}	wt. %Cr CORR.
975	.654	-2.509	-2.495	-.013	1.91
976	.640	-2.499	-2.494	-.005	1.90
977	.648	-2.504	-2.495	-.009	1.90
973	.716	-2.548	-2.498	-.049	4.72
974	.712	-2.545	-2.498	-.047	4.72
978	.813	-2.603	-2.503	-.100	9.36
980	.793	-2.592	-2.502	-.090	9.36
981	.805	-2.599	-2.503	-.096	9.36
971	.922	-2.657	-2.508	-.149	14.3
972	.929	-2.661	-2.509	-.152	14.3
982	1.01	-2.698	-2.513	-.185	18.8
983	.977	-2.682	-2.511	-.171	18.8
968	1.14	-2.748	-2.519	-.229	23.2
969	1.15	-2.754	-2.520	-.234	23.2
966	1.38	-2.832	-2.531	-.301	30.9
967	1.40	-2.837	-2.532	-.305	30.9
963	1.89	-2.968	-2.556	-.412	36.9
964	1.82	-2.953	-2.553	-.400	36.5
961	1.90	-2.972	-2.557	-.415	37.9
962	1.93	-2.978	-2.558	-.419	37.5

SEE ALSO FIG. 25

TABLE 21

TERNARY SYSTEM
IRON - SULPHUR - CHROMIUM

EFFECT OF CHROMIUM ON THE
ACTIVITY COEFFICIENT OF SULPHUR AT

1690°C

$$\left(\frac{P_{H_2S}}{P_{H_2}}\right)_{CORR.} = 0.00267$$

WEIGHT PERCENT SCALE

RUN	wt. %S	<LOG K'>	<LOG K'>	LOG f _S ^{Cr}	wt. %Cr CORR.
1024	.863	-2.510	-2.497	-.013	1.87
1025	.870	-2.513	-2.497	-.016	1.87
1033	.862	-2.510	-2.497	-.013	1.87
1022	.950	-2.552	-2.501	-.051	4.66
1023	.957	-2.555	-2.501	-.054	4.66
1032	.961	-2.557	-2.502	-.055	4.71
1020	1.08	-2.608	-2.507	-.101	9.24
1021	1.02	-2.583	-2.504	-.079	9.24
1031	1.08	-2.608	-2.507	-.101	9.34
1018	1.23	-2.664	-2.514	-.150	14.1
1019	1.21	-2.656	-2.513	-.143	14.1
1030	1.16	-2.640	-2.511	-.129	13.8
1016	1.35	-2.703	-2.519	-.183	18.7
1017	1.32	-2.695	-2.518	-.177	18.7
1029	1.31	-2.693	-2.518	-.175	18.4
1013	1.48	-2.743	-2.526	-.218	23.1
1014	1.42	-2.725	-2.523	-.202	22.6
1028	1.41	-2.723	-2.522	-.200	22.7
1010	1.68	-2.800	-2.535	-.265	30.7
1011	1.56	-2.768	-2.530	-.238	29.9
1012	1.44	-2.733	-2.524	-.209	29.1
1008	1.97	-2.869	-2.549	-.320	36.6

SEE ALSO FIG. 26

TABLE 22

 TERNARY SYSTEM
 IRON - SULPHUR - CHROMIUM

 EFFECT OF CHROMIUM ON THE
 ACTIVITY COEFFICIENT OF SULPHUR AT

1755°C

$$(P_{H_2S}/P_{H_2})_{CORR.} = 0.00120$$

WEIGHT PERCENT SCALE

RUN	wt. %S	<LOG K'>	<LOG K'>	LOG f_S^{Cr}	wt. %Cr CORR.
680	.366	-2.484	-2.469	-.014	1.91
684	.366	-2.484	-2.469	-.014	1.91
685	.381	-2.500	-2.470	-.030	1.88
686	.353	-2.468	-2.469	.001	1.86
687	.387	-2.508	-2.470	-.037	4.65
688	.388	-2.509	-2.470	-.039	4.61
689	.392	-2.513	-2.471	-.042	4.58
690	.400	-2.522	-2.471	-.051	4.54
693	.429	-2.552	-2.472	-.080	9.25
694	.418	-2.541	-2.472	-.069	9.18
697	.427	-2.550	-2.472	-.078	14.2
698	.436	-2.559	-2.473	-.086	14.1
701	.467	-2.590	-2.474	-.116	18.6
702	.456	-2.579	-2.474	-.106	18.5
705	.485	-2.606	-2.475	-.131	23.3
706	.484	-2.605	-2.475	-.130	23.1
709	.529	-2.643	-2.477	-.167	27.7
710	.522	-2.638	-2.476	-.162	27.5
717	.519	-2.635	-2.476	-.159	32.5
718	.515	-2.632	-2.476	-.155	32.0
713	.610	-2.706	-2.480	-.225	38.9
714	.608	-2.704	-2.480	-.224	38.3

SEE ALSO FIG. 27

TABLE 23

TERNARY SYSTEM
IRON - SULPHUR - CHROMIUM

EFFECT OF CHROMIUM ON THE
ACTIVITY COEFFICIENT OF SULPHUR AT

1525°C

$$(P_{H_2S}/P_{H_2}) \text{ CORR.} = 0.00204 \quad \text{OR} \\ 0.00253$$

LATTICE RATIO SCALE

RUN	wt. %S	Z _S	<LOG K' ¹ >	<LOG K'>	LOG Ψ _S ^{Cr}	Z _{Cr}	wt. %Cr CORR.
824 *	.861	.0154	-.783	-.764	-.019	.021	1.92
825 *	.867	.0155	-.786	-.764	-.022	.021	1.93
823	.641	.0114	-.747	-.751	.004	.021	1.90
820	.708	.0126	-.791	-.755	-.036	.052	4.81
821	.725	.0129	-.801	-.756	-.045	.053	4.81
822	.731	.0130	-.805	-.756	-.049	.053	4.81
827 *	1.12	.0201	-.900	-.780	-.121	.105	9.54
828 *	1.11	.0200	-.898	-.779	-.119	.104	9.50
829 *	1.14	.0204	-.907	-.781	-.126	.105	9.54
816	.987	.0177	-.938	-.772	-.167	.160	14.6
817	.975	.0174	-.933	-.771	-.162	.160	14.6
818	.988	.0177	-.939	-.772	-.167	.160	14.6
833 *	1.57	.0285	-1.051	-.807	-.244	.211	19.1
834 *	1.57	.0285	-1.052	-.807	-.245	.211	19.1
814	1.31	.0237	-1.066	-.792	-.275	.264	24.1
815	1.36	.0245	-1.081	-.794	-.287	.264	24.1
830 *	2.23	.0415	-1.214	-.850	-.364	.322	28.8
831 *	2.25	.0418	-1.218	-.852	-.367	.322	28.8
832 *	2.29	.0425	-1.225	-.854	-.371	.324	28.9
810	1.87	.0343	-1.226	-.827	-.400	.373	33.8
811	1.90	.0349	-1.234	-.829	-.405	.374	33.8
812	1.84	.0338	-1.221	-.825	-.396	.372	33.7
813	1.33	.0241	-1.073	-.793	-.280	.264	24.1
804	2.41	.0449	-1.343	-.862	-.482	.452	40.5
807	2.39	.0445	-1.340	-.860	-.479	.453	40.5
808	2.55	.0477	-1.369	-.871	-.498	.452	40.3
809	2.37	.0442	-1.336	-.859	-.477	.447	40.0

SEE ALSO FIG. 30

* Runs carried out with $(P_{H_2S}/P_{H_2}) \text{ CORR.} = 0.00253$

TABLE 24

TERNARY SYSTEM
IRON - SULPHUR - CHROMIUM

EFFECT OF CHROMIUM ON THE
ACTIVITY COEFFICIENT OF SULPHUR AT

1600°C

= 0.00203

LATTICE RATIO SCALE

RUN	wt. %S	Z _S	<LOG K' _S >	<LOG K'>	LOG Ψ _S ^{Cr}	Z _{Cr}	wt. %Cr CORR.
975	.654	.0116	-.757	-.744	-.013	.021	1.91
976	.640	.0113	-.748	-.744	-.004	.021	1.90
977	.648	.0115	-.753	-.744	-.009	.021	1.90
973	.716	.0127	-.797	-.748	-.049	.052	4.72
974	.712	.0126	-.794	-.748	-.047	.052	4.72
978	.813	.0145	-.853	-.753	-.100	.102	9.36
980	.793	.0141	-.842	-.752	-.090	.102	9.36
981	.805	.0143	-.849	-.753	-.096	.102	9.36
971	.922	.0165	-.909	-.760	-.150	.156	14.3
972	.929	.0166	-.913	-.760	-.153	.156	14.3
982	1.01	.0181	-.951	-.765	-.186	.205	18.8
983	.977	.0175	-.935	-.763	-.172	.204	18.8
968	1.14	.0204	-1.002	-.772	-.231	.252	23.2
969	1.15	.0207	-1.009	-.773	-.236	.253	23.2
966	1.38	.0249	-1.090	-.786	-.304	.337	30.9
967	1.40	.0253	-1.095	-.787	-.308	.337	30.9
963	1.89	.0346	-1.232	-.816	-.416	.407	36.9
964	1.82	.0334	-1.216	-.812	-.404	.401	36.5
961	1.90	.0350	-1.237	-.817	-.419	.418	37.9
962	1.93	.0354	-1.242	-.819	-.423	.413	37.5

SEE ALSO FIG. 29 AND 30

TABLE 25

TERNARY SYSTEM
IRON - SULPHUR - CHROMIUM

EFFECT OF CHROMIUM ON THE
ACTIVITY COEFFICIENT OF SULPHUR AT

1690°C

$$(P_{H_2S}/P_{H_2})_{CORR.} = 0.00267$$

LATTICE RATIO SCALE

RUN	wt. %S	Z _S	<LOG K'>	<LOG K'>	LOG ψ_{S}^{Cr}	Z _{Cr}	wt. %Cr CORR.
1024	.863	.0154	-.762	-.748	-.014	.021	1.87
1025	.870	.0155	-.765	-.748	-.017	.021	1.87
1033	.862	.0154	-.761	-.748	-.013	.021	1.87
1022	.950	.0170	-.804	-.752	-.052	.051	4.66
1023	.957	.0171	-.807	-.753	-.055	.051	4.66
1032	.961	.0172	-.809	-.753	-.057	.052	4.71
1020	1.08	.0194	-.862	-.759	-.103	.102	9.24
1021	1.02	.0183	-.836	-.756	-.080	.101	9.24
1031	1.08	.0194	-.862	-.759	-.103	.103	9.34
1018	1.23	.0222	-.920	-.767	-.153	.155	14.1
1019	1.21	.0217	-.911	-.766	-.145	.155	14.1
1030	1.16	.0209	-.895	-.764	-.131	.152	13.8
1016	1.35	.0243	-.960	-.774	-.186	.206	18.7
1017	1.32	.0239	-.952	-.772	-.180	.206	18.7
1029	1.31	.0238	-.950	-.772	-.178	.202	18.4
1013	1.48	.0268	-1.002	-.781	-.222	.254	23.1
1014	1.42	.0257	-.983	-.777	-.206	.249	22.6
1028	1.41	.0255	-.981	-.777	-.204	.249	22.7
1010	1.68	.0308	-1.062	-.792	-.270	.339	30.7
1011	1.56	.0284	-1.028	-.785	-.242	.328	29.9
1012	1.44	.0262	-.991	-.779	-.213	.318	29.1
1008	1.97	.0363	-1.134	-.808	-.326	.405	36.6

SEE ALSO FIG.30

TABLE 26

TERNARY SYSTEM
IRON - SULPHUR - CHROMIUM

EFFECT OF CHROMIUM ON THE
ACTIVITY COEFFICIENT OF SULPHUR AT

1755°C

$$(P_{H_2S}/P_{H_2})_{CORR.} = 0.00120$$

LATTICE RATIO SCALE

RUN	wt. %S	Z _S	<LOG K'>	<LOG K'>	LOG Ψ_S^{Cr}	Z _{Cr}	wt. %Cr CORR.
680	.366	.0064	-.729	-.718	-.011	.021	1.91
684	.366	.0064	-.729	-.718	-.011	.021	1.91
685	.381	.0067	-.746	-.718	-.028	.020	1.88
686	.353	.0062	-.713	-.717	.004	.020	1.86
687	.387	.0068	-.753	-.719	-.035	.050	4.65
688	.388	.0068	-.755	-.719	-.036	.050	4.61
689	.392	.0069	-.758	-.719	-.040	.050	4.58
690	.400	.0071	-.768	-.719	-.049	.049	4.54
693	.429	.0076	-.798	-.721	-.078	.100	9.25
694	.418	.0074	-.787	-.720	-.067	.099	9.18
697	.427	.0075	-.796	-.721	-.076	.153	14.2
698	.436	.0077	-.805	-.721	-.084	.151	14.1
701	.467	.0082	-.836	-.723	-.114	.200	18.6
702	.456	.0081	-.826	-.722	-.104	.198	18.5
705	.485	.0086	-.853	-.723	-.129	.249	23.3
706	.484	.0085	-.852	-.723	-.128	.247	23.1
709	.529	.0094	-.891	-.726	-.165	.296	27.7
710	.522	.0092	-.885	-.725	-.160	.293	27.5
717	.519	.0092	-.882	-.725	-.157	.346	32.5
718	.515	.0091	-.879	-.725	-.154	.340	32.0
713	.610	.0108	-.954	-.730	-.224	.413	38.9
714	.608	.0108	-.952	-.730	-.223	.407	38.3

SEE ALSO FIG.30

- A PALLADIUM CATALYST
- B MAGNESIUM PERCHLORATE
- C GAS SAMPLING DEVICE
- D GAS FLOWMETER
- E NEEDLE VALVES
- F DIBUTYL PHTHALATE
- H HF GENERATOR
- J LEVITATION COIL
- K TWO-COLOUR PYROMETER

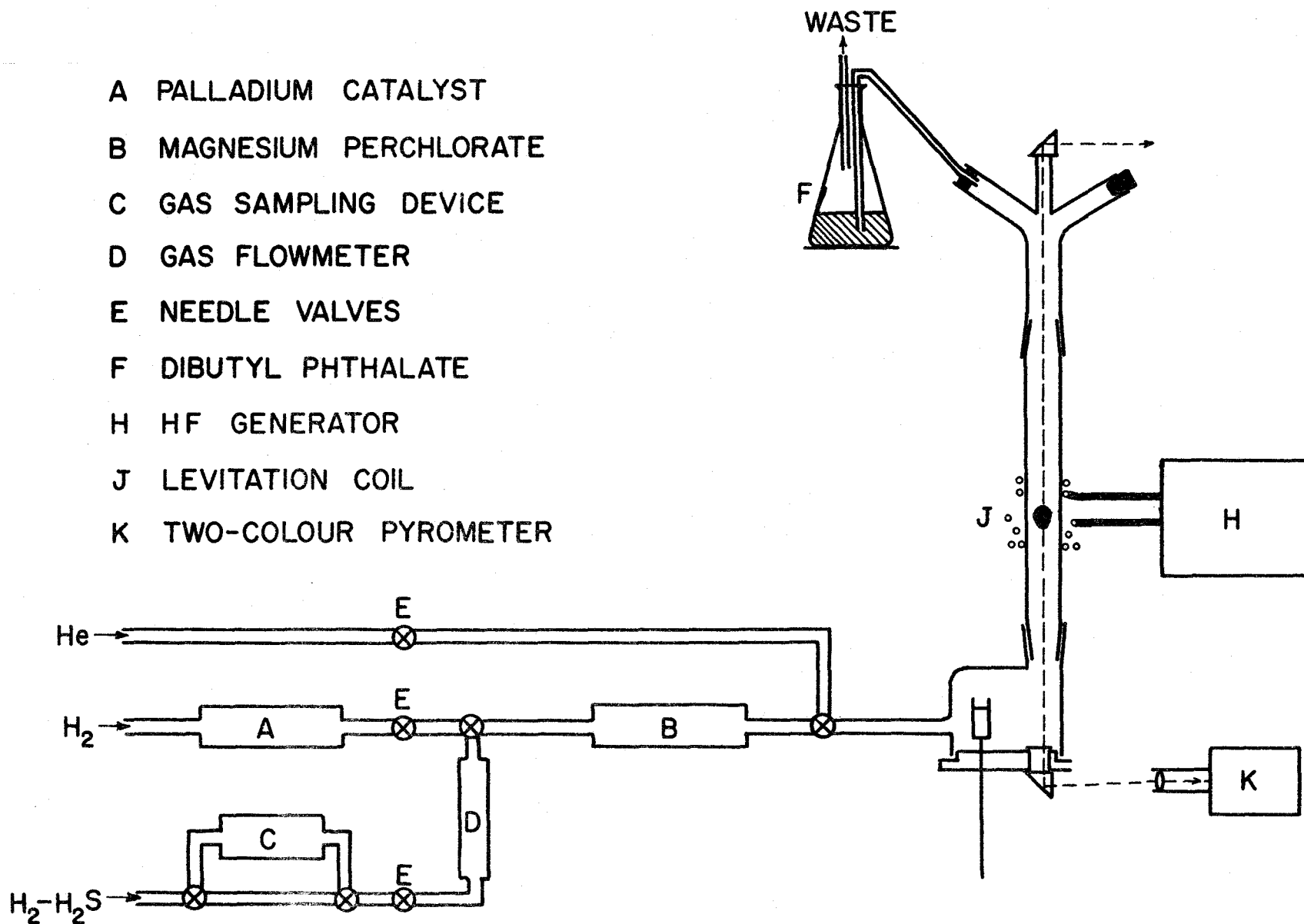


FIG. 1: SCHEMATIC DIAGRAM OF THE LEVITATION APPARATUS.

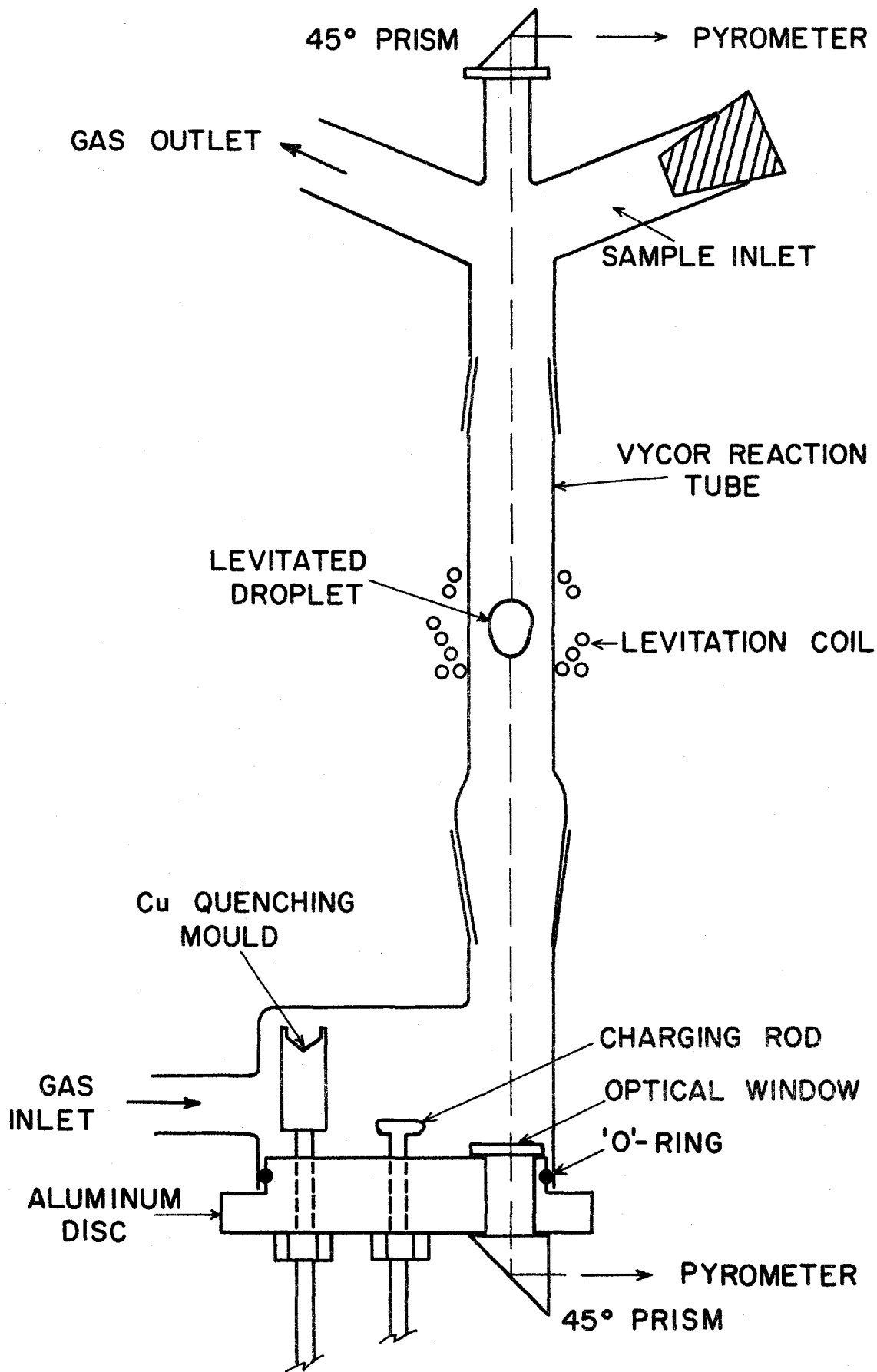
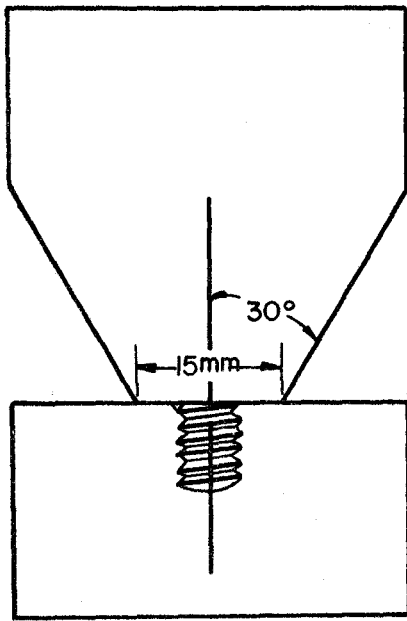
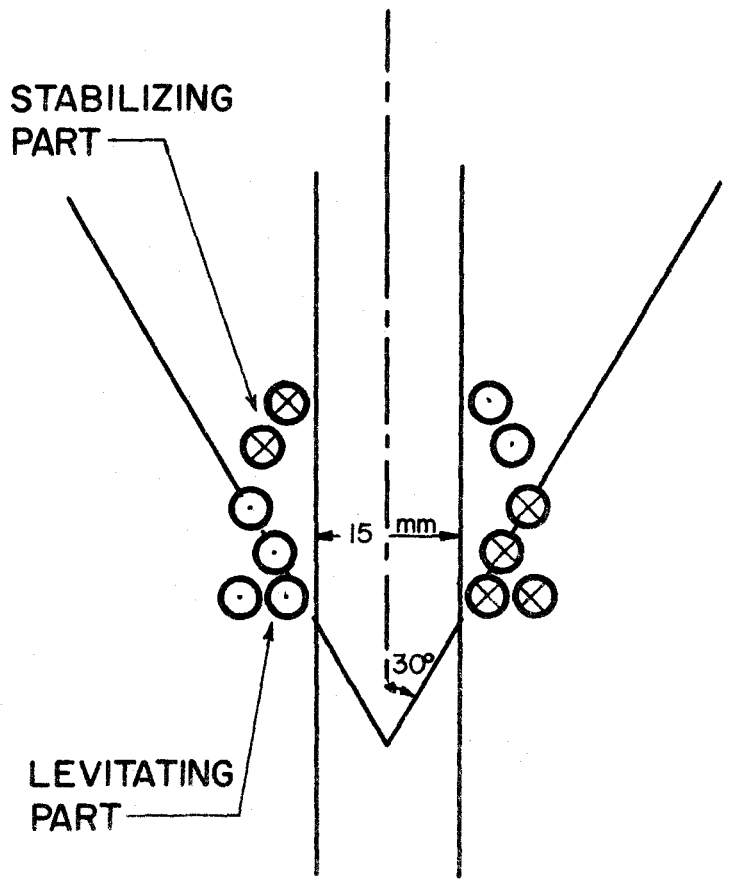


FIG. 2 : REACTION CHAMBER.

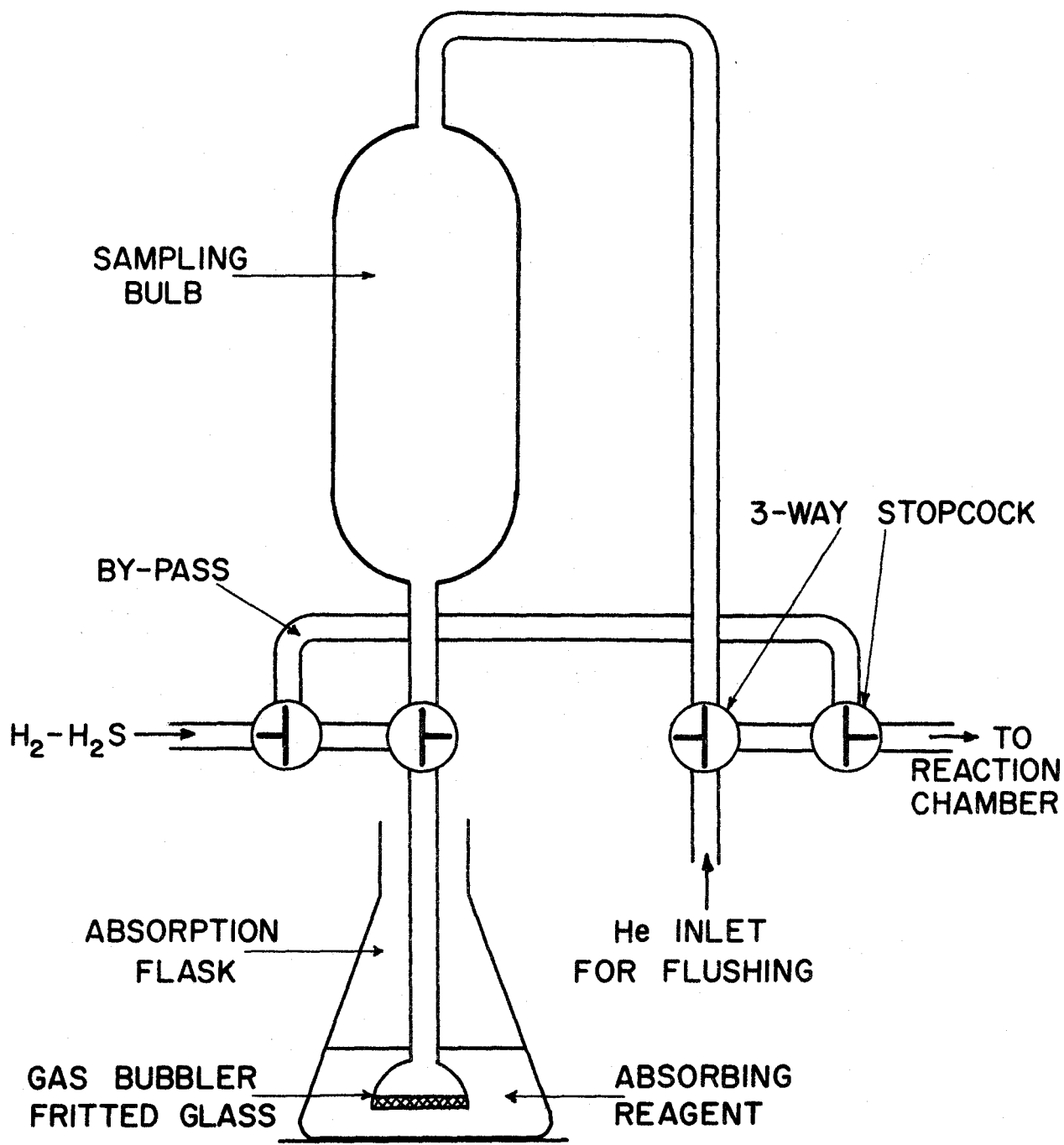


THE FORMER



THE COIL

FIG. 3 :



TAPS ARE IN POSITION FOR GAS ANALYSIS.

FIG. 4: GAS SAMPLING DEVICE.

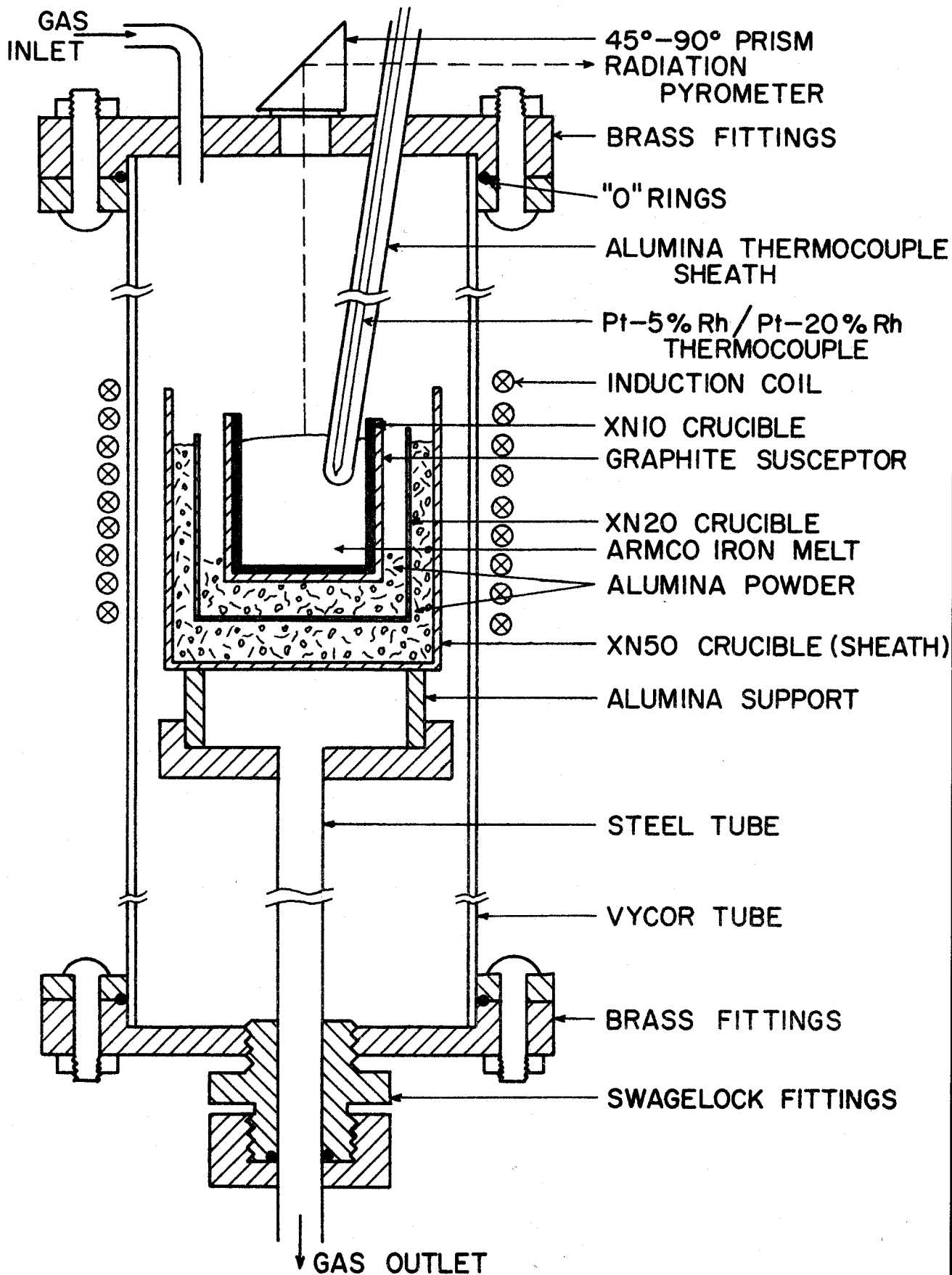


FIG. 5: PYROMETER CALIBRATION APPARATUS.

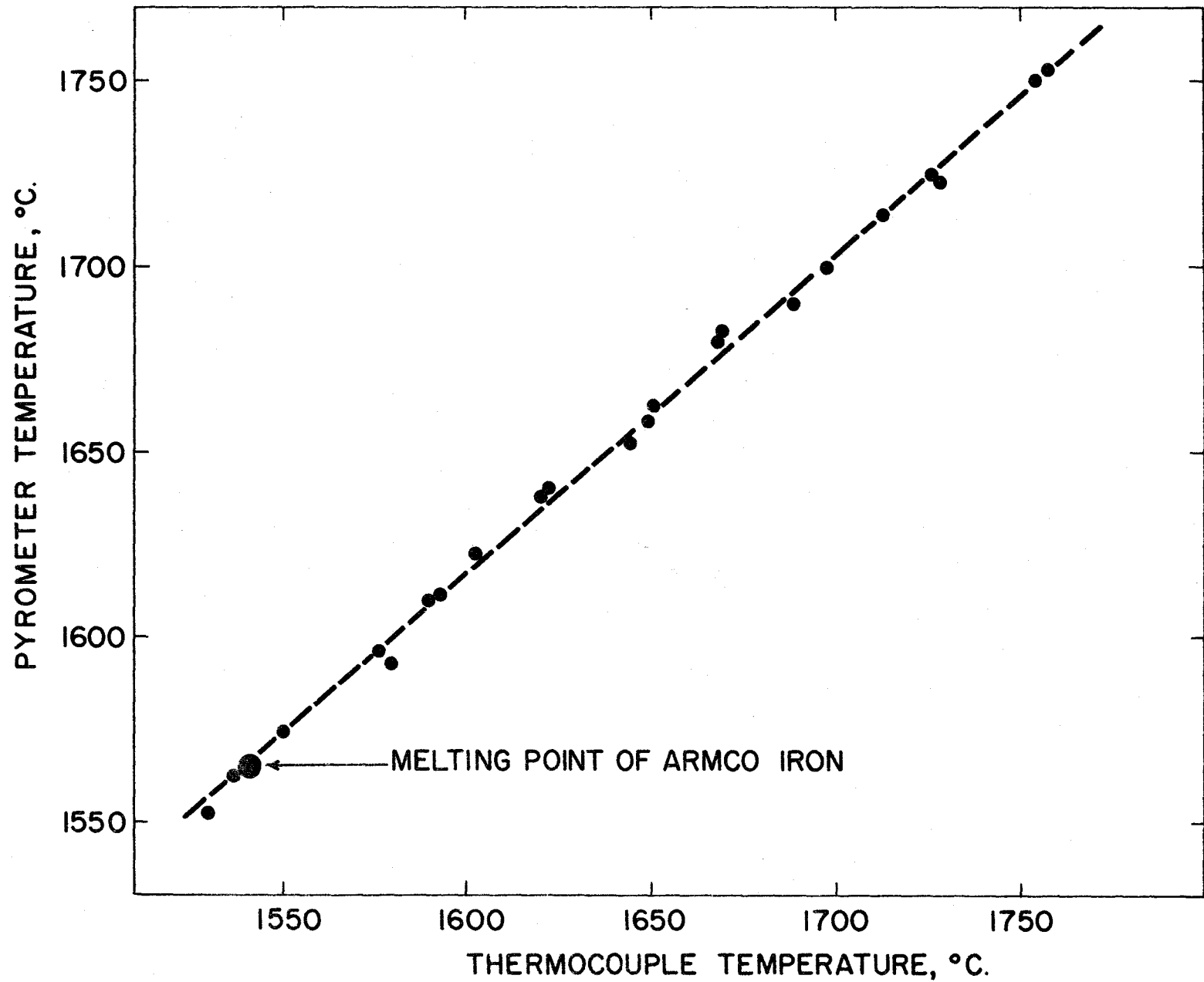


FIG. 6:

PYROMETER CALIBRATION CURVE .

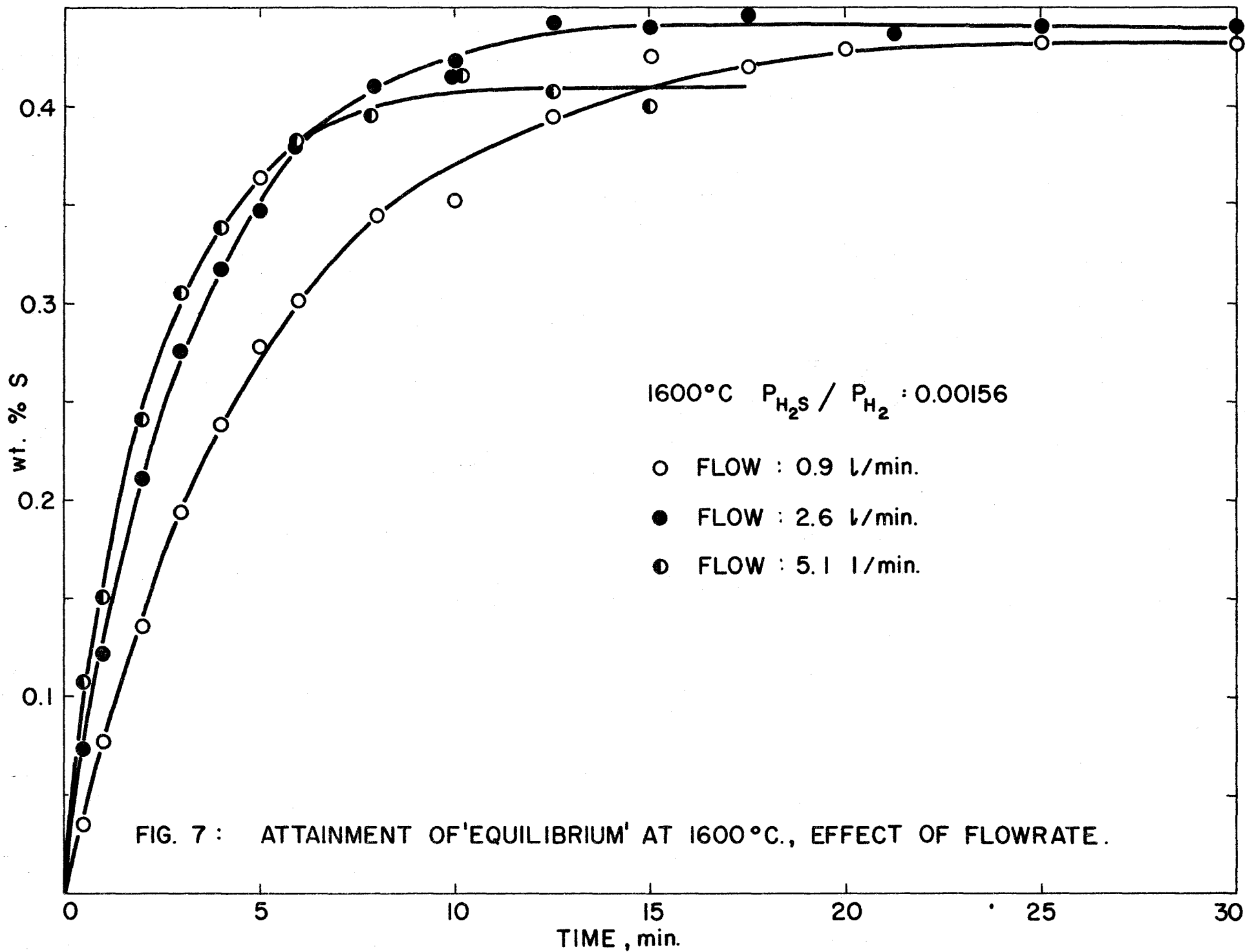


FIG. 7 : ATTAINMENT OF 'EQUILIBRIUM' AT 1600°C., EFFECT OF FLOWRATE.

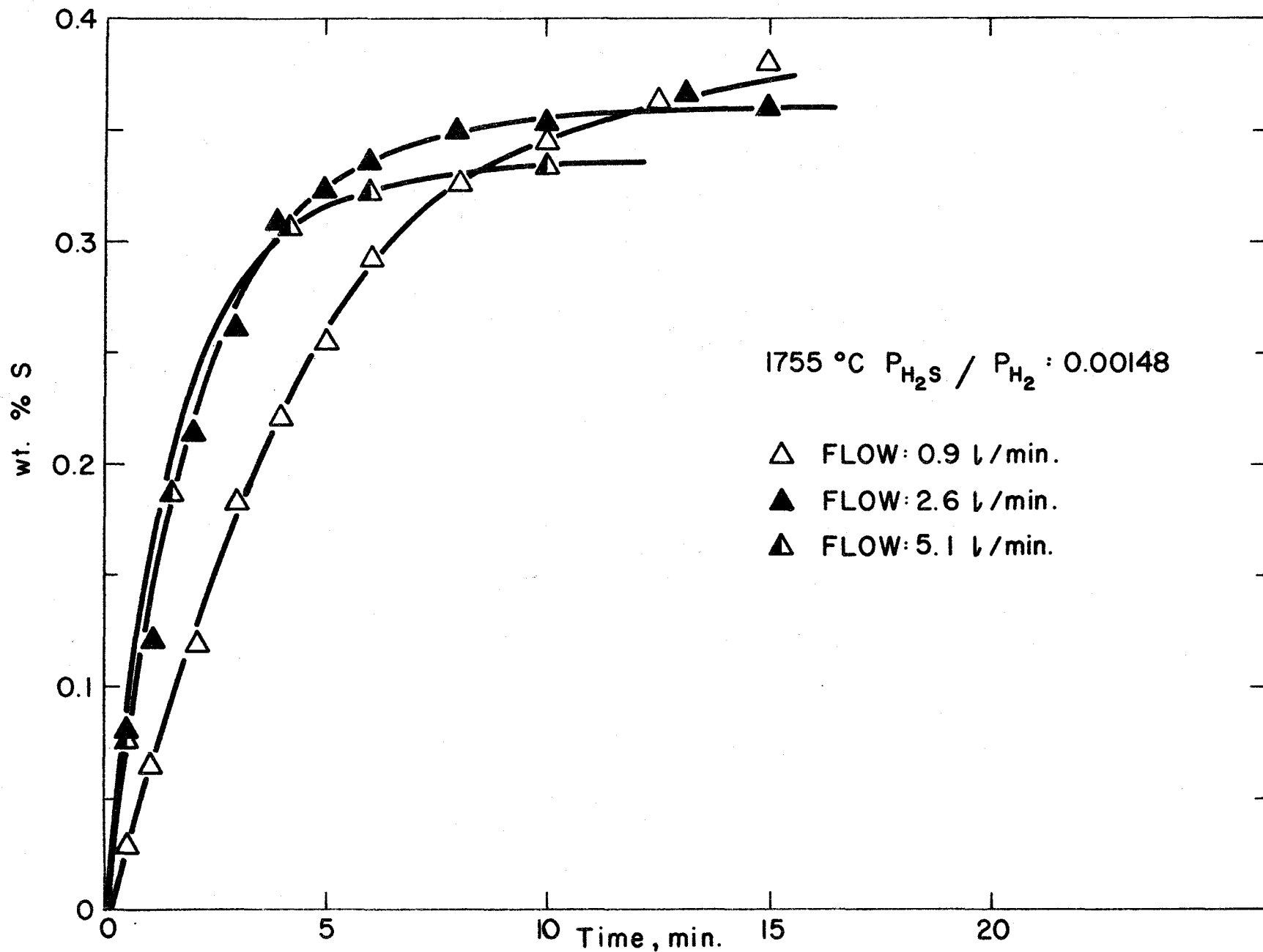


FIG. 8: ATTAINMENT OF 'EQUILIBRIUM' AT 1755 °C., EFFECT OF FLOW RATE .

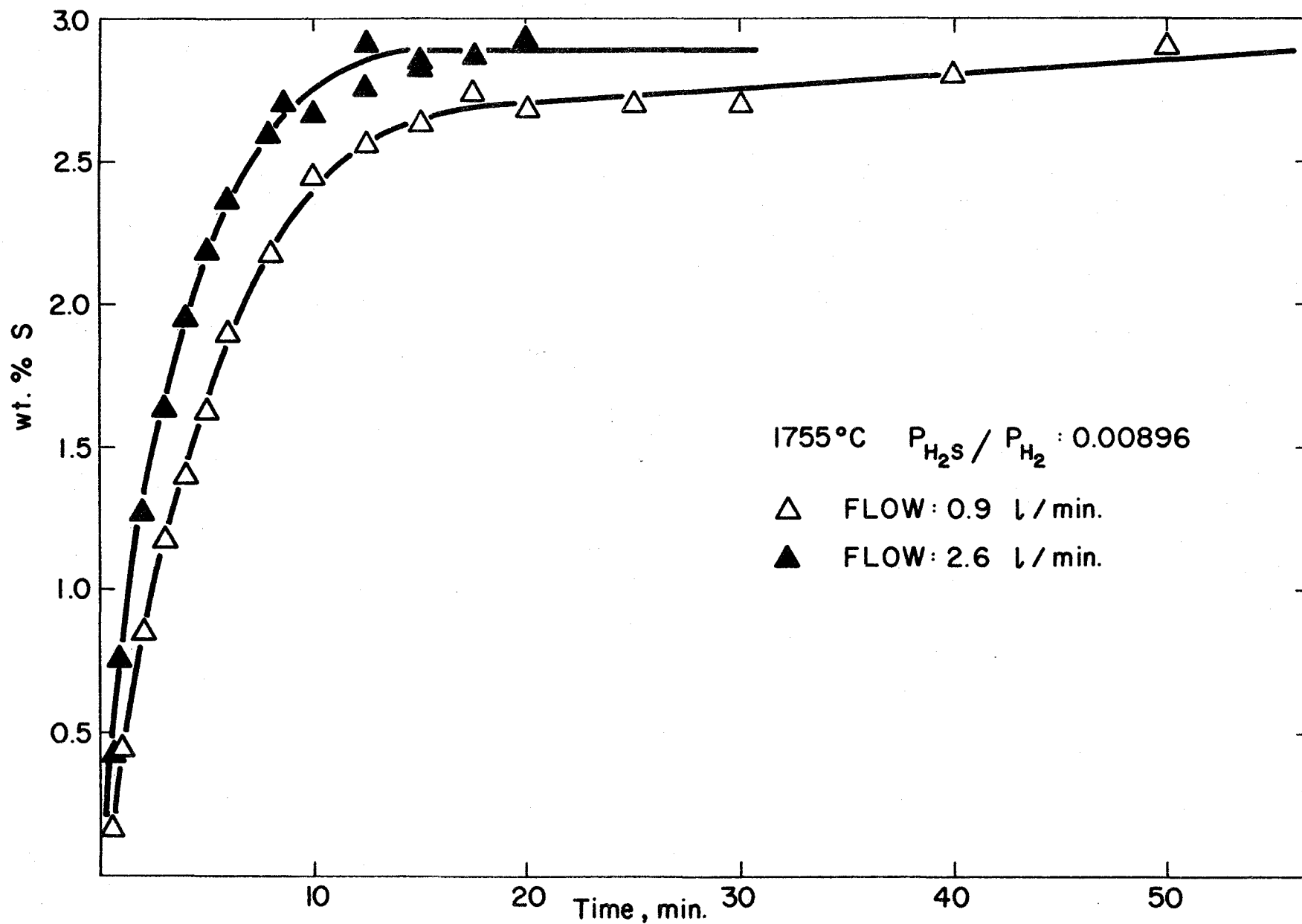


FIG. 9: ATTAINMENT OF 'EQUILIBRIUM' AT 1755 °C: EFFECT OF FLOWRATE.

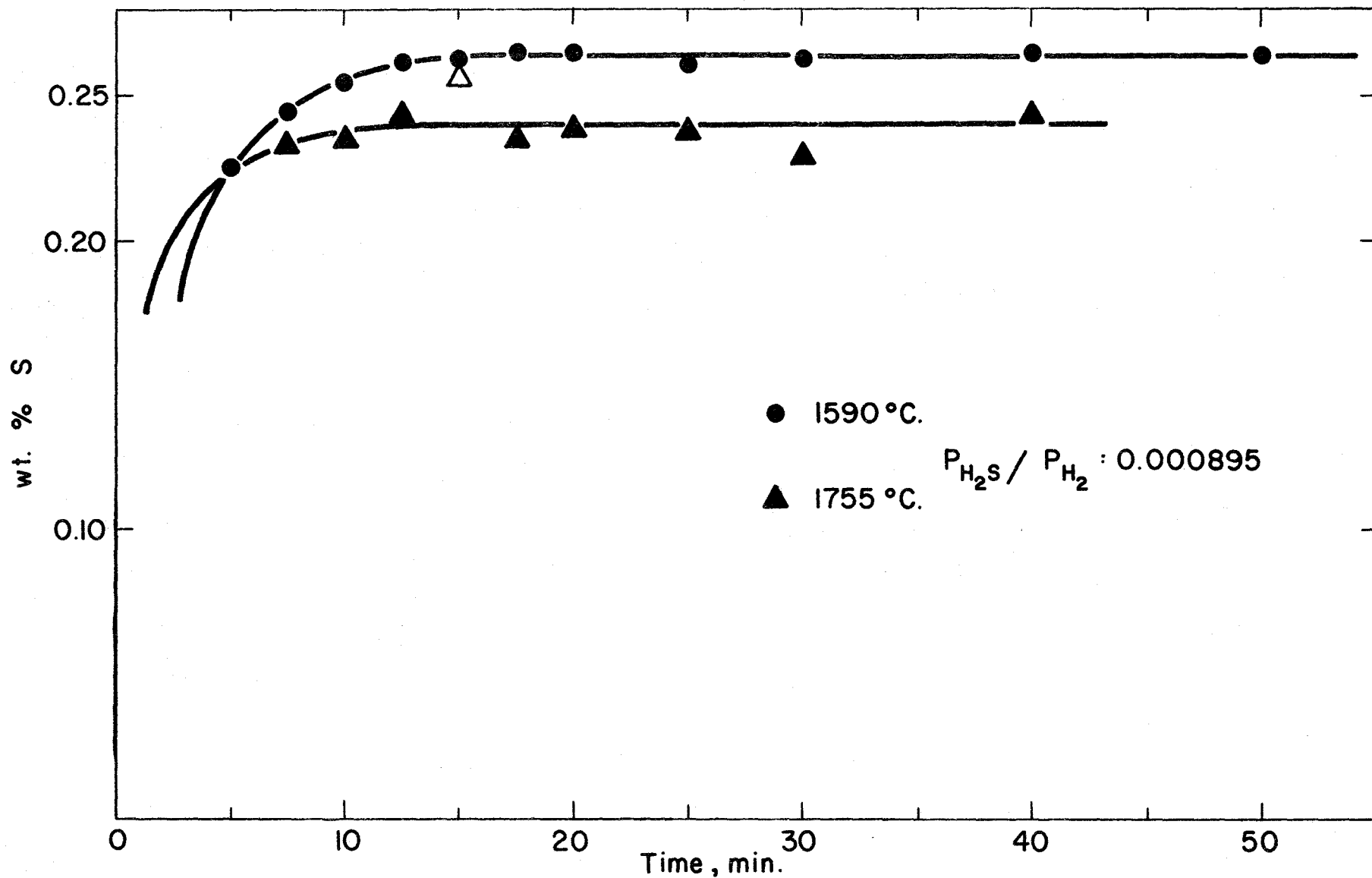


FIG. 10: ATTAINMENT OF 'EQUILIBRIUM' FOR VERY LOW VALUE OF P_{H_2S} / P_{H_2} : EFFECT OF TEMP.

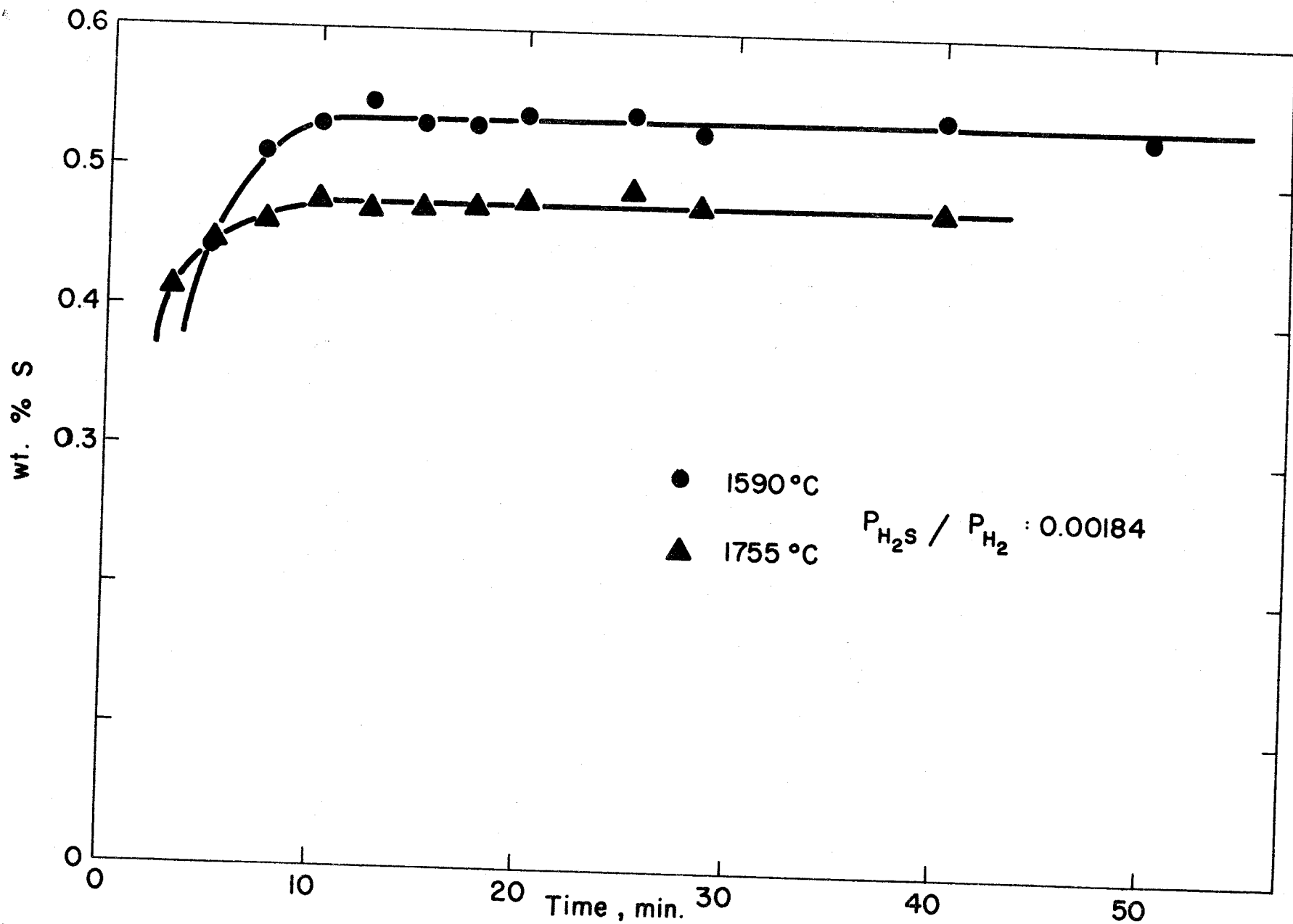


FIG. II: ATTAINMENT OF 'EQUILIBRIUM' FOR LOW VALUE OF P_{H_2S} / P_{H_2} , EFFECT OF TEMP.

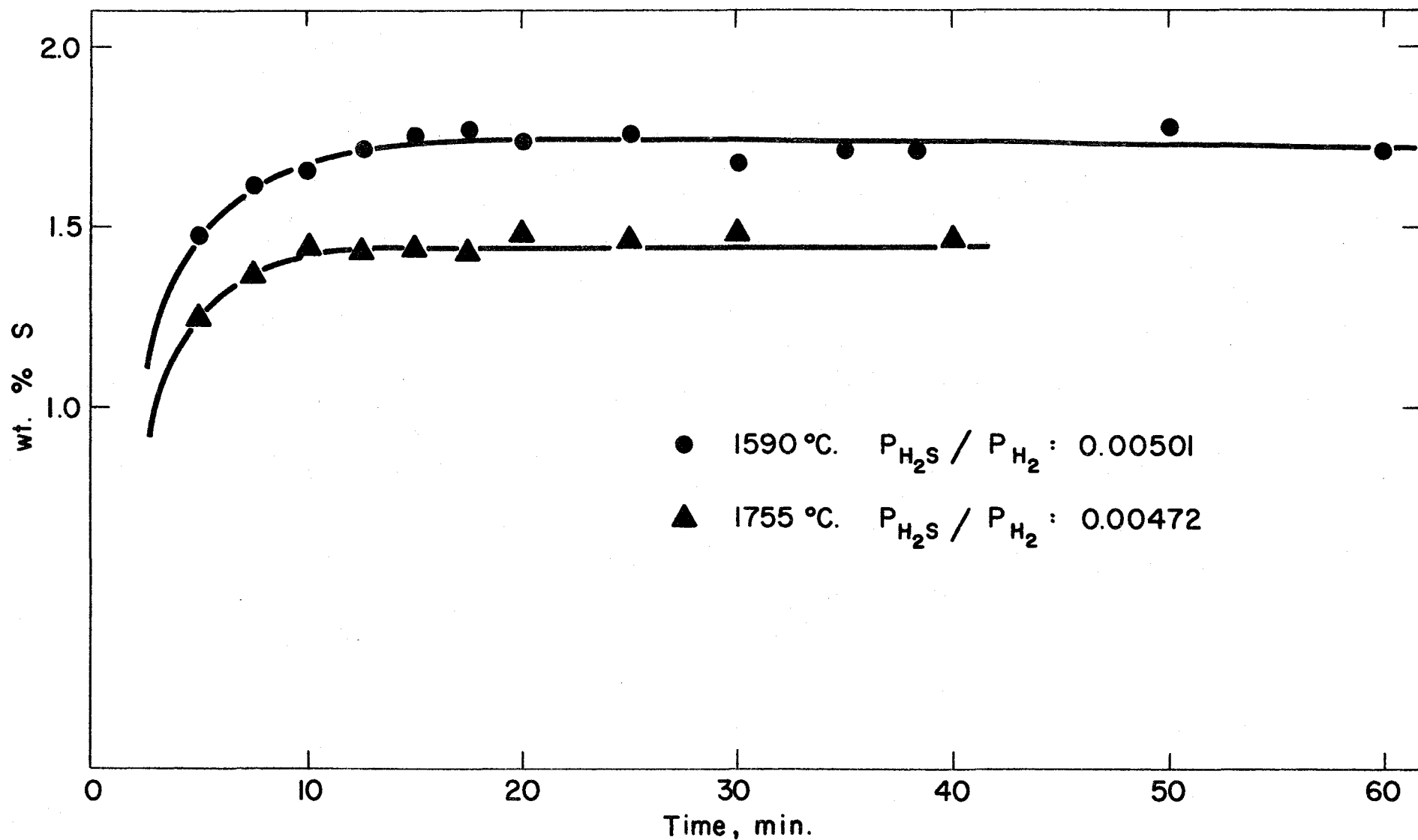


FIG. 12: ATTAINMENT OF 'EQUILIBRIUM' FOR MEDIUM VALUE OF P_{H_2S}/P_{H_2} , EFFECT OF TEMP.

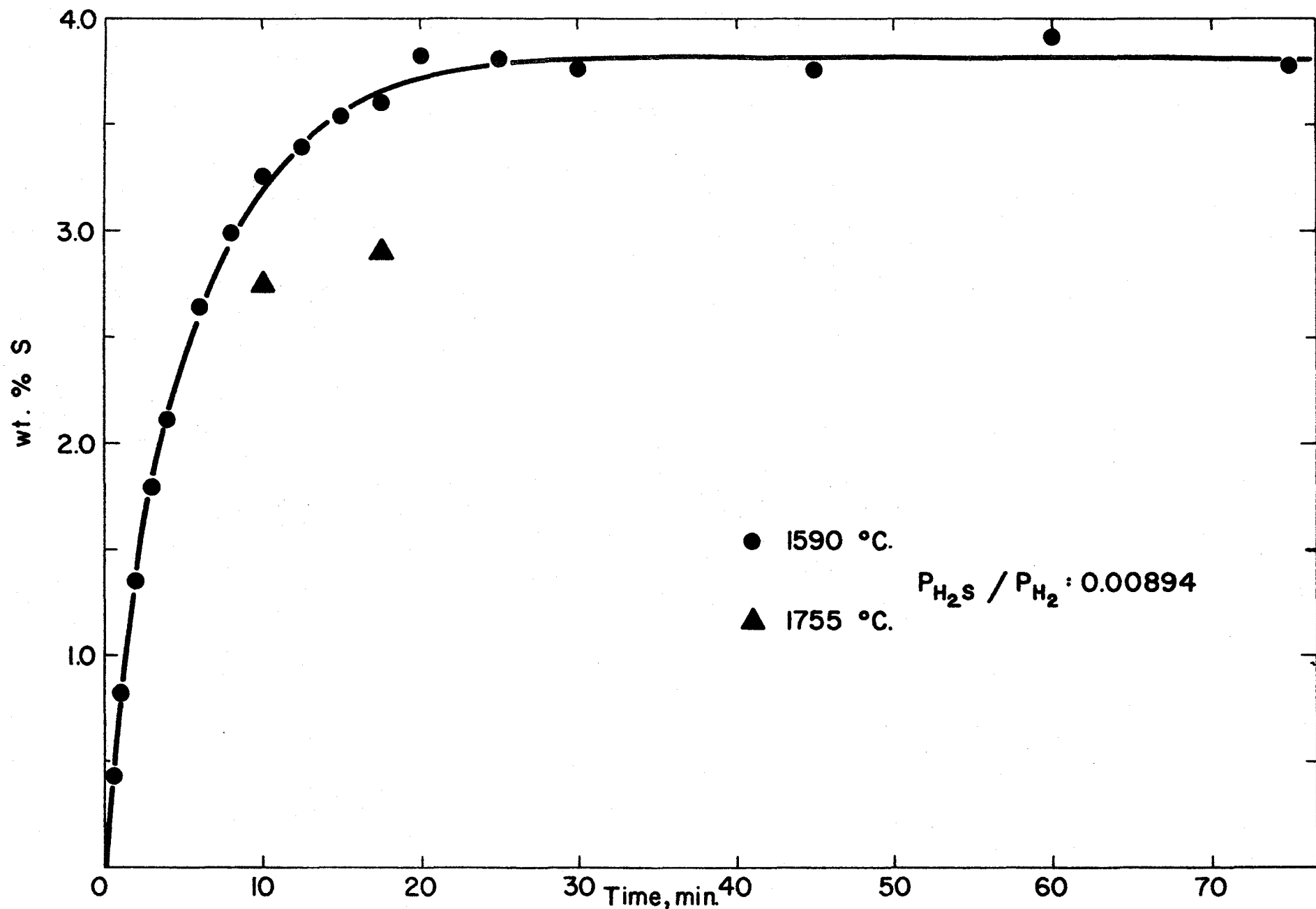


FIG. 13: ATTAINMENT OF 'EQUILIBRIUM' FOR HIGH VALUE OF P_{H_2S} / P_{H_2} : EFFECT OF TEMP.

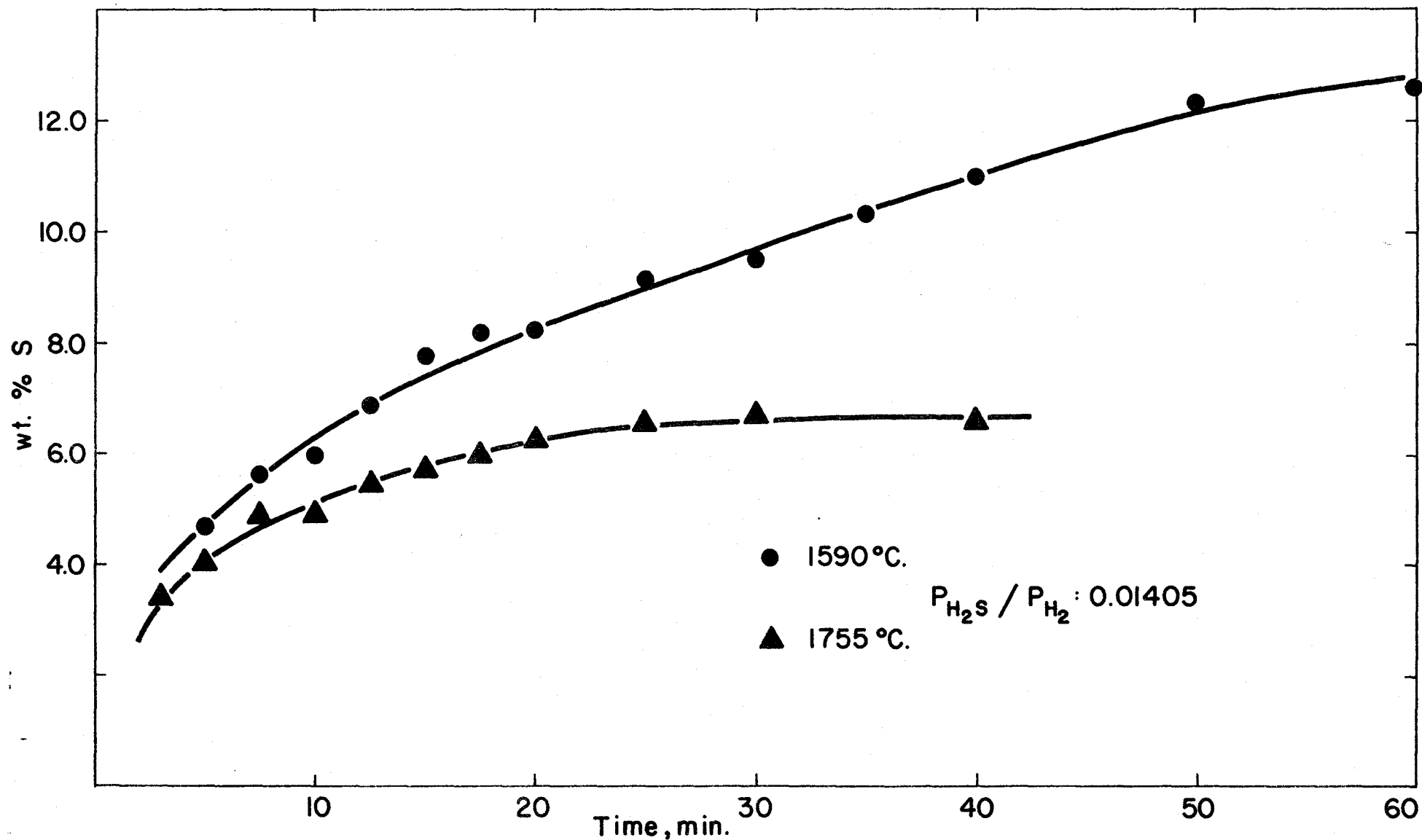


FIG. 14: ATTAINMENT OF 'EQUILIBRIUM' FOR VERY HIGH VALUE OF P_{H_2S}/P_{H_2} : EFFECT OF TEMP.

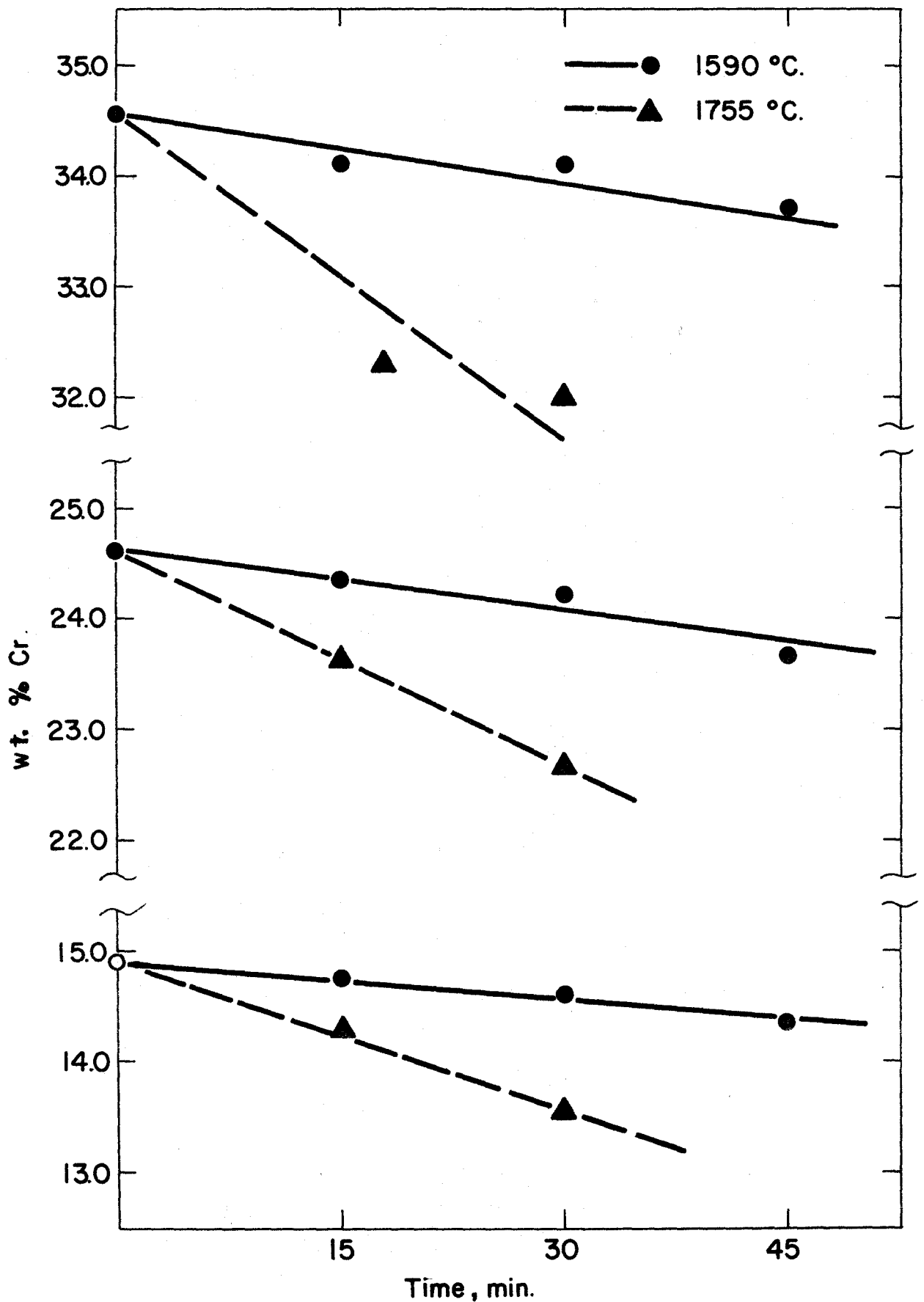


Fig. 15 : Effect of levitation time on Cr loss at 1590 °C and 1755 °C.

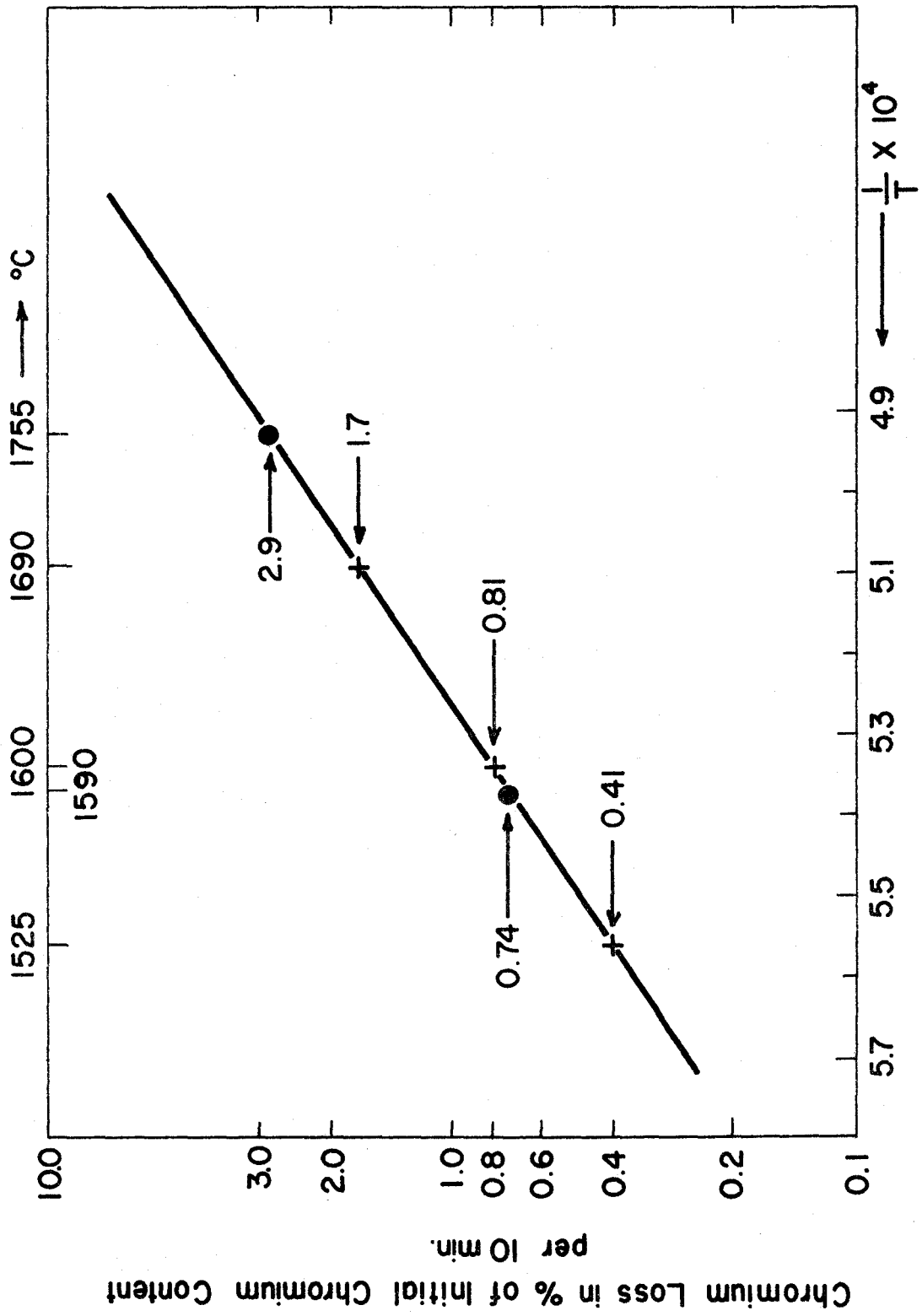


FIG. 16: CHROMIUM LOSS DURING LEVITATION, EFFECT OF TEMPERATURE.

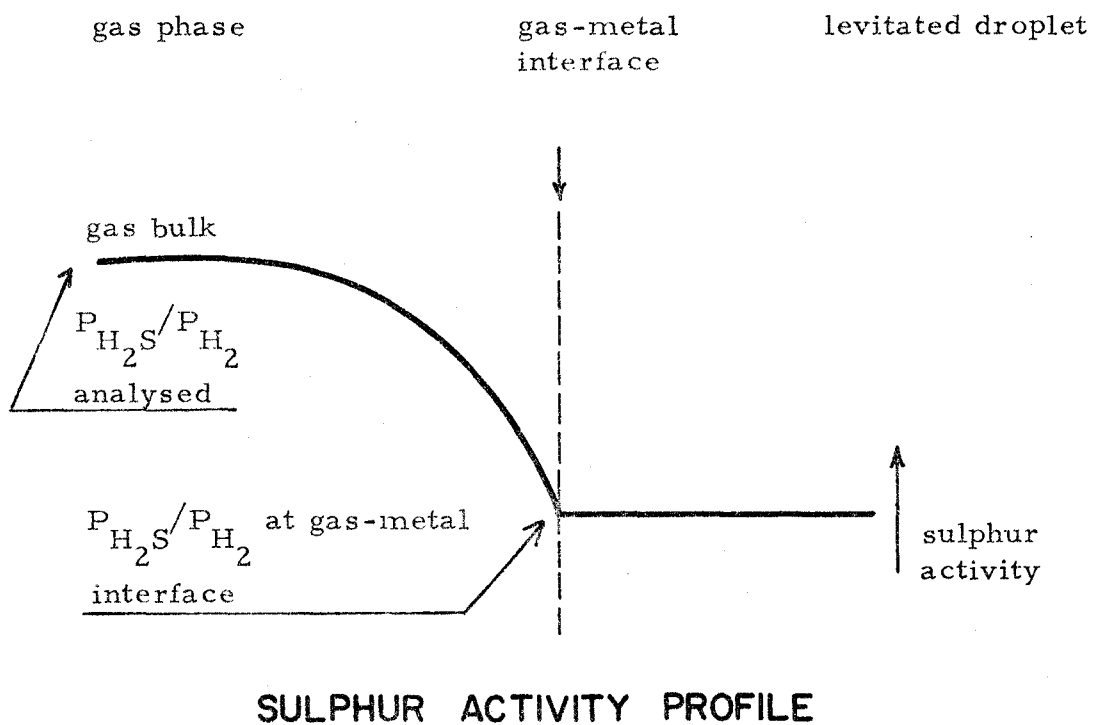
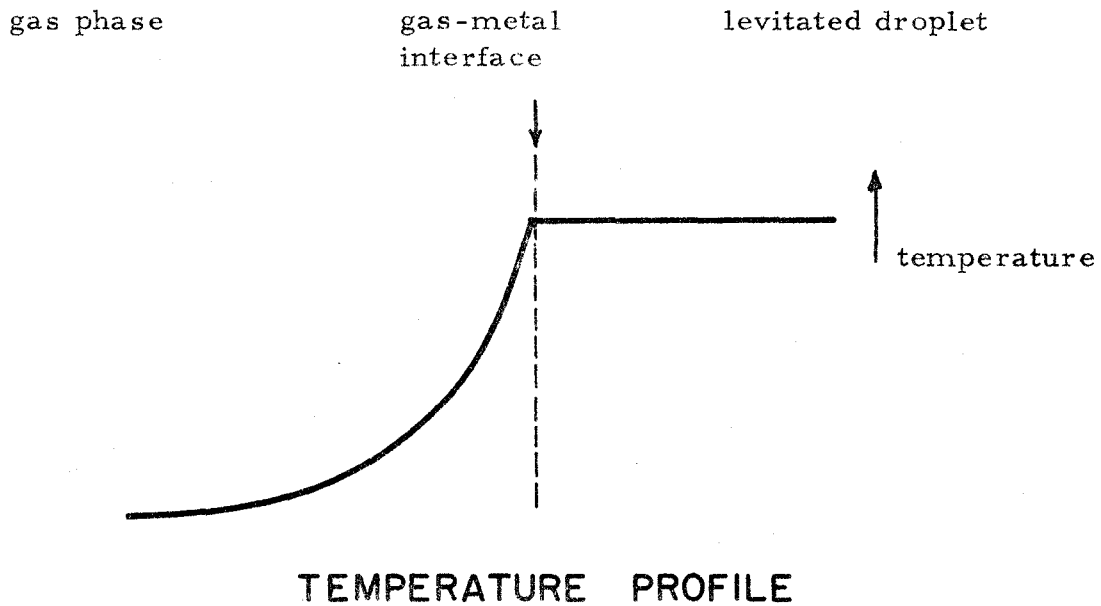


FIG 17: EFFECT OF THERMAL DIFFUSION

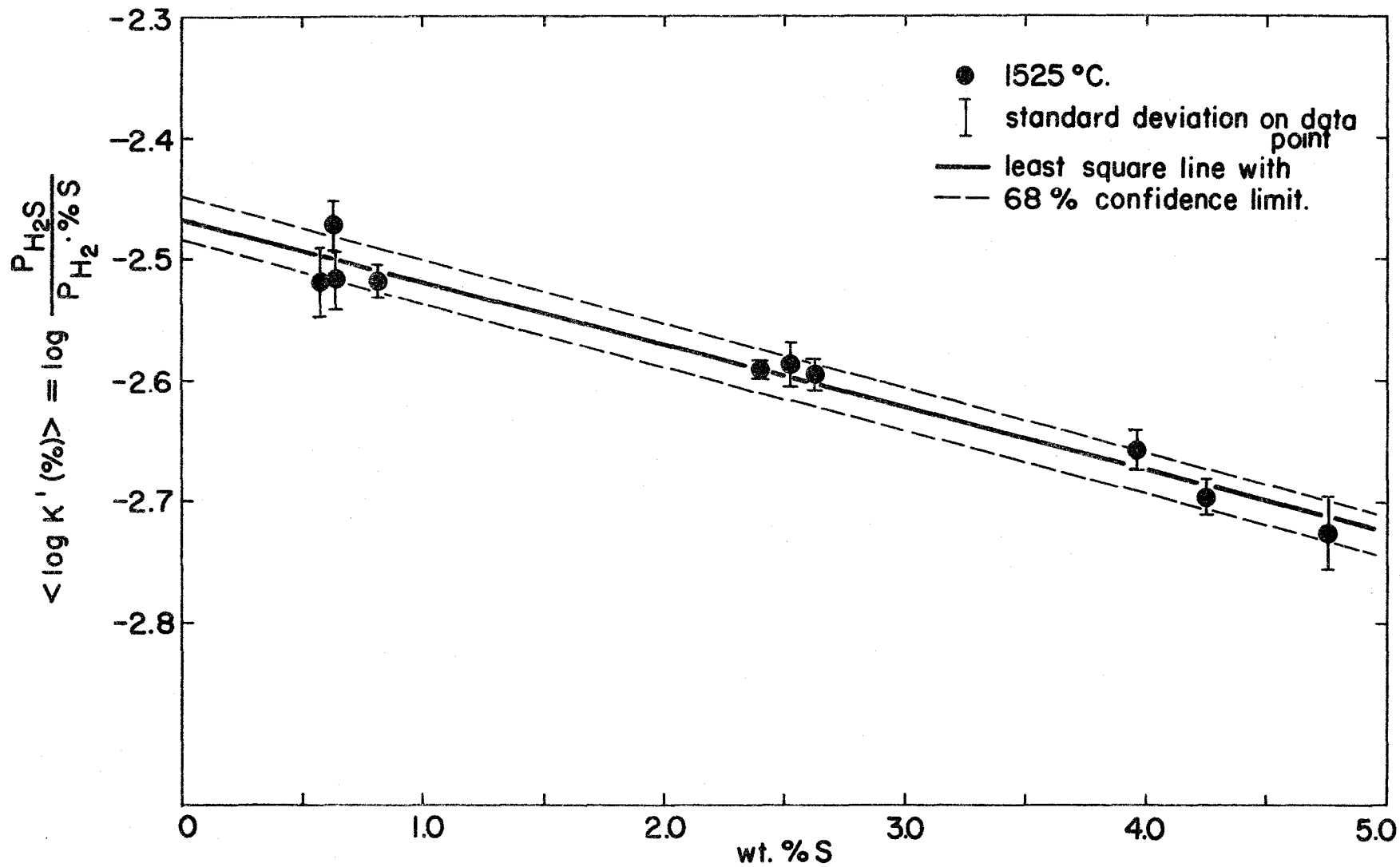


FIG. 18: $\langle \text{LOG } K'(\%) \rangle$ VERSUS WT. % S AT 1525°C

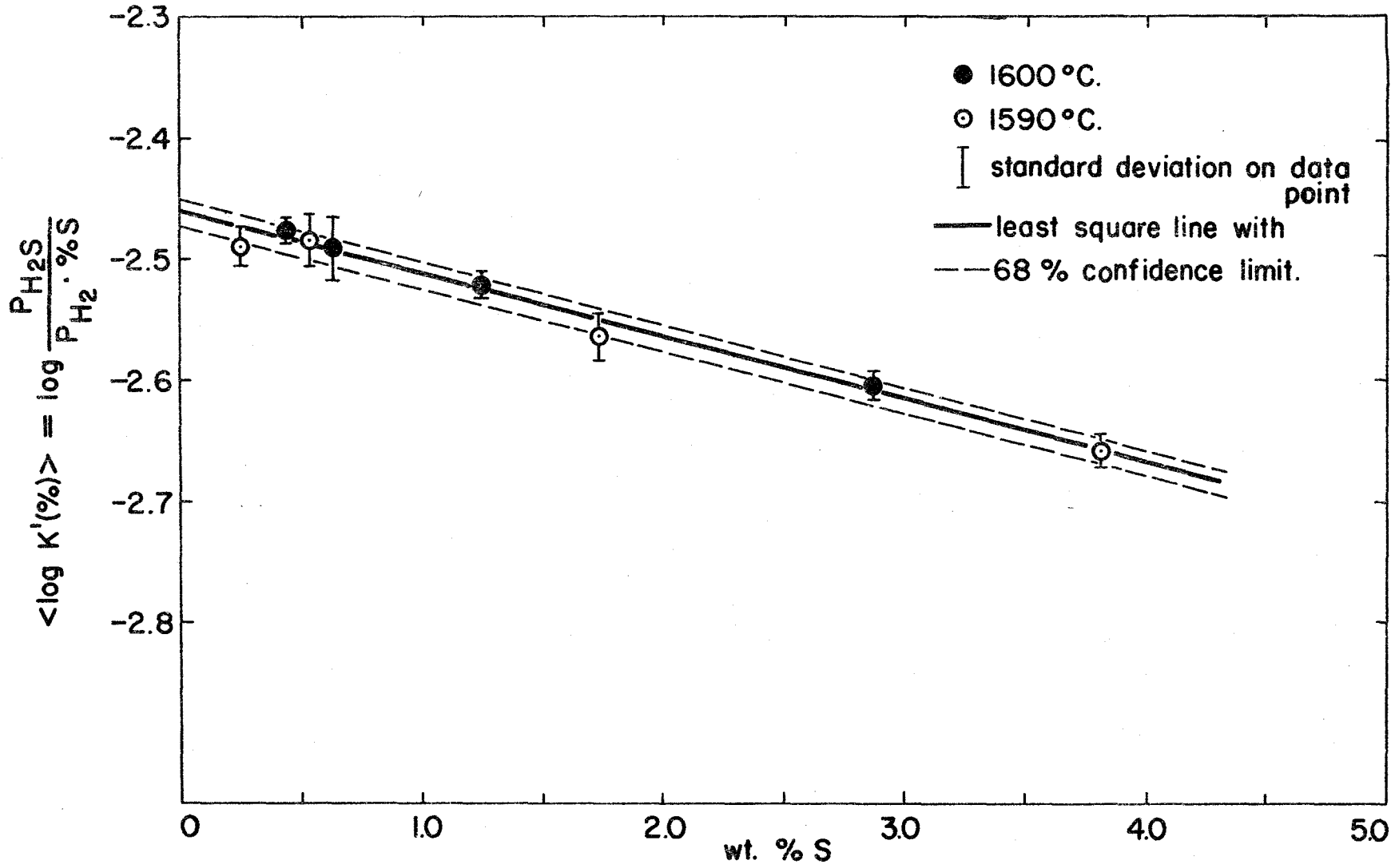


FIG. 19: $\langle \text{LOG } K'(\%) \rangle$ VERSUS WT. %S AT 1600°C

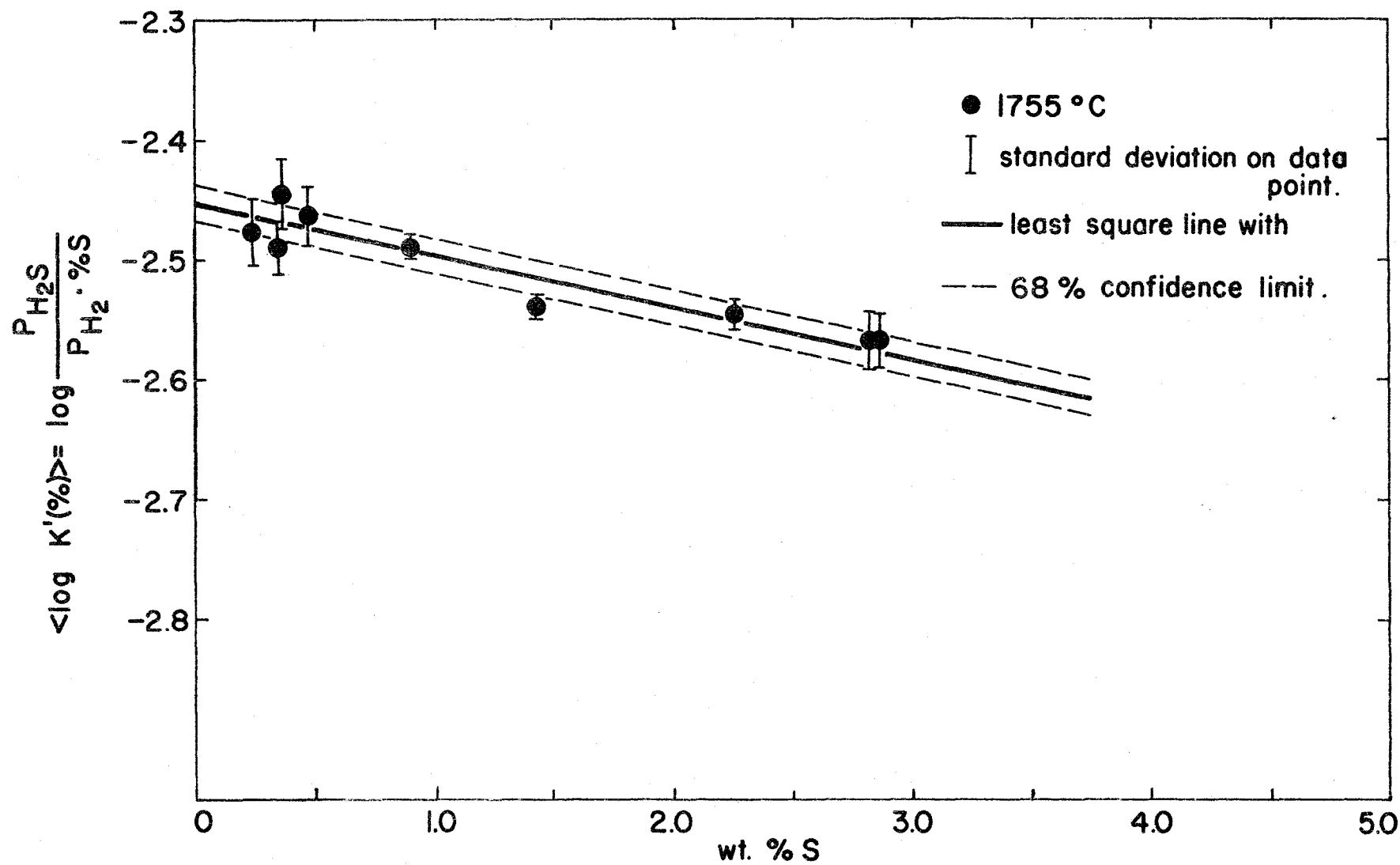


FIG. 20: $\langle \text{LOG } K'(\%) \rangle$ VERSUS WT. %S AT 1755°C

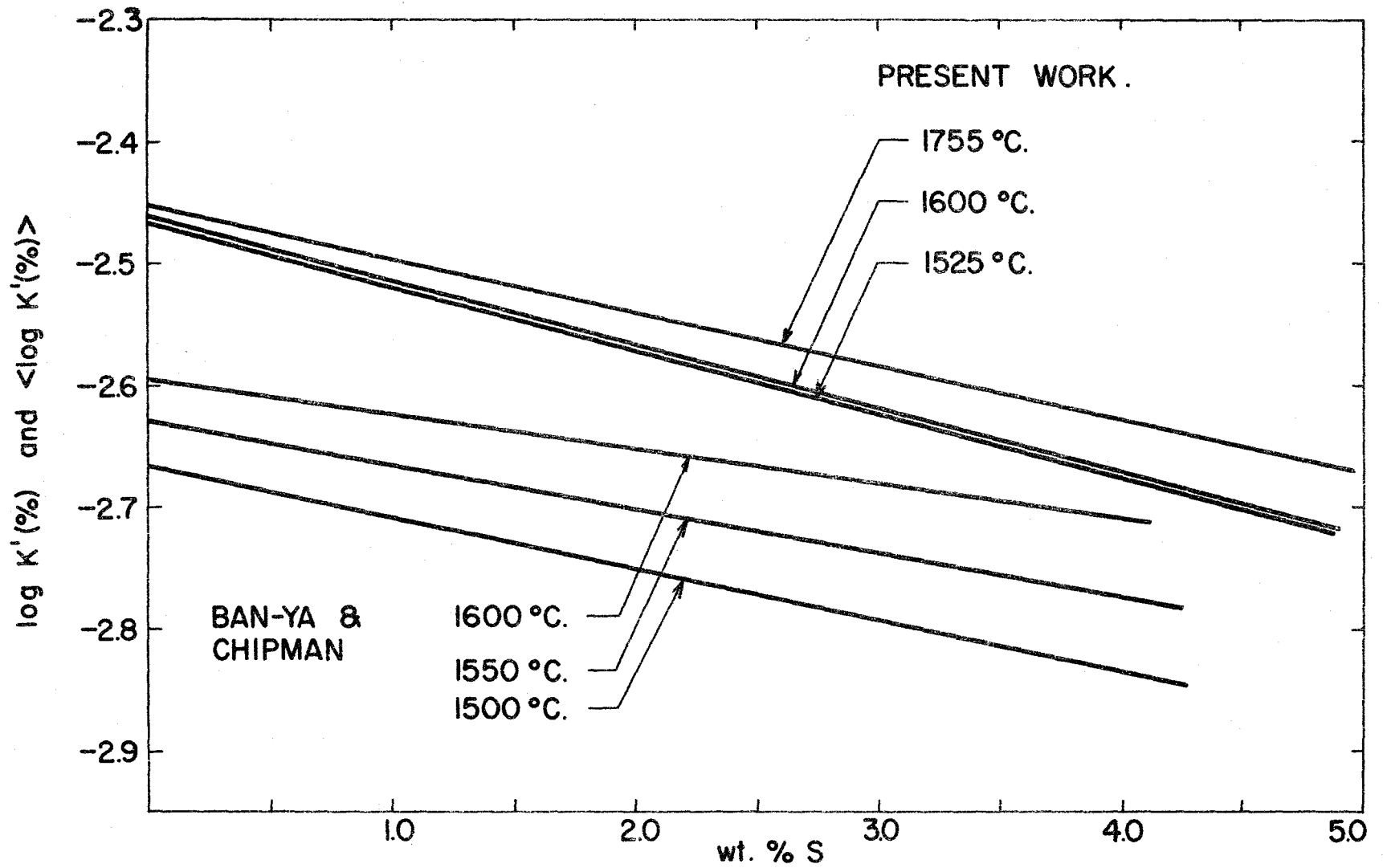


FIG. 21: EFFECT OF TEMPERATURE ON LOG K' (%) AND $\langle \text{LOG K}'(\%) \rangle$

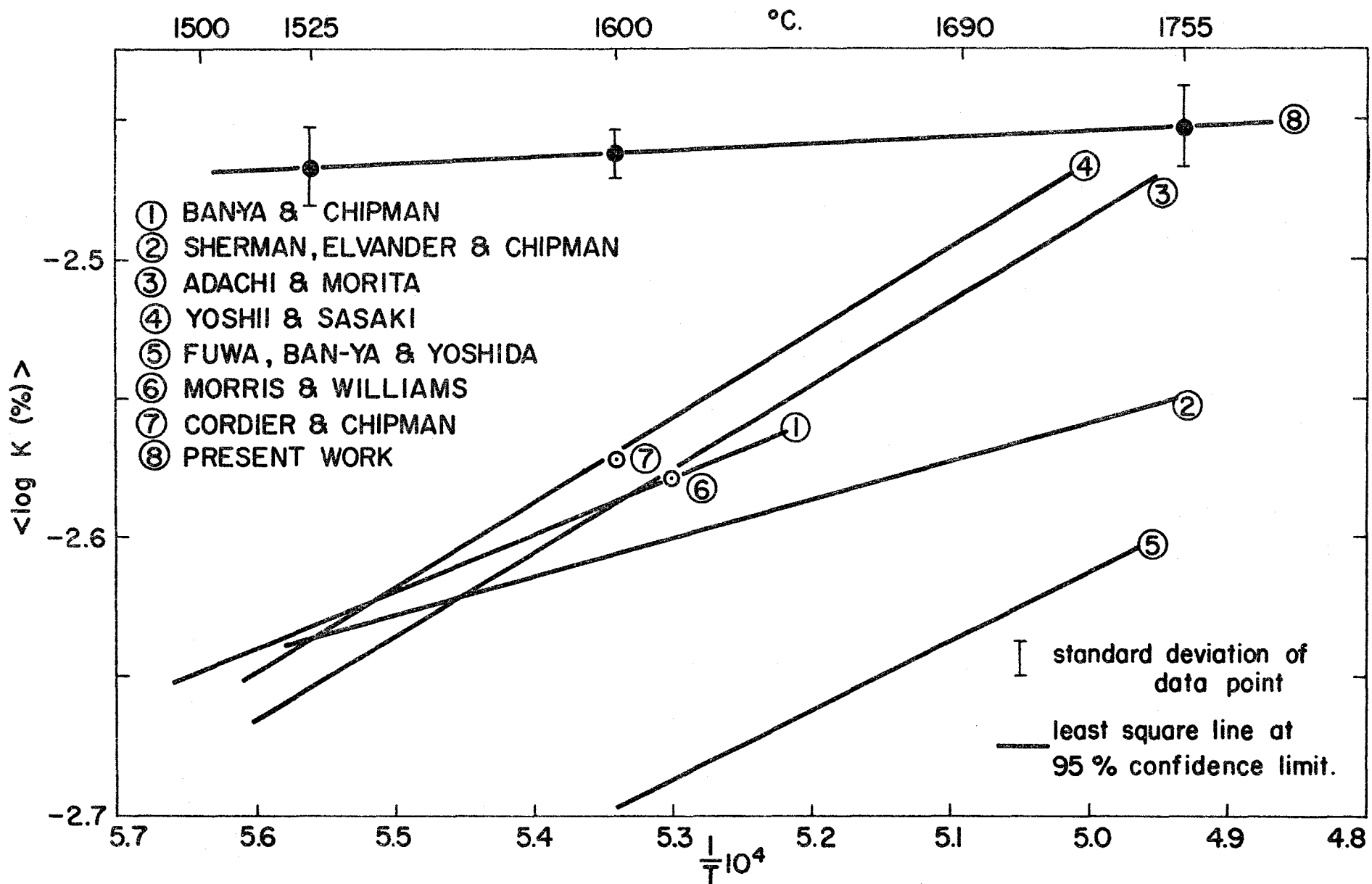


FIG. 22: COMPARATIVE DIAGRAM: TEMPERATURE DEPENDENCE OF LOG K(%) OR < LOG K(%)>

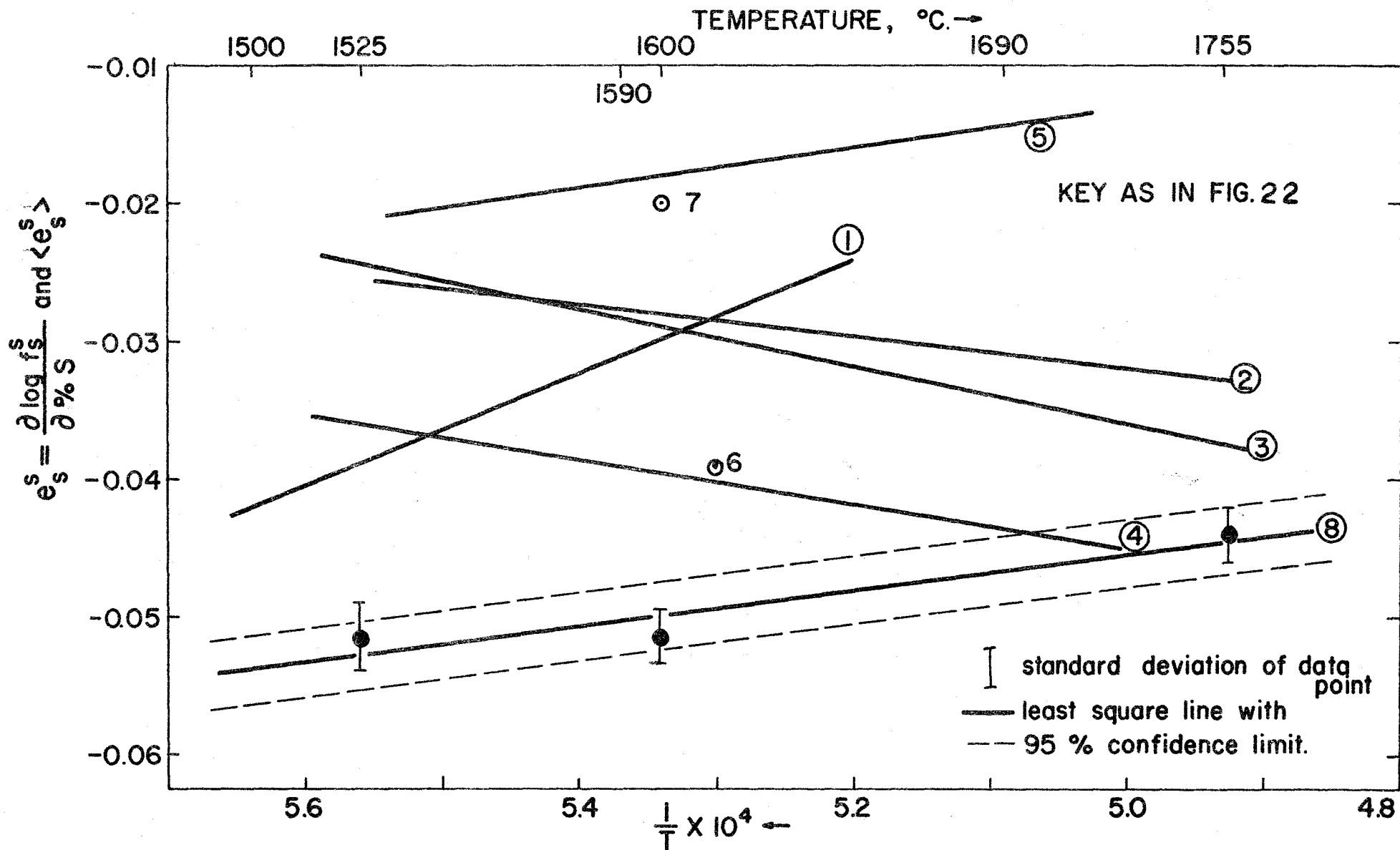


FIG. 23: COMPARATIVE DIAGRAM: TEMPERATURE DEPENDENCE OF e_s^S AND $\langle e_s^S \rangle$

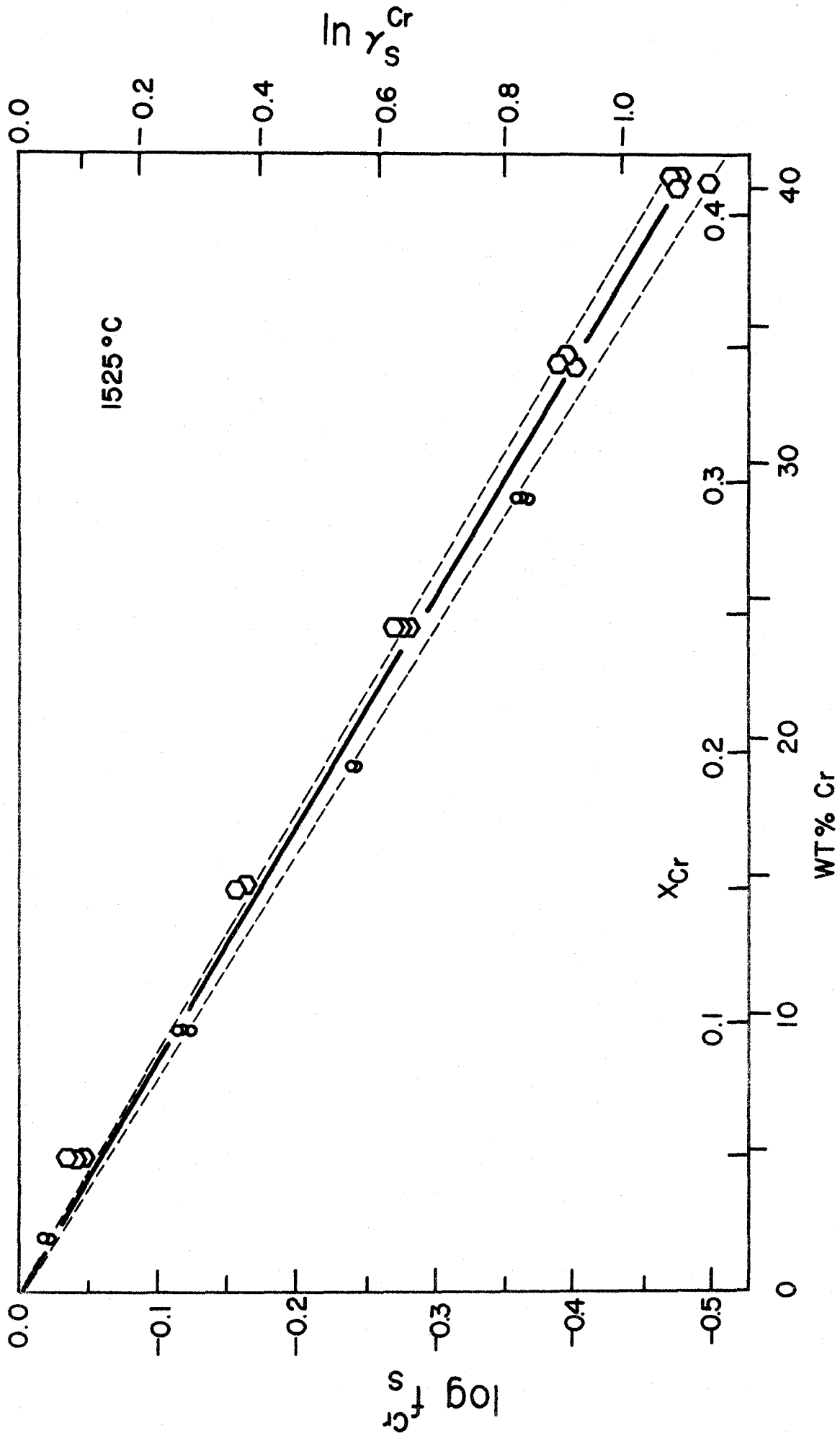


FIG. 24: EFFECT OF Cr ON THE ACTIVITY COEFFICIENT OF S AT 1525 °C

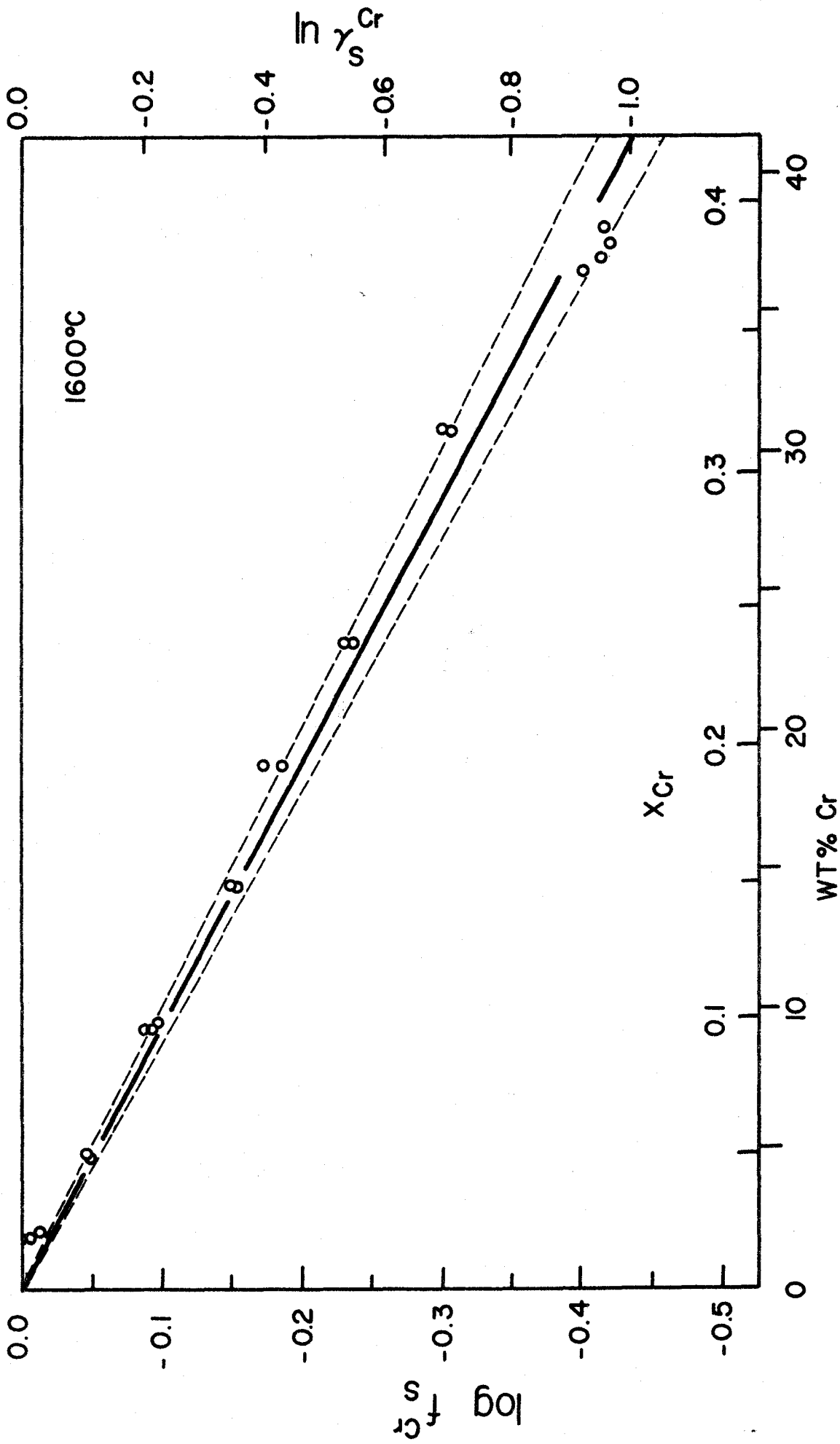


FIG. 25: EFFECT OF Cr ON THE ACTIVITY COEFFICIENT OF S AT 1600°C

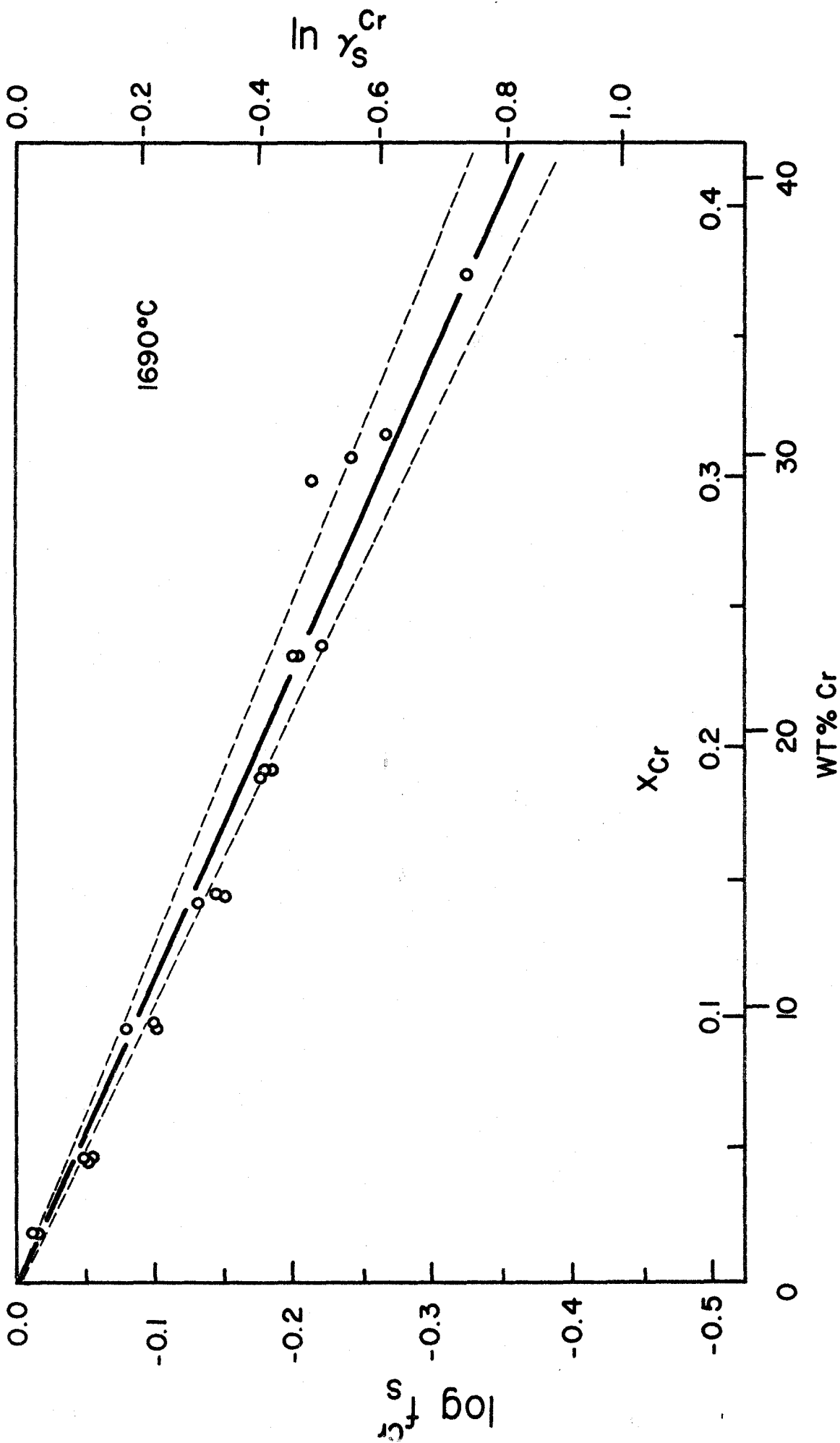


FIG. 26: EFFECT OF Cr ON THE ACTIVITY COEFFICIENT OF S AT 1690°C

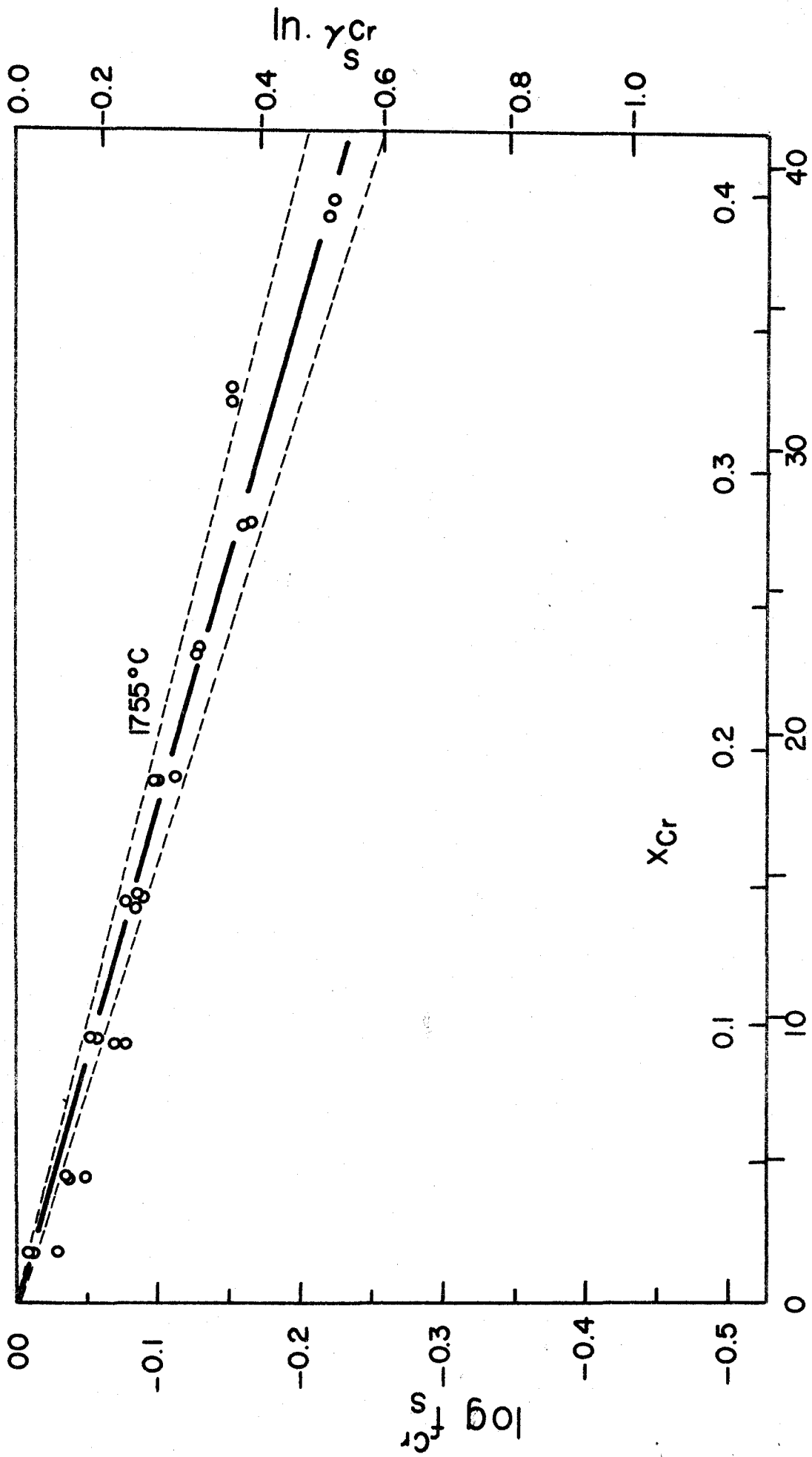


FIG. 27: EFFECT OF Cr ON THE ACTIVITY COEFFICIENT OF S AT 1755°C

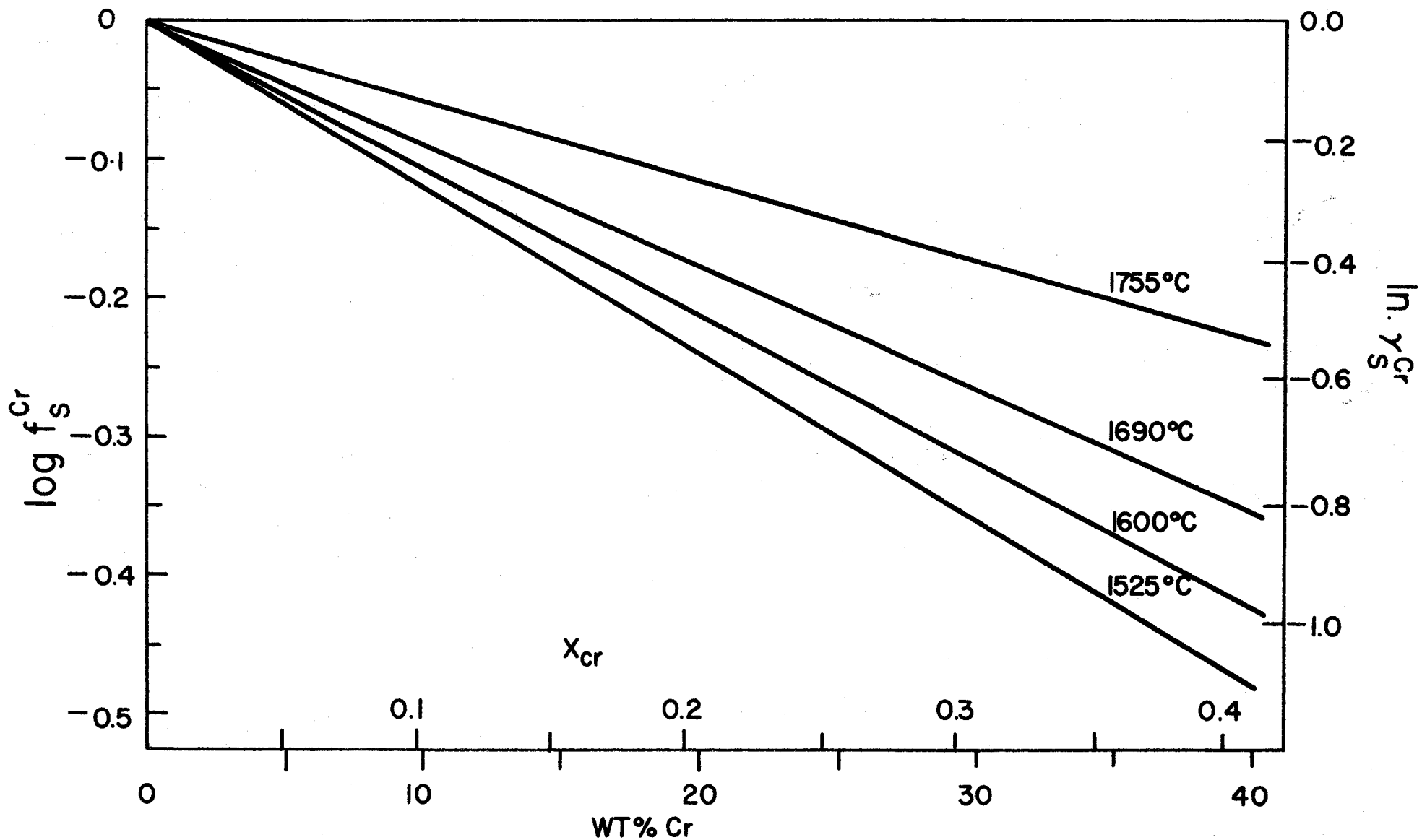


FIG. 28: EFFECT OF Cr AND TEMPERATURE ON THE ACTIVITY COEFFICIENT OF S

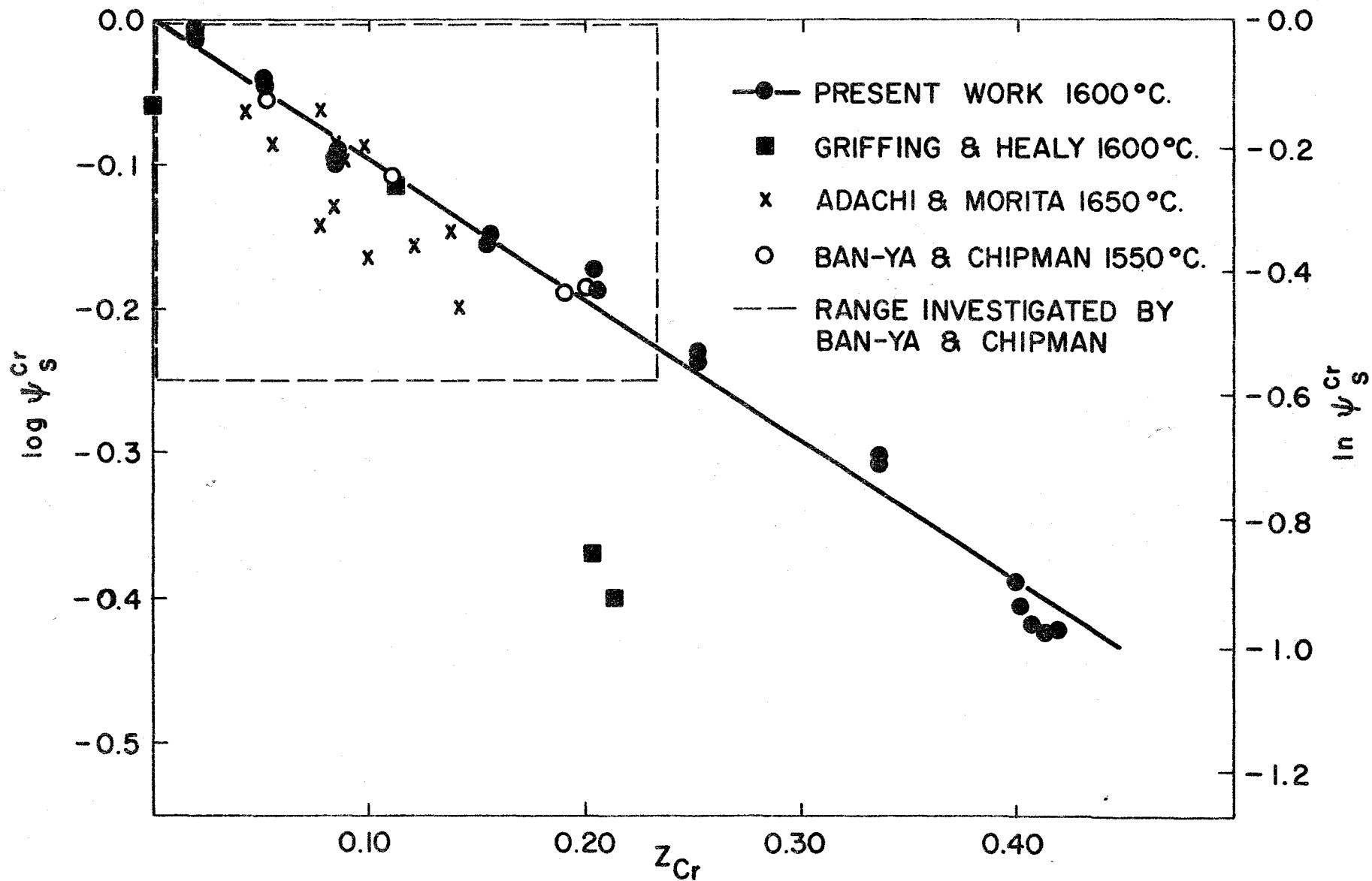


FIG. 29: COMPARATIVE STUDY OF THE EFFECT OF Cr ON THE ACTIVITY COEFFICIENT OF S
 $v_{Cr} = +1$

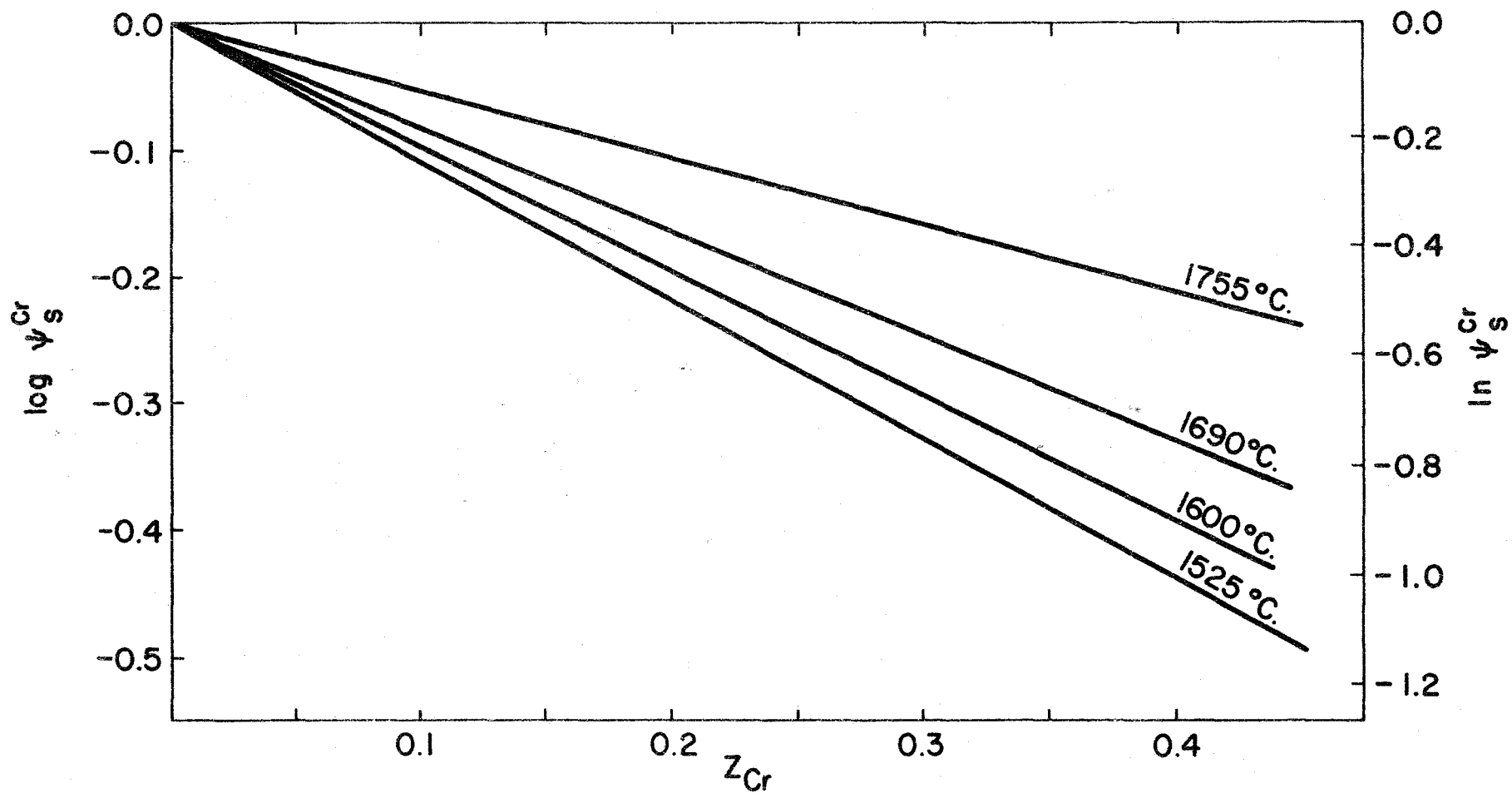


FIG. 30: EFFECT OF Cr AND TEMPERATURE ON THE ACTIVITY COEFFICIENT OF S

$$v_{\text{Cr}} = +1$$

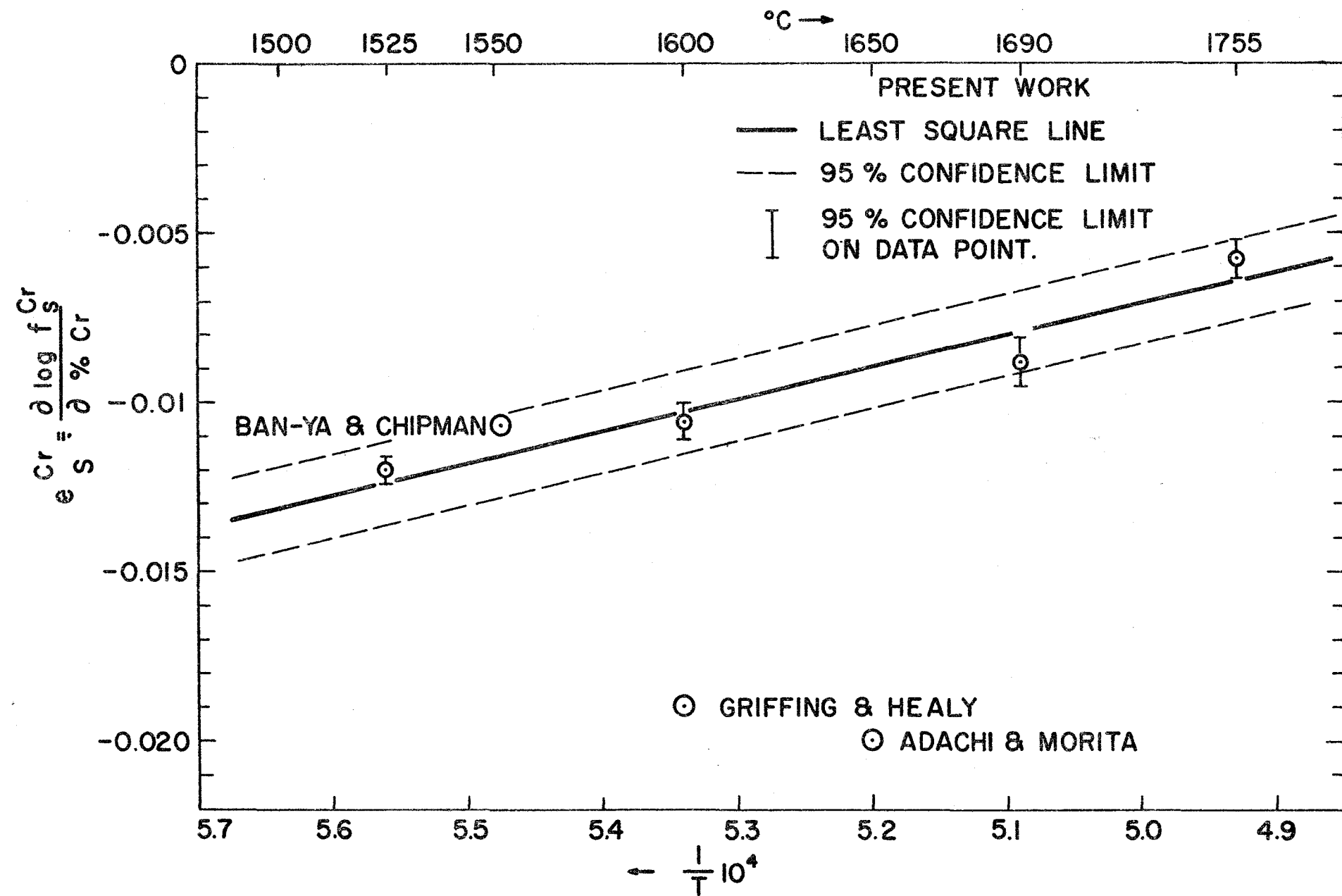


FIG. 31: TEMPERATURE DEPENDENCE OF e_S^{Cr} , COMPARATIVE STUDY

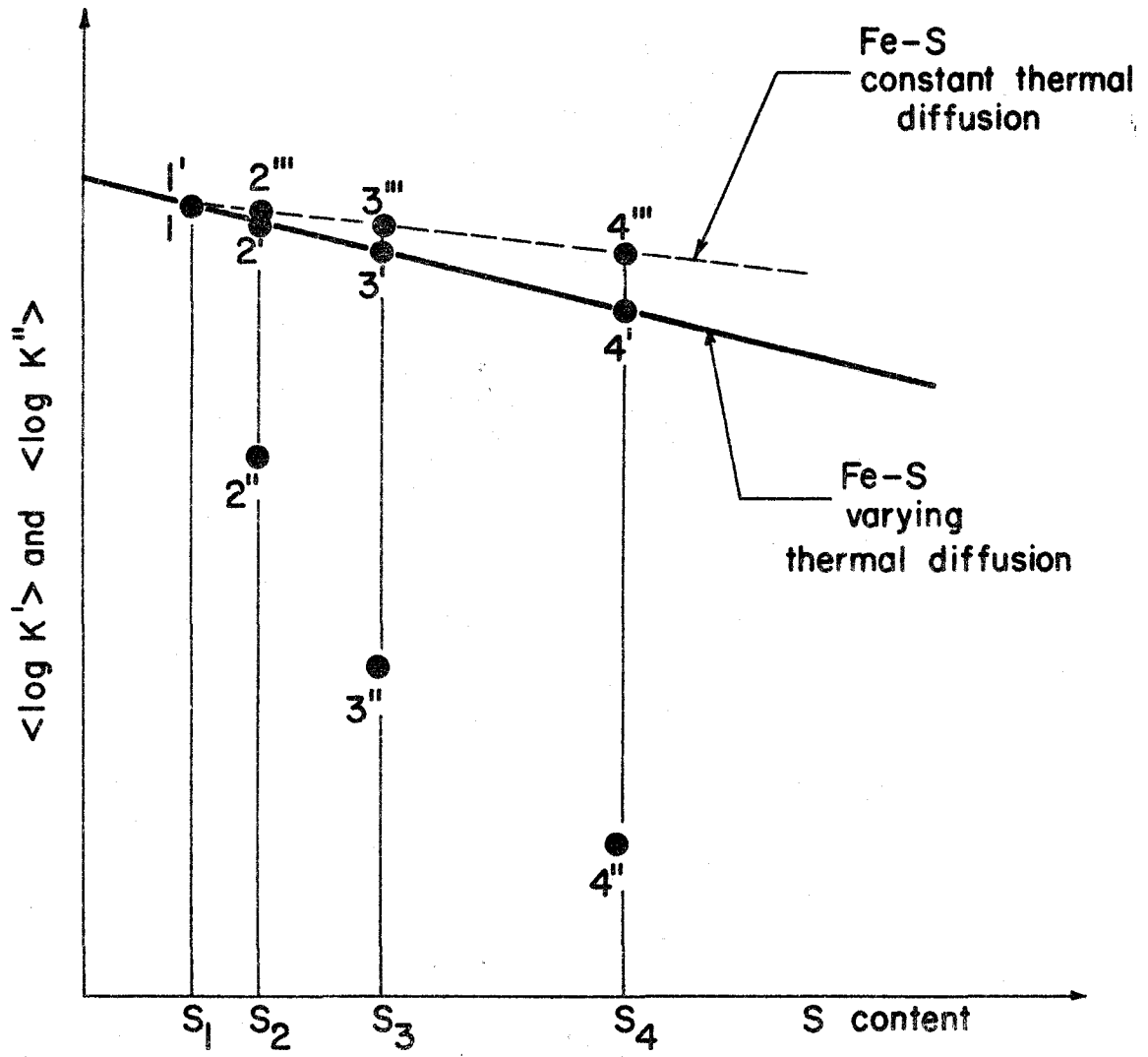


FIG. 32: THERMAL DIFFUSION EFFECT DUE TO A VARIATION IN GAS COMPOSITION

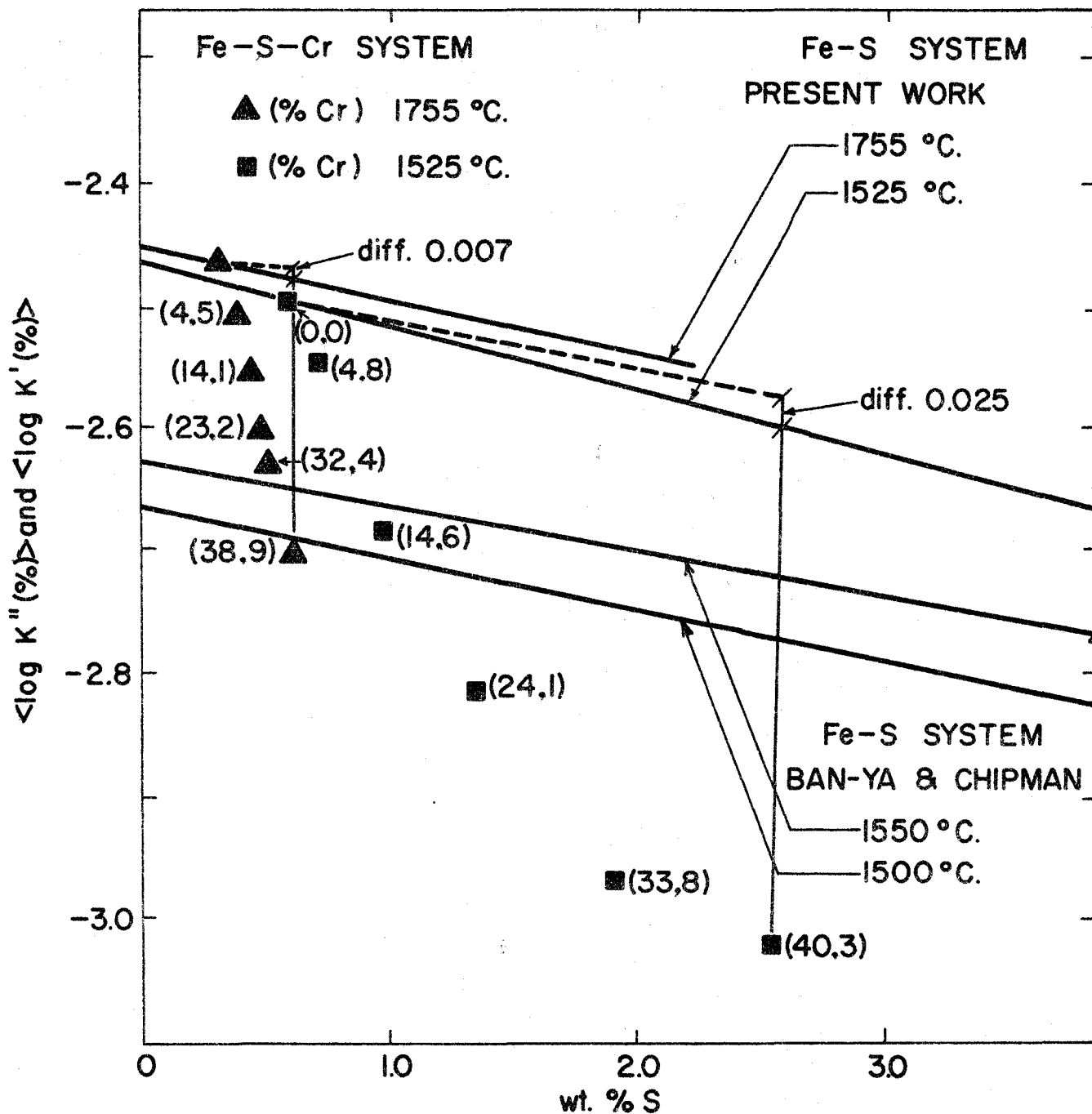


FIG 33: EFFECT OF GAS COMPOSITION UPON THE THERMAL DIFFUSION EFFECT, EXPERIMENTAL ESTIMATION